SPbGASU
1832

ARCHITECTURE & ENGINEERING

Volume 8
Issue 3
September, 2023

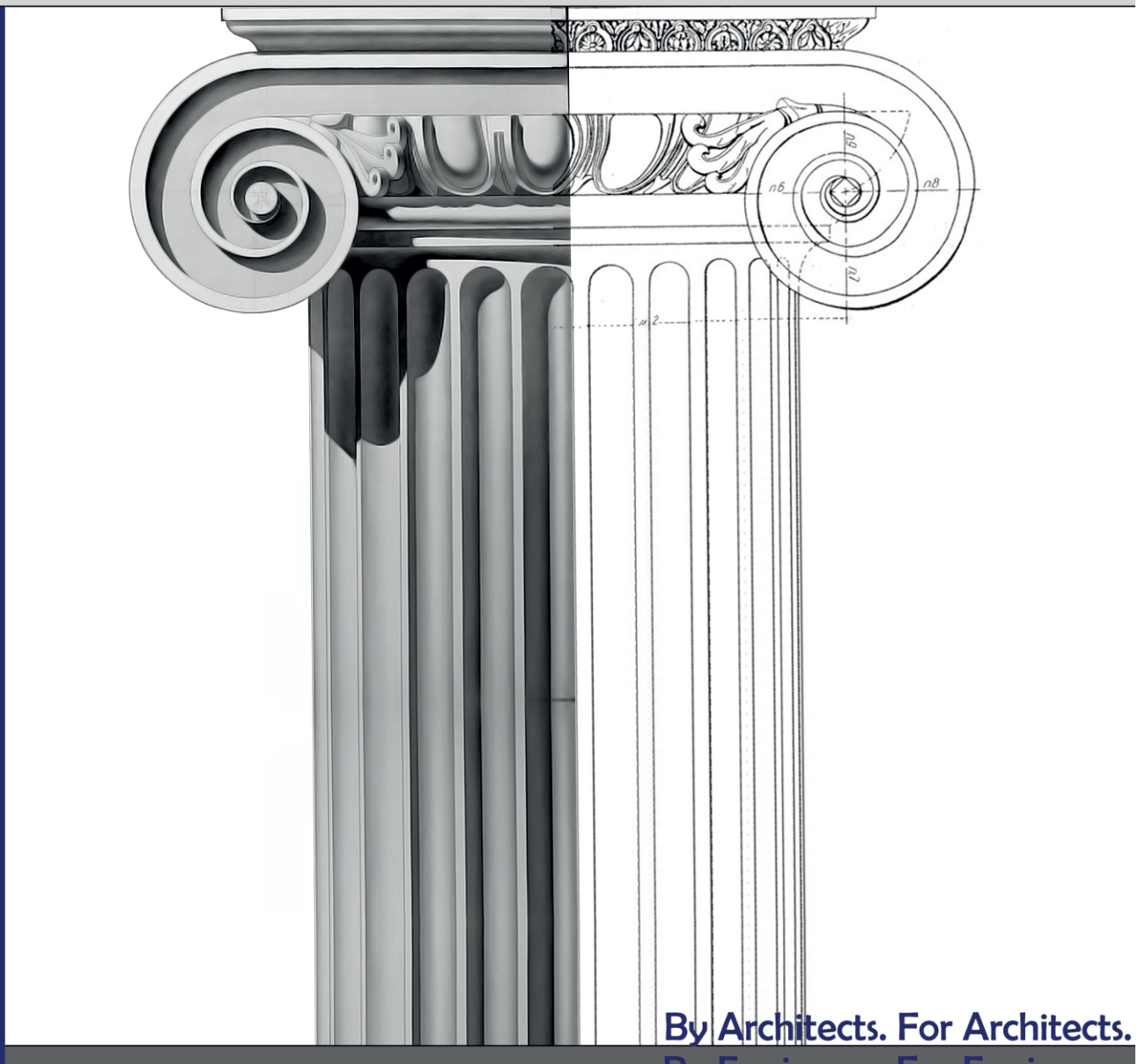

By Architects. For Architects.
By Engineers. For Engineers.

Architecture
Civil and Structural Engineering
Mechanics of Materials
Building and Construction
Urban Planning and Development
Transportation Issues in Construction
Geotechnical Engineering and Engineering Geology
Designing, Operation and Service
of Construction Site Engines

eISSN: 2500-0055
http://aej.spbgasu.ru/

Architecture and Engineering

Volume 8 Issue 3 (2023)

ISSN: 2500–0055

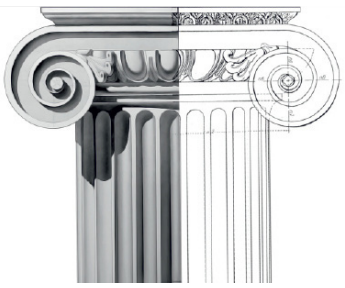

CONTENTS

Architecture and Engineering
peer-reviewed scientific journal
Start date: 2016/03
4 issues per year

Founder, Publisher:
Saint Petersburg State University of Architecture and Civil Engineering

Indexing:
Scopus, Russian Science Citation Index, Directory of Open Access Journals (DOAJ), Google Scholar, Index Copernicus, Ulrich's Periodicals Directory, WorldCat, Bielefeld Academic Search Engine (BASE), Library of University of Cambridge and CyberLeninka

Corresponding address:
4 Vtoraya Krasnoarmejskaja Str.,
St. Petersburg, 190005, Russia

Website: http://aej.spbgasu.ru/
Phone: +7(812) 316 48 49
Email: aejeditorialoffice@gmail.com

Date of issue: September 29, 2023

The Journal was re-registered by the Federal Service for Supervision of Communications, Information Technologies and Mass Communications (Roskomnadzor) on May 31, 2017;
registration certificate of media organization El No. FS77–70026

DOI: 10.23968/2500-0055-2023-8-3-3-13

MODERN ARCHITECTURAL APPROACHES TO SMART CITIES AND EDUCATIONAL FACILITIES

Numan Abu-Hammad

Khawarizmi University Technical College, Amman, Jordan

E-mail: abuhammad@bau.edu.jo

Abstract

Introduction: This article aims to provide readers with an overview of significant modern architectural approaches to creating sustainable smart city models. Different architectural approaches have piqued the interest of many researchers that study ancient and modern buildings, specifically their characteristics and execution methods. **Purpose of the study:** Interest toward smart architecture has grown due to the extensive development of technology and its integration into all aspects of human and city life, including the learning environment, the psychological effect of various spaces, and environmental impact. **Methods:** Architects, designers, engineers, and psychologists alike must consider these key developments and choose approaches to spaces and buildings that properly reflect the smart building philosophy. Many case studies have been adopted in the current investigation. **Results:** Over the recent years, due to the increasing strain of real estate demands, which led to overcrowding in cities, the need to find the most suitable housing solutions has emerged as a key problem. Architects and researchers are considering the best modern architectural approaches to building a sustainable model for smart cities.

Keywords: modern architecture; architectural approaches; smart cities; sustainable models; sustainable cities; design; engineering; smart architecture; smart buildings; concrete; facade; finishing materials.

Introduction

Today's ever-increasing expansion of smart technology, which is being adopted rapidly even in remote corners of the planet, coupled with intricate connections between information and data, paints a realistic and evolving picture of smart cities. Smart technology is one of the main pillars that support the future of smart cities.

The term "smart cities" relates to virtual cities, from which the concept of digital cities also derives. The most prominent outcome is the electronic or virtual space (Romano et al., 2018). The Smart Community Forum defined such spaces in 2006 as areas that foster creativity and provide means of communication and data for the local community. Information and communication technologies combine the intelligence of people and organizations to support learning, creativity, and digital spaces, thus enabling innovation and control over knowledge. Academics and practitioners are becoming increasingly interested in expanding the use of smart technology, including computer technologies and communication media. It is important to know how to unify and interconnect a given facility's systems to increase resource efficiency and to regulate the cost of operation and maintenance, as well as the space's psychological effects and environmental impact. In the era of smart cities and communications, the technological features of modern facilities have come to play a critical role in knowledge acquisition, which overlaps with their information technology role, as they help support the establishment of smart cities. This includes interconnected and integrated knowledge facilities, transforming the role of digital connectivity from standalone buildings in a given space to an entire interlinked system. This approach to the technology behind smart installations and smart facilities centers on a variety of inputs to provide data in a coordinated and up-to-date manner.

The following sections will outline the types of modern architecture, including concrete, facade and finishing materials, and their potential applications. This will be followed by a discussion section that will highlight the effects on learning environments, spatial psychological effects, and environmental impact, based on key case studies, including Storey's Field Center, the teaching and learning facilities at the Eddington Nursery, the Düsseldorf Stadttor building, and the Bahrain World Trade Center. The conclusion will provide recommendations for practitioners and outline a future scope for the next steps.

Modern Architecture Types and Applications

"Sustainable architecture" is a general term that describes environmentally conscious design techniques in the field of architecture (Foster, 2020). It can be defined as designing buildings that respect the

environment and are energy-, material- and resource-efficient, while minimizing the effects of construction and achieving harmony with the natural environment (Bielek, 2016). The corresponding architectural finishes and engineering designs are deployed in smart cities using materials and configurations that can respond to stimuli from the internal and external environment (Elattar, 2013). These materials have the ability to detect and "feel" the various stimuli and adapt to them by integrating functions into their structures. Such stimuli may be electrical or magnetic in nature and are utilized in smart cities to achieve sustainability (Juaristi et al., 2018).

Modern Applications of Concrete in Smart Cities

Many construction materials have been created over the ages, characterized by their smart features and ability to respond to the conditions in the environment around the building. Some examples of these materials are:

Carbon fiber concrete: Short carbon fibers are added to conventional concrete mixes, enabling the detection of even minor pressure and small cracks. Any defects in the concrete structure are located and repaired through the use of electrical sensors installed on the outside of the concrete structure, measuring the underground pressure and predicting earthquakes. This concrete type can also be used for monitoring building occupancy and traffic flow (Elattar, 2013).

Light transmitting concrete: This mixture of concrete and optical fibers offers a view on the space's external surroundings, as it lets light pass through it, creating a contrast between various segments depending on wall thickness.

Transparent concrete: Made of crushed glass and plastic, transforming the building facade into a large glass window. This material is superior to conventional concrete in terms of bearing compression and bending (Brownell, 2016).

Aerated concrete: Invented in 1914 in Sweden. When aluminum powder is added to cement, lime and water, it produces a foamy mixture. After melding and hardening, it is treated in pressurized steam rooms, which results in lightweight concrete that can be used at high altitudes and the inner walls of the building.

Pervious concrete: A type of concrete with a porous structure that lets rainwater pass through it to the ground. Used in sidewalks and floors, and characterized by strength and durability. It consists of Portland cement and coarse rocks (Dogne and Choudhary, 2014).

Smart bricks: Bricks filled with sensors, processors and wireless signal connections to send warnings about hidden stress and damage in the aftermath of natural disasters such as earthquakes and hurricanes. These bricks can monitor the building's temperature, vibration and movement, transmitting signals at regular intervals. This provides firefighters and rescue teams with important and necessary information, keeping both them and disaster victims safe (Elattar, 2013).

Smart cement: Contains magnesium carbonate instead of calcium carbonate and absorbs carbon dioxide from the atmosphere (0.4 tons of carbon dioxide per ton of cement) (Brownell, 2016).

Modern Applications of Facades in Smart Cities

Digital facades: Considered an integral part of a digital building, an element essential to the building's internal life (Funari et al., 2021). Conceptually, digital facades are presented as practical and instrumental to reducing energy consumption and improving the building's internal conditions through responding to external changes mechanically and automatically (Zolfagharpour et al., 2022). They interact with external changes, either through material elements (like canvas) that are affixed at the facade or through digital materials with characteristics that respond to changes in external conditions (Wigginton and Harris, 2002). Double facades are considered an exciting modern development as they allow for isolating the interior (Vasileva et al., 2022). Double facades can be created by adding a layer of glass outside the facade in order to provide buildings with ventilation and sound insulation, which is one of their most critical functions (Knaack et al., 2007).

Second-skin facade: This facade type features a second layer of glass along the outer surface of the whole building. It is distinguished by technical and structural simplicity, but provides little ability to control the internal environment (Strahle, 2012).

Corridor facade: Such facades are divided horizontally. Vertical joints separate the internal and external facade to reduce airflow horizontally and prevent fires. This, however, does not insulate against noise.

Shaft-box facade: Divided into square openings, or openings of other shapes, which distribute internal air depending on pressure differences and allow it to spill over vertically between floors to increase thermal efficiency.

Double digital facades: Come in different types, depending on the nature of external facades that help with moving air within the internal space and providing suitable ventilation.

Interactive facades: Interactive facades are considered as the ideal technique in the field of smart architecture, as they can respond to different environmental conditions. They are powered by control systems, where the automation process can be adjusted in order to guarantee ideal building performance and the highly efficient exploitation of the available natural resources, such as lighting and ventilation (Dewidar et al., 2010).

Kinetic facade: Kinetic facades are distinguished by their ability to modify their shape, shift, and create a given number of openings depending on various external environmental conditions, including temperature, moisture, and wind. These facades are considered to have a high impact on reducing energy. These facades need to be accounted for at the very first stages of the designing process, making it possible to integrate them into all parts of the building and thus achieve automation and reduce energy consumption.

Solar facades: Solar facades are contributing to reducing energy consumption, as they use renewable solar energy. Their structure is based on solar and photovoltaic cells that produce electricity, which can be used for heating, cooling, and lighting purposes. Such facades are compatible with sustainable green buildings (Ghaffarianhoseini et al., 2012).

Digital building upgrades must account for many aspects, the most important of which is the building facades, which can play an effective role in optimal energy performance. Many studies recommend making digital facades from sustainable materials to reduce energy consumption, reach zero level of non-renewable energy, and increase the facades' ability to respond to stimuli inside and outside the building.

Modern Applications of Finishing Materials in Smart Cities

The finishing materials have varied over the years, evolving to keep pace with the technical and technological development of the buildings themselves. Examples of smart finishing materials include:

Reflective indoor coating: A type of paint that reflects light better than ordinary paints, thus enhancing illumination and space perception. It further helps to reduce the amount of energy used in industrial lighting and increases perception and energy consumption by up to 20%. Such materials can last for 5–10 years without losing their performance and reliability. Reflective paint is suitable for regions with limited daylight intensity and duration, such as Central and Northern Europe (Bax et al., 2013).

Super black: An ultra-black paint that reflects 10–20 times less light than normal paint and is used to reduce unwanted reflections (Dogne and Choudhary, 2014).

Luminous bricks: Initially used in international art installations, these bricks are made out of polycarbonate panels and characterized by high strength. They successfully bear greater loads than normal bricks and are 50% lighter than glass. Furthermore, they come in different transparency levels and colors, and can be either molded, curved or sculpted, with a glossy or matte surface.

Shutoff valves: Valves containing sensors that cut off the flow of water in the event of a leak, thereby preventing flooding damage and providing live usage data (Elattar, 2013).

Optical fiber: Optical fibers are devices that direct waves and optical signals and are used for remote sensors. They can be made out of silica, sapphire, fluoride, or neodymium doped silica, with the transmission and sensing speed varying from material to material (Sun, 2015).

Glass: Glass still plays a major role in construction and has evolved into an advanced construction material, now considered a key feature of smart architecture.

Discussion and Case Studies

Digital building is a key architectural term and concept that relates to the production, development, and progress of architectural methods and concepts. The concept integrates modern technological and architectural thoughts, as both aim to fulfill the users' needs. While working on developing definitions and standards for digital buildings and identifying their characteristics, many researchers have stated that digital buildings are specialized entities and communities. The most important aspect is the ability to identify what is inside and outside. The building needs to function as efficiently as possible and respond to the users' needs, providing comfort and protection.

This architectural pattern developed quickly, eventually posing special design requirements, including smart materials that can change their physical properties as an automatic response to the surrounding conditions (Kamila, 2013; Sadeghi et al., 2011). Different smart systems emerged as well, utilizing sensors linked to the building's central control system. Smart facades are an important building feature, as they allow for controlling its internal environment according to external conditions, thus meeting the space requirements and changing needs. From here, it becomes clear that the use of these modern architectural features makes the new smart cities the focus of attention for people that search for distinctive housing with all the elements of smart cities. Eventually, these cities will transform, becoming greener and more architecturally sustainable. It is also worth noting that several famous cities in the world have already implemented modern architecture, turning certain areas into smart sustainable city spaces.

This research office building (Fig. 1), also known as the environmental building, is an example of using technological smart systems. It is considered an important landmark and demonstrates how smart architecture can be applied in environmental buildings. The building is located in Garston in the United Kingdom. The British government considers it a paragon of British innovation, recognizing it through the Millennium nomination. The eco-building's owners wanted it to be a model for other

Fig. 1. Garston Building Research Establishment

future buildings in the United Kingdom. The facade designs were equipped with the smart systems and linked into an internal work network, and the building was also provided with different sensors for measuring the temperature, wind speed and sunlight direction. The system was also pre-programmable, which made automatic control of the building faster while not restricting it as the only option. Instead, there was still room for the users to manually adjust the surrounding environment conditions. It is worth noting that the practical application of the ecological building concept must overlap with the architectural notions of smart architecture, giving the designer a preconceived perception of how to employ smart building features to achieve this, while also considering the best systems and methods and ways of connecting them for the best architectural results (Wigginton and Harris, 2002).

Case Study: Düsseldorf Stadttor ("City Gate")

This structure, located in Düsseldorf, Germany, was designed by Petzinka Pink und Partner for a 1991 competition to construct a new building over a tunnel that attracts traffic to the city center. The building contains offices, studios and media headquarters, and was completed in 1997. It is designed to rely on natural factors such as ventilation and lighting, in addition to the introduction of smart systems (Fig. 2). Moreover, the building utilizes air facades, where there is a distance ranging between 1.4 and 0.9 meters between the inner and outer facade (Strahle, 2012).

Case Study: Bahrain World Trade Center

The Bahrain World Trade Center is the first smart building in Bahrain, and the building includes many smart technological features, the most important of which is the use of a high-speed Internet connection system, in addition to telephone communication via Internet protocols and unified wireless messages in one network for audio and visual data. The building management system functions by connecting the Internet networks to a dedicated computer device, downloading dynamic schedules, and monitoring system integration. The system reduces costs and allows the building occupants to receive a single bill that includes fees for energy use, rent, and information and communication technology. The building uses advanced, smart security systems for protection, monitoring, and response to alarms (Fig. 3).

Case Study: Storey's Field Center, the Teaching and Learning Facilities at the Eddington Nursery, and Their Psychological Impact

This segment of the study aims to evaluate the environmental influence on psychological awareness and attitude, as well as explore the psychological impact of digital learning spaces on students at Storey's Field Center and the Eddington Nursery (Fig. 4). Furthermore, we shall discuss the relationship between the modern architecture's

Fig. 2. Düsseldorf Stadttor building

applications and students at Storey's Field Center and the Eddington Nursery, and the role of the working environment in the students' lives. The paper by Schuilenburg and Peeters (2018) discusses spatial psychology among students and evaluates the impact of the environment and architectural design on flexible and productive outcomes. It presents a comprehensive assessment of psychological effects on students. Architectural design institutes contribute to a better understanding of environmental influences. Various institutes offer both numerous traditional study spaces and a selection of innovative, flexible study spaces. The educational norms that drive this transition offer an intriguing research backdrop, and the tension between various types of learning spaces is now prominent in many other places. Furthermore, the choice also depends on the study participants and access to appropriate resources. Learning spaces can greatly emphasize discipline and group thinking, which is reflected in their traditional theoretical architectural styles and interior features. The space tends to create a relaxed interdisciplinary environment with rich color combinations, comfortable interiors, location and flexibility, and an increased sense of ownership and autonomy (Adams-Hutcheson and Johnston, 2019).

Fig. 3. Bahrain World Trade Center

Fig. 4. Storey's Field Center and Eddington Nursery

To go beyond this historical approach to learning environments, we provide the following set of guidelines for designing and executing university spaces. Hopefully, these principles will result in facilities that are less prescriptive and functionally specific than they are now. The aim is to foster a sense of community ownership among students through using and occupying certain campus spaces (Lam et al., 2019). We believe that new spaces should be used in conjunction with existing design concepts rather than replacing them. Instead of expressing a new set of intentions, emphasis shifts to the way these environments are used (Fig. 5).

Learning spaces are designed to be optimal for specific purposes (such as transcription in lecture halls, computer-based activities in computer labs, and use of tools other than information and communication technology during tutorials or group classes). This is the current strategy for building new facilities for Storey's Field Center and the Eddington Nursery. The design of the new learning environment must be flexible enough to accommodate a wide range of functions. This covers teacher-centered and student-centered approaches, formal planned meetings, and various unstructured ways in which students use technology (Simpeh and Shakantu, 2019). Using a student-centered collaborative learning approach, along with consultative assessment, will increase the diversity of student engagement at Storey's Field Center and the Eddington Nursery (Fig. 5).

The online space and official website must gradually adapt to the needs of informal users, such as students who use the facilities outside of planned courses. As pointed out in (Schmidt, 2020), students spend 80% of their time on campus engaging in social and extracurricular activities. As a result, when they are not in formal classrooms, they are forced to gather in libraries or cafes, which are not ideal for big student groups working together. This situation is unsustainable from a pedagogical and economic point of view. Information and communication technology may be required when appropriate infrastructure is unavailable, or when remaining in an authorized formal classroom areas may hinder collaborative activities (Foteinaki et al., 2018).

Since its inception, architecture has predominantly focused on how to use ground space. The possibilities offered by the creative use of vertical dimensions should be utilized better. Whiteboards and other collaboration tools can be placed on the wall for students to plan and document their ideas, as well as work together with others. Stage performances can benefit from a raised floor. Ceilings and skylights can be created to enhance the spontaneity and visual value of specific architectural spaces (Fig. 6).

Where feasible, campus amenities should be added to prevent current services and functions from becoming isolated. Facilities that serve food and drinks, communal spaces for casual conversation, and comfortable furniture will allow students to enjoy this environment and integrate social interactions and personal activities into it. Covered walkways, arcades, galleries, and corridors serve as a convenient transition zone between interior and outdoor spaces and should be explicitly considered when designing areas outside of the architectural space.

It should be assumed that teachers and students can completely control the facility's functionality and environment. Videoconferencing or computer labs can become expensive and intrusive if they

Fig. 5. Nursery classroom design (source: Hartman, 2018)

Fig. 6. Main hall (source: Hartman, 2018)

rely on tech support from a single location. In most cases, tech support is prioritized for official, teacher-led activities, which makes it much less accessible in informal student-led environments without the teacher's personal intervention.

As university campuses offer a variety of lessons, courses, and extracurricular activities, it is necessary for them to provide a variety of formal and informal learning environments. For instance, if a science test site is structured to have an extensive study area supplemented by some smaller, more specialized rooms, a laboratory could be classified as such. To reduce the number of large, underutilized special-purpose laboratories that can become barriers to the adoption of alternative pedagogical practices, enhanced through information and communication technology, it is necessary to downsize these laboratories.

It is vital to review requirements from every field of study in order to assess how educational objectives are currently being met, including what new technologies have been suggested and which other advancements or trends may become important in the future.

Students are developing an increased sense of responsibility for their own learning experience. The overall controlled environment hampers the results that most organizations envision for their campus services. A student-centered approach requires resources that are available to students 24/7 (such as libraries, information and communication technology-equipped areas, and classrooms).

It is possible to improve a facility's visual design without compromising its function. To nurture people who think critically and actively embrace social difference, we must counter the tendency to institutionalize and standardize design. Students should have plenty of opportunities to develop a sense of ownership of the building and its maintenance in the locations that they use daily, especially department- or faculty-specific ones.

In the mid-1990s, the capital management program at the Australian National University Learning Studio opened several new facilities with a planning horizon of over 5 years ahead. Many of those buildings offered new teaching and learning resources, including technology. In 1997, a decision was made to establish an experimental "learning studio" for testing different spatial arrangements. The proposal included high-tech classroom furniture arrangement that differed significantly from existing arrangements (Dane, 2019).

Case Study: Technology at Storey's Field Center and the Eddington Nursery

This learning space, housed in a former commercial bank building in Eddington, welcomes students from both international, domestic and indigenous backgrounds. The teaching team's experience with pedagogical and architectural issues highlights many of the critical components we mentioned earlier. The architecture of an educational facility should facilitate a certain learning style while also considering the surrounding cultural context (Dane, 2019). According to the program's coordinator, encouraging inquisitiveness is the most important organizational aspect of the curriculum, both in general terms of teaching and learning, and specifically in the context of the program. Both the individual and the community highly value the wisdom of their fellow humans. The personal and cultural experiences of students and their families are valued, and the focus is on informal contacts and strong community relationships, as well as on practice and on making personal theories after a period of intensive study. The project's ultimate goal is to provide public access to natural areas that are currently inaccessible, such as rivers and woodlands. This concept has been applied throughout the building, resulting in a learning environment that is both integrated and informal. First- and second-year students will be able to learn from one another because the same subjects will be taught in both years simultaneously. Instead of confining individuals and putting them in "boxes", the surrounding environment could be used to foster a universal sense of belonging. Furthermore, there must be enough room for students to read, talk to one another, and do research.

Here, the building greatly benefits from having a large open area in the center. One of the classrooms has been converted into a small kitchen area, where students may now prepare their tea or coffee. The individual in charge of the project most likely worked at the bank's management office. There is a carving on one of the main walls in the third room. The remaining room was initially empty, leaving the teachers and students to use it as they pleased. They partitioned the space using whiteboards and overhead projectors. If necessary, seats and tables may also be set up. In 1999, many students visited the center to study numerous subjects.

Choosing the facility's teaching philosophy is critical when constructing a new campus infrastructure that emphasizes student-centered learning practices. Children learn in various formal and informal ways, and educators have long recognized this. The teacher should aid them in their educational endeavors rather than simply impart knowledge. Moreover, students and elders from the indigenous community come to exchange knowledge and work as a team to better their education. The learning process of this specific group of children has been influenced by several indigenous tribes' stories.

They were instructed to utilize all of the resources available to them at the time of getting an education.

As students worked alone or in groups, instructors were more motivated, and consequently more likely, to deliver lectures for small classes. Although students were required to meet deadlines, they were also encouraged to study and collaborate at their own speed, regardless of circumstances. Due to the nature of activity and the high number of students that participated, the furniture had to be moved. Courses were held on campus and in surrounding parks to maximize efficiency and make the most of the group's landholdings.

Rearranging the furniture proved easier in open spaces. Teachers and students could design multi-activity learning environments suited to their unique requirements. If there were enough attendees to warrant it, the institution would remain open late, and the staff would sometimes offer midnight events for those who could not make it during normal business hours. While most students were expected to attend specific courses, they were encouraged to work on campus as much as they wanted. Because of the educational institution's location, it was required to offer a kitchenette and other facilities. Local companies provided meals for the campus dining hall. The curriculum requirements were predicated on the idea that students were responsible for their own education and living environment. Instructors were given much freedom in how they used the facilities.

Future Scope

This paper explored the ways in which higher education is evolving, specifically in terms of location and physical space. There have been several studies on these learning environment elements, but we believe that none of them looked at how educational institutions teach and influence their students. From the papers included in the current issue of Higher Education Research and Development, it is clear that, despite recent advances in pedagogy and classroom design, these innovations have not yet been fully integrated into the education system. This is what will be considered in this section.

A concerted attempt to examine how instructors and students interact with constructed settings today and in the future is highly likely to lead to improvements in on-campus teaching and learning facilities. Yet getting resources in this sector is already challenging, and it remains uncertain how things will progress in the future. Instead, a stage designer may be able to develop an original solution. Rather than following our notion of developing a physical structure to serve as a *shell* for educational activities, the way things are done today is incompatible with our concept. The idea of designing a *shell* is inspired by stage and set design techniques that focus on the capacity to move freely within the boundaries of a confined area, as well as within environmental and budgetary constraints. An on-campus teaching and learning facility similar to those discussed above may serve as an exemplary model for other institutions.

Conclusion

In light of the issues covered above, many collaboration opportunities should be made more accessible in the classroom for instructors and students to use. If the relevant fixtures and fittings were readily accessible, it would be far easier to tailor them to satisfy the specific requirements of different groups of individuals. It is important to be more flexible when integrating information and communication technology to avoid reducing mobility and participation. New teaching and learning environments may be created and implemented throughout the whole school or just a few departments. A single building acts as the focal point for the entire process. There are plans to make construction projects more strategic and institutional in nature, reducing duplication across departments.

This transition will need adjustments in the strategic facility management planning. Similarly, if instructors and students decided to design and build their classrooms and learning environments from the ground up, the results would be the same. In either case, it would be impossible to function without the same authorization. The expansion of academic departments' responsibilities during the last decade has resulted in a wide range of tasks that they need to complete, including designing and managing the physical settings where study activities take place. Later on, information and communication technology and constructed environments will be combined with teaching and learning. Let us suppose that new information and communication technologies will not modify the relationship between pedagogy and the physical environment. In that case, students will be forced to attend classes in a facility constructed decades ago for purposes that are opposed to those they are pursuing today.

Recommendations

Consequently, designers who adopt this architectural trend should consider:

Identifying the nature of the building's conditions and functions, including the system of spatial arrangement and the mechanism of bringing the spaces together.

Identifying common environmental conditions and the suitable building and finishing materials that can adjust to them. Identifying and customizing spaces suitable for the building's main control systems. Studying the building's facades and architectural design in order to select the most suitable option, integrated into the building's concept. Engaging with stakeholders from diverse fields, including psychology, engineering, and design, and getting them involved in the conceptualization and planning phases of smart architectural spaces.

References

Adams-Hutcheson, G. and Johnston, L. (2019). Flourishing in fragile academic workspaces and learning environments: Feminist geographies of care and mentoring. *Gender, Place and Culture,* Vol. 26, Issue 4, pp. 451–467. DOI: 10.1080/0966369X.2019.1596885.

Bax, L. Cruxent, J. and Komornicki, J. (2013). *Innovative chemistry for energy efficiency of buildings in smart cities*. [Online] Available at: https://cefic.org/app/uploads/2019/01/Innovative-Chemistry-for-Energy-Efficiency-of-Buildings-in-SmartCities-BROCHURE-iNNOVATION.pdf [Date accessed September 18, 2023].

Bielek, B. (2016). Green building — towards sustainable architecture. *Applied Mechanics and Materials*, Vol. 824, pp. 751–760. DOI: 10.4028/www.scientific.net/AMM.824.751.

Brownell, B. (2016). *Transmaterial: A catalog of materials, products and processes that are redefining our physical environment*. [Online] Available at: http://www.eskyiu.com/aainter1/index_files/transmaterial.pdf [Date accessed September, 20 2016].

Dane, J. E. (2019). *New generation learning environments in higher education*. PhD Thesis. Monash University.

Dewidar, K., Mahmoud, A. H., Magdy, N., & Ahmed, S. (2010). The role of intelligent façades in energy conservation. In International Conference on Sustainability and the Future: Future Intermediate Sustainable Cities, (FISC) Vol. 1. Cairo-Egypt.

Dogne, N. and Choudhary, A. (2014). *Smart construction materials and techniques. National Conference on Alternative & Innovation Construction Materials & Techniques*. [Online] https://www.researchgate.net/publication/297167802_SMART_CONSTRUCTION_MATERIALS_TECHNIQUES [Date accessed September 5, 2016].

Elattar, S. M. S. (2013). Smart structures and material technologies in architecture applications. *Academic Journals*, Vol. 8 (31), pp. 1512–1521. DOI: 10.5897/SRE2012.0760.

Foster, G. (2020). Circular economy strategies for adaptive reuse of cultural heritage buildings to reduce environmental impacts. *Resources, Conservation and Recycling*, Vol. 152, 104507. DOI: 10.1016/j.resconrec.2019.104507.

Foteinaki, K., Li, R., Heller, A., and Rode, C. (2018). Heating system energy flexibility of low-energy residential buildings. *Energy and Buildings*, Vol. 180, pp. 95–108. DOI: 10.1016/j.enbuild.2018.09.030.

Funari, M. F., Hajjat, A. E., Masciotta, M. G., Oliveira, D. V., and Lourenço, P. B. (2021). A parametric scan-to-FEM framework for the digital twin generation of historic masonry structures. *Sustainability*, Vol. 13, Issue 19, 11088. DOI: 10.3390/su131911088.

Ghaffarianhoseini, A., Berardi, U., and Makaremi, N. (2012). Intelligent facades in low-energy buildings. *British Journal of Environment & Climate Change*, Vol. 2, Issue 4, pp. 437–464. DOI: 10.9734/BJECC/2012/2912.

Hartman, H. (2018). *RIBA Stirling Prize 2018: Storey's Field Centre and Eddington Nursery MUMA,* Cambridge. [Online] Available at: https://www.architectsjournal.co.uk/buildings/riba-stirling-prize-2018-%E2%80%8Bstoreys-field-centre-and-eddington-nursery-by-muma [Date accessed 18/09/2023].

Juaristi, M., Monge-Barrio, A., Knaack, U., and Gómez-Acebo, T. (2018). Smart and multifunctional materials and their possible application in facade systems. *Journal of Facade Design and Engineering*, Vol. 6, No. 3, pp. 19–33. DOI: 10.7480/jfde.2018.3.2475.

Kamila, S. (2013). Introduction, classification and applications of smart materials: an overview. *American Journal of Applied Sciences*, Vol. 10, No. 8, pp. 876–880. DOI: 10.3844/ajassp.2013.876.880.

Knaack, U., Klein, T., Bilow, M., and Auer, T. (2007). *Facades. Principles of construction*. Berlin: Birkhäuser Verlag AG, 43 p.

Lam, E. W. M., Chan, D. W. M., and Wong, I. (2019). The architecture of built pedagogy for active learning—a case study of a university campus in Hong Kong. *Buildings*, Vol. 9, Issue 11, 230. DOI: 10.3390/buildings9110230.

Romano, R., Aelenei, L., Aelenei, D., and Mazzucchelli, E. S. (2018). What is an adaptive facade? Analysis of recent terms and definitions from an international perspective. *Journal of Facade Design and Engineering*, Vol. 6, No. 3, pp. 65–76. DOI: 10.7480/jfde.2018.3.2478.

Sadeghi, M., Masudifar, P., and Faizi, F. (2011). *The function of smart material's behaviour in architecture. In: International Conference on Intelligent Building and Management,* Vol. 5. 317-322. [online] Available at: https://www.researchgate.net/profile/Foad-Faizi/publication/267233873_The_Function_of_Smart_Material%27s_behavior_in_architecture/links/56998e1708aeeea98594a403/The-Function-of-Smart-Materials-behavior-in-architecture.pdf [Date accessed September 18, 2023].

Schmidt, P. (2020). Living on Campus: An Architectural History of the American Dormitory by Carla Yanni (review). *The Review of Higher Education*, Vol. 43, No. 4, pp. E-43–E-45. DOI: 10.1353/rhe.2020.0024.

Schuilenburg, M. and Peeters, R. (2018). Smart cities and the architecture of security: pastoral power and the scripted design of public space. *City, Territory and Architecture*, Vol. 5, 13. DOI: 10.1186/s40410-018-0090-8.

Simpeh, F. and Shakantu, W. (2019). Prioritisation of on-campus university student housing facility spaces. *Journal of Construction Project Management and Innovation*, Vol. 9, No. 1, pp. 19–33. DOI: 10.36615/jcpmi.v9i1.179.

Strahle, C. G. (2012). *An environmental skin: enhancing thermal performance with double□skin facades in Hawai`i's climate*. PhD Thesis in Architecture. School of Architecture, University of Hawai`i at Mānoa.

Sun, B.H. (2015). *Smart materials and structures. Lecture at Swiss Federal Institute of Technology Zurich (ETH)*. [Online] Available at: https://www.researchgate.net/publication/281836834_Smart_Materials_and_Structures [Date accessed November 16, 2016].

Vasileva, I. L., Nemova, D. V., Vatin, N. I., Fediuk, R. S., and Karelina, M. I. (2022). Climate-adaptive facades with an air chamber. *Buildings*, Vol. 12, Issue 3, 366. DOI: 10.3390/buildings12030366.

Wigginton, M. and Harris, J. (2002). *Intelligent skins*. London: Routledge, 184 p. DOI: 10.4324/9780080495446.

Zolfagharpour, A., Shafaei, M., and Saeidi, P. (2022). Responsive architecture solutions to reduce energy consumption of high-rise buildings. *International Journal of Architectural Engineering & Urban Planning*, Vol. 32, Issue 3. DOI: 10.22068/ijaup.679.

СОВРЕМЕННЫЕ АРХИТЕКТУРНЫЕ ПОДХОДЫ К УМНЫМ ГОРОДАМ И ОБРАЗОВАТЕЛЬНЫМ УЧРЕЖДЕНИЯМ

Нуман Абу-Хаммад

Прикладной университет Эль-Балка, Амман, Иордания

E-mail: abuhammad@bau.edu.jo

Аннотация
Введение: Цель настоящей статьи — ознакомить читателя с основными современными архитектурными подходами к созданию устойчивых моделей умного города. Различные архитектурные подходы представляют интерес для исследователей, изучающих древние и современные здания, в частности их характеристики и методы исполнения. **Цель исследования:** Интерес к «умной» архитектуре растет благодаря активному развитию технологий и их интеграции во все аспекты жизни общества и города, включая образовательную среду, психологический эффект различных пространств и воздействие на окружающую природу. **Методы:** Специалисты — как архитекторы, дизайнеры и инженеры, так и психологи — должны учитывать столь существенные перемены и выбирать подходы к созданию пространств и сооружений, должным образом отражающие философию «умного здания». **Результаты:** В последние годы поиск рациональных решений в сфере жилья стоит на повестке дня, поскольку спрос на недвижимость неуклонно растет, приводя к перенаселению в городах. Архитекторы и исследователи рассматривают оптимальные современные архитектурные подходы к созданию устойчивой модели умного города.

Ключевые слова: современная архитектура; архитектурные подходы; умные города; устойчивые модели; устойчивые города; дизайн; проектирование; умная архитектура; умные здания; бетон; фасад; отделочные материалы.

DOI: 10.23968/2500-0055-2023-8-3-14-22

ON THE AUTOGENOUS SHRINKAGE OF CEMENT PASTES

Abdelghafour Saadi*, Abdelmalek Brahma

University Saâd Dahlab Blida 1, Algeria

*Corresponding author's e-mail: Saadi.abdelghafour@yahoo.fr

Abstract

Introduction: This study focuses on autogenous shrinkage in cement pastes and presents a novel calculation method considering variations in internal relative humidity (IRH). IRH significantly influences autogenous shrinkage, and its evolution is modeled based on decline curves. The proposed method accurately evaluates autogenous shrinkage and aligns well with experimental data. Additionally, we calculate capillary depression and meniscus radius using the Laplace–Kelvin equation. **Methods:** To address early autogenous shrinkage in construction materials, we developed our calculation method, emphasizing IRH variation. We analyzed decline curves to model IRH and validated our model using literature-based experimental data. **Results:** Our validated model for predicting IRH and autogenous shrinkage in Portland cement pastes, based on cement paste hydration degree, water-to-cement ratio (w/c), and the critical degree of hydration (α_{cr}), closely aligns with experimental data and existing models.

Keywords: cement paste, autogenous shrinkage, internal relative humidity, prediction, modeling, decline curves.

Introduction

Autogenous shrinkage refers to the chemical shrinkage due to Le Chatelier contraction derived by the difference in density between hydration products and reactants (Davis, 1940); generally, it is a phenomenon caused by three parameters: depression capillary, superficial tension, and disjoining pressure (Mounanga, 2004).

A decrease in w/c ratio leads to an increase in autogenous shrinkage; this is due to the spacing between the particles. A low value of the radius of the meniscus generates a difficult circulation of water (capillary depression) which creates stresses in the matrix leading to its contraction.

Due to its complex composition, there are difficulties with modeling the shrinkage of cement paste. The researchers work on two types of models: macro (or phenomenological) and micromechanical models. Both have limitations because they do not take into consideration that cement paste is a porous medium, and fail to take into account time-dependent properties. In addition, identifying the model parameters for most of these models is rather complicated as well (Mounanga, 2004).

Internal relative humidity (IRH) plays a role in the development of capillary depression. During the progression of hydration, the reduction of IRH generates capillary tension in the interstitial water, then a modification of the radius of the capillaries to balance compressive stress in the solid skeleton; compressive stresses are accompanied by deformations (van Breugel, 2001).

IRH is a key parameter influencing the microstructure and durability of cement-based materials. Understanding the relationship between IRH and autogenous shrinkage is important for the design and performance evaluation of these materials. The evolution of degree of hydration, which is influenced by factors such as cement composition, curing conditions, and environmental exposure, affects both IRH and autogenous shrinkage. In this context, several models (Bažant and Prasannan, 1989; Bentz et al., 1994; Eguchi and Teranishi, 2005; Haecker et al., 2005; Hua et al., 1995, 1997; Koenders and van Breugel, 1997; Lura et al., 2003; Mabrouk et al., 2004; Neubauer et al., 1996; Paulini, 1994; Shimomura and Maekawa, 1997; Ulm et al., 2004; Xi and Jennings, 1997) have been proposed to predict the variation of autogenous shrinkage over time. However, the majority of these models do not account for the evolution of hydration degree, which limits their accuracy and applicability. Additionally, there are models predicting other properties such as IRH, Young's modulus, and temperature, all of which are in direct relationship with the progression of hydration degree.

The main goal of this study was to develop a comprehensive calculation method for early autogenous shrinkage in construction materials. To achieve this goal, we took into account the variation of IRH as a crucial factor in the shrinkage process. In a second step, we analyzed decline curves to model IRH. Furthermore, we validated the proposed model using experimental data from the literature

For citations: Saadi, A., Brahma, A. (2023). On the autogenous shrinkage of cement pastes. Architecture and engineering, No 2 (8), pp. 14-22. DOI: 10.23968/2500-0055-2023-8-3-14-22.

and compared its performance with that of other models. The paper is organized as follows. Section 2 describes the method used to calculate autogenous shrinkage. Section 3 presents the proposed model for predicting IRH. Section 4 presents the validation results of the proposed model and calculation method and compares their performance with that of other models. Section 5 presents a discussion. Finally, Section 6 summarizes the conclusions of the study.

Calculation of Autogenous Shrinkage

Let us consider a small piece of material located in the full mass of the paste of cement subjected to compressive stress generated by the depression of the water in the capillaries (Fig. 1). The interstitial fluid in depression exerts a pressure on the element in question so that the element is subjected to a uniform triaxial stress (Fig. 2).

We can write the volume change ε as:

$$\varepsilon = \frac{\Delta V}{V} = \varepsilon_x + \varepsilon_y + \varepsilon_z. \quad (1)$$

By applying this equation to a differential element of volume and then integrating it, we can obtain the change in volume of a body even when the normal strains vary throughout the body.

By Hooke's law in mechanics of materials, the element is subjected to triaxial stress (beer et al, 2012):

$$\varepsilon = \frac{1-2\nu}{E}\left(\sigma_x + \sigma_y + \sigma_z\right). \quad (2)$$

In the case of uniaxial stress (prismatic specimen in compression), Eq. 2 is simplified to:

$$\varepsilon = \frac{\Delta V}{V} = \frac{(1-2\nu)}{E}\sigma, \quad (3)$$

where ν is Poisson's ratio and E is the elastic modulus of cement paste.

The determination of the deformation (ε) requires the knowledge of stress (σ), which is the value of the constraint generated by capillary depression. At younger ages, deformation mechanism by capillary depression is dominant due to high internal relative humidity; stress σ in this case is given by the Laplace–Kelvin equation:

$$\sigma = \frac{2\gamma}{r} = -\frac{RT}{V_m}\mathrm{Ln}(\mathrm{IRH}), \quad (4)$$

where σ is the capillary depression (Pa), R is the universal gas constant [8.314 J/(mol K)], T is the internal temperature in (K), V_m is the molar volume of water [18.02 10^{-6} m^3/mol], and IRH is the internal relative humidity (with values between 0 and 1), γ is the superficial tension (N/m) and r is the meniscus radius (m).

By bringing Eq. 4 into Eq. 3, we can deduce the equation of autogenous shrinkage:

$$\varepsilon = -\frac{(1-2\nu)}{E}.\frac{Ln(IRH)RT}{V_m}. \quad (5)$$

The unknowns in this equation are IRH, E, ν and T. There are several models proposed in literature to calculate these variables. For example, L. Stefan et al. (2010) proposed an equation to predict the evolution of E as a function of hydration degree (Eq. 6); other authors considered the relationship between adiabatic temperature and degree of hydration (Cervera et al., 1999) (Eq. 7):

$$E(\alpha) = E(\alpha = \alpha_\infty)\left[\left\langle \frac{\alpha - \alpha_0}{\alpha_\infty - \alpha_0}\right\rangle^+\right]^\beta, \quad (6)$$

where β = w/c is a material parameter, α_∞ = 0.75 (Cervera et al., 1999) and α_0 = 0.2.

$$\frac{\alpha}{\alpha_\infty} = \frac{T}{T_\infty^{ad} - T_0}, \quad (7)$$

where T_∞^{ad} = 80°C and T_0 = 20°C.

In the upcoming section, we will present a model that predicts the IRH variable, which is the primary cause of autogenous deformations in Portland cement pastes. This model is a function of the degree of hydration developed and validated using the

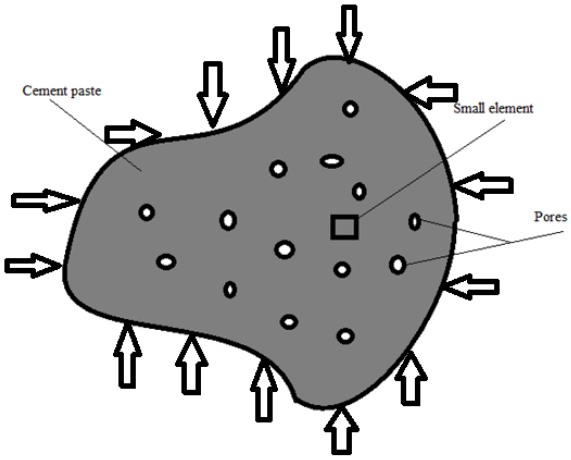

Fig. 1. Cement paste subjected to capillary depression

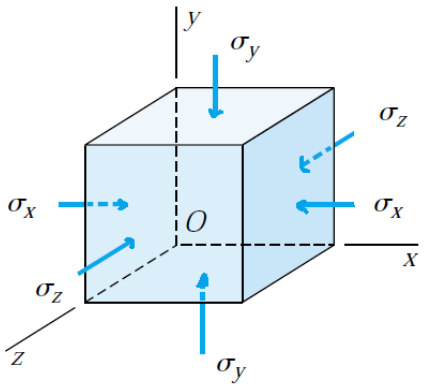

Fig. 2. Element in triaxial stress

data from previous studies. To accomplish this, we connect all variables in Eq. 5 to a single parameter, the degree of hydration (α), which we calculate using the three-parameter model (TPM) (Schindler and Folliard, 2005):

$$\alpha = \alpha_u \exp\left(\left(\frac{\tau}{t_{eq}}\right)^{\beta'}\right), \quad (8)$$

where τ and β' are parameters of the model, α_u is the ultimate degree of hydration and a function of w/c ratio, with the following equations:

$$\alpha_u = \frac{1{,}031\ \mathrm{w/c}}{0{,}194 + \mathrm{w/c}}; \quad (9)$$

$$\tau = 66.78 P_{C_3A}^{-0.154} P_{C_3S}^{-0.401} Blaine^{-0.804} P_{SO_3}^{-0.758}; \quad (10)$$

$$\beta = 181.4 P_{C_3A}^{0.146} P_{C_3S}^{0.227} Blaine^{-0.535} P_{SO_3}^{0.558}, \quad (11)$$

where P is the weight ratio in terms of total cement content.

The equivalent age can be defined as the same level of maturity of cement (mechanical properties and degree of hydration) acquired by specimens of the same composition but under different temperature history. Using the Arrhenius Law, we obtain (Hansen and Pedersen, 1977):

$$t_{eq} = \int_0^t \exp\left(-\frac{E_a}{R}\left(\frac{1}{T(\tau)} - \frac{1}{T_{ref}}\right)\right) d\tau, \quad (12)$$

where E_a is the activation energy, $T(\tau)$ is the temperature history, and T_{ref} is the reference temperature generally equal to 20°C, R is the universal gas constant; the ratio E_a/R = 4000 for $T \geq 20$°C for Portland cement (RILEM TC 119-TCE, 1997).

Modeling of Internal Relative Humidity

From the research of Bentz et al.(2004), we can deduce that the fineness of cement has no significant influence on the IRH–α relation. An IRH reduction is less in the systems with higher w/c ratio, due to low values of capillary depression. This is due to the initially larger spacing between cement particles (larger pore radius) (Bentz and Aïtcin, 2008), and is demonstrated mathematically by the Laplace–Kelvin relation.

As shown in Fig. 3, the variation of IRH with the progression of hydration degree is influenced by the w/c ratio. The evolution of IRH with the degree of hydration exhibits a critical point where a decrease begins; we call it the critical degree of hydration (α_{cr}).

The critical degree of hydration (α_{cr}) corresponds to the maximum value of the degree of hydration at which the decrease of IRH begins. It varies linearly between different ratios, as shown in Fig. 4, and can be determined through experimental tests.

In Fig. 5, we observe a simplified representation of the variation of IRH with the ratio *f*, where *f* (abscissa) is divided into two parts – negative and positive. The first part corresponds to the initial stages of hydration when the cement matrix is in a saturated state, while the second part exhibits an almost linear decrease in IRH with the degree of hydration, indicating the consummation of combined water with the progression of hydration reactions. To predict the IRH variation with *f*, we employ the classical analysis of decline curves (Arps, 1945).

The loss ratios are represented by an arithmetic series (Fig. 6), where the difference between successive loss ratios is the hyperbolic exponent *n*, which is approximately constant. Using this information, we can establish the following differential equation:

$$\frac{d\left(\frac{\mathrm{IRH}}{d(\mathrm{IRH})/df}\right)}{df} = -n. \quad (13)$$

Integration of Eq. 13 gives:

$$\frac{\mathrm{IRH}}{d(\mathrm{IRH})/df} = -nf - a_0. \quad (14)$$

The constant loss ratio at f = 0 is denoted by a_0. We can simplify the above equation as follows:

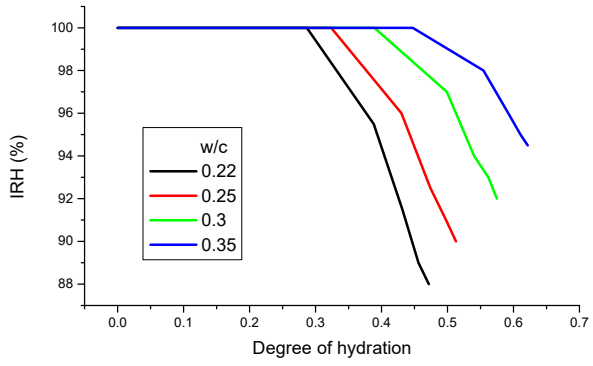

Fig. 3. Relation between IRH and degree of hydration (experimental data from Wyrzykowski and Lura (2013))

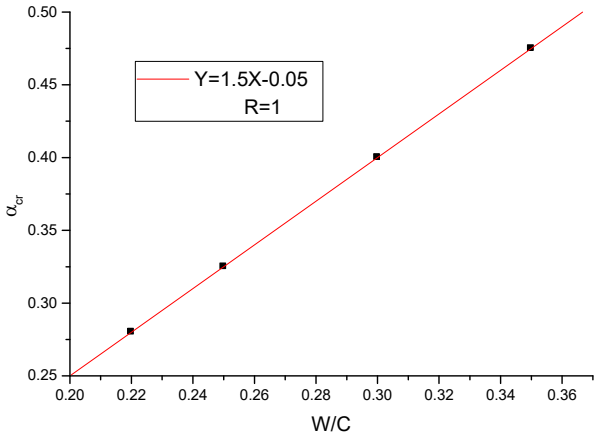

Fig. 4. Variation of the critical degree of hydration with w/c ratio

$$\frac{d(\mathrm{IRH})}{\mathrm{IRH}} = -\frac{df}{a_0 + nf}. \quad (15)$$

To eliminate the constants of integration from the previous second-order differential equation, we assume that IRH is equal to IRH_0, which is 100% for f = 0. This results in the following relationship between IRH and f:

$$\mathrm{IRH} = \mathrm{IRH}_0 \left(1 + \frac{nf}{a_0}\right)^{-1/n}. \quad (16)$$

We pose: $\frac{n}{a_0} = -k$.

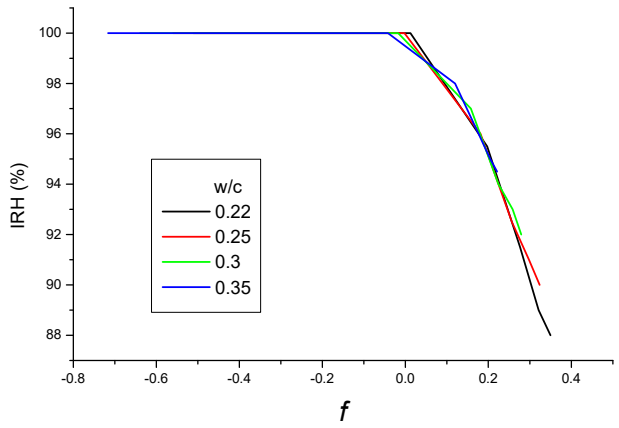

Fig. 5. Evolution of IRH with f ($f = \frac{\alpha - \alpha_{cr}}{\alpha_u}$)

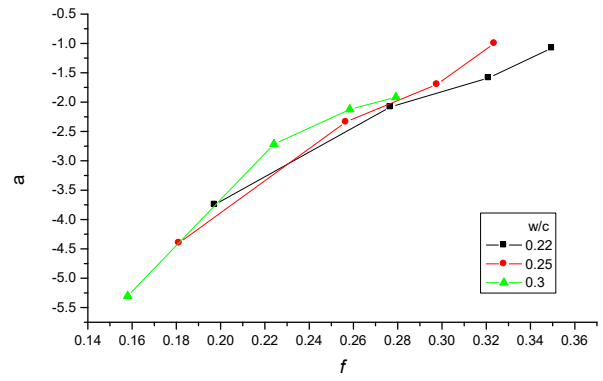

Fig. 6. Variation of the loss ratios $a = \frac{\mathrm{IRH}}{\frac{\Delta(\mathrm{IRH})}{\Delta f}}$ with f

The equation to predict the variation of IRH with α can be expressed as follows:

$$\mathrm{IRH} = \begin{cases} 100\ \% & \text{when } \alpha \le \alpha_{cr} \\ \mathrm{IRH}_0 \left(1 - k\left(\frac{\alpha - \alpha_{cr}}{\alpha_u}\right)\right)^{-n^{-1}} & \text{when } \alpha \ge \alpha_{cr} \end{cases}, \quad (17)$$

where n and k are parameters of the model that can be determined with regression from experiments as a function of w/c ratio and cement composition (C_3S and C_3A contribute most to heat release at early ages).

Validation

The free method for measuring autogenous shrinkage of cement pastes involves the preparation of unrestrained specimens, typically prismatic or cylindrical in shape. These specimens are allowed to undergo natural shrinkage without any external restraints, and their dimensional changes over time are measured. Various techniques such as linear displacement sensors, dilatometers, or image analysis can be employed to accurately monitor the specimen's length or volume. By analyzing the collected data, the autogenous shrinkage behavior of cement paste can be evaluated, providing insights into the material's intrinsic characteristics. The free shrinkage method offers a direct measurement of the unrestrained behavior of cement pastes, allowing for a better understanding of their volume changes and potential cracking risks.

To validate the proposed IRH model, we used the calculated degree of hydration values (obtained using Eq. 8) of the cements reported in literature (Huangand Ye, 2016; Kumarappa et al., 2018; Lu et al., 2020; Wei et al., 2015; Wyrzykowski and Lura, 2013). Subsequently, we used the last proposed method to calculate autogenous shrinkage for the experiments conducted in the work of Song et al. (2020). Table 1 presents the parameters of the proposed IRH model for various cement pastes.

Fig. 7 depicts the predicted values of the proposed IRH model with an overlay on experimental data from

Table 1. **Values of the IRH model parameters**

References	w/c	α_{cr}	α_u	$-K$	$-n$
Wyrzykowski and Lura, 2013	0.22	0.28	0.5479	1.997	8.938
	0.25	0.325	0.5805	2.13	10.65
	0.3	0.4	0.626	2.696	16.85
	0.35	0.475	0.663	6.14	18.49
Huang and Ye, 2016	0.25	0.31	0.5805	2.41	9.44
Lu et al., 2020	0.3	0.38	0.626	2.47	10.7
	0.4	0.52	0.69427	1.95	9.92
Huang and Ye, 2016	0.25	0.1	0.5805	1.19	12.63
Wei et al., 2015	0.3	0.2	0.626	1.495	15.8
Wyrzykowski and Lura, 2013	0.35	0.3	0.663	1.986	34.35
Kumarappa et al., 2018	0.4	0.4	0.694	2.68	63.395

literature (Huang and Ye, 2016; Lu et al., 2020). The results show a strong agreement between the model predictions and the experimental tests, indicating the effectiveness of the proposed model in predicting the variation of IRH with α. This validates the use of the model for further analysis and predictions in similar experiments.

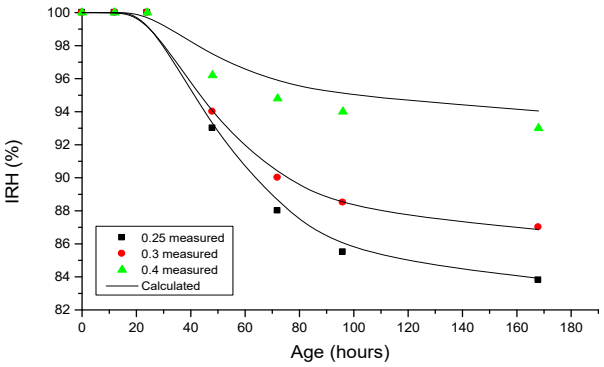

Fig. 7. Measured and calculated IRH (experimental data from Huang and Ye (2016), Lu et al. (2020))

In Figs. 8 to 11, we present the validation results of our proposed model using data from previous studies (Huang and Ye, 2016; Kumarappa et al., 2018; Wei et al., 2015; Wyrzykowski and Lura, 2013). Additionally, we compare the performance of our model with that of two other models in literature, namely the Song model (Song et al., 2020) and the Shen model (Shen et al., 2018).

Upon examining the figures (Figs. 8–11), it is evident that the proposed model exhibits an excellent agreement with the measured data, thus establishing its reliability in predicting the behavior of IRH. Moreover, a comparative analysis with two other models (Song (Song et al., 2020) and Shen (Shen et al., 2018)) demonstrated that the proposed model's performance was comparable to these existing models. This validation process offers robust evidence of the accuracy of the proposed model in predicting IRH.

For the 11 mixtures (Table 1) found in literature, we suggest the following equations of the parameters of the proposed IRH model:

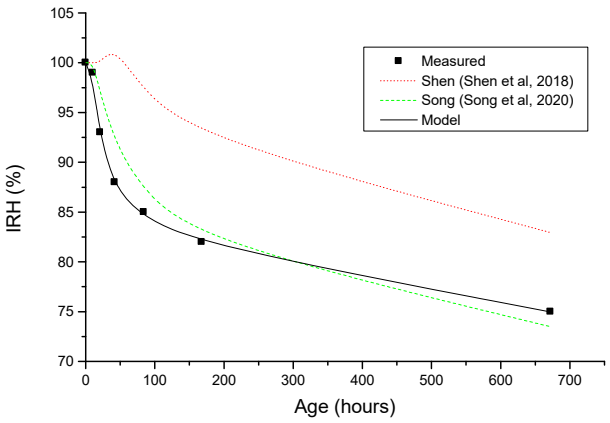

Fig. 8. Measured and calculated IRH for w/c = 0.25 (experimental data from Huang and Ye (2016))

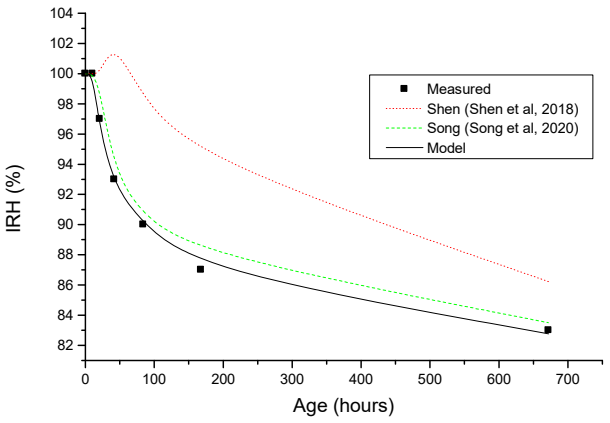

Fig. 9. Measured and calculated IRH for w/c = 0.3 (experimental data from Wei et al. (2015))

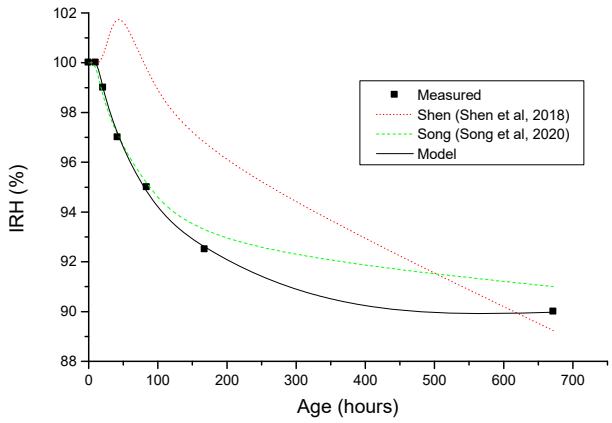

Fig. 10. Measured and calculated IRH for w/c = 0.35 (experimental data fromWyrzykowski and Lura (2013))

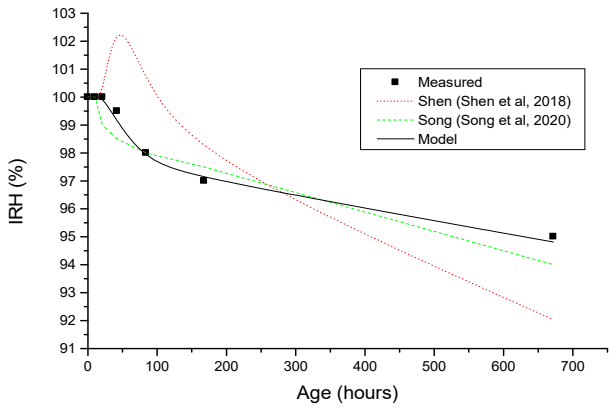

Fig. 11. Measured and calculated IRH for w/c = 0.4 (experimental data fromKumarappa et al. (2018))

$$k = \frac{1.02 - 2.663\left(\frac{E}{C}\right)}{1 - 4.52\left(\frac{E}{C}\right) + 4.94\left(\frac{E}{C}\right)^2}; \quad (18)$$

$$n = 8.05P_{C_3S} - 36.24P_{C_3A} - $$
$$-190.27(\ln\left(\frac{E}{C}\right)) + 5.81\left(P_{C_3S}\right)\ln\left(\frac{E}{C}\right) -$$
$$-25.92(P_{C_3A})\left(\ln\left(\frac{E}{C}\right)\right) - 250.37. \quad (19)$$

The observed small *p*-values (0.01) indicate significant relationships between the independent variables and the IRH parameters. The F-test shows improved prediction accuracy with each additional variable.

The following tables (Tables 2–5) present the calculated values of IRH and autogenous shrinkage along with their corresponding parameters. The results are then compared to the experimental data from Song et al. (2020).

Upon examining the tables (Tables 2–5), we can conclude that the autogenous shrinkage values obtained from the proposed model are in very good agreement with the experimental results from Song et al. (2020). Additionally, the calculated values of capillary depression are consistent with the values reported in literature (Lu et al., 2020; Song et al., 2020).

Discussion

The proposed model for predicting the internal relative humidity (IRH) and autogenous shrinkage of Portland cement pastes was validated using the data from previous studies. The model is based on the degree of hydration of the cement paste and takes into account the water-to-cement ratio (w/c) and the critical degree of hydration (α_{cr}) at which IRH starts to decrease. The validation results show that the proposed model fits very well with the experimental data and is comparable with other models in literature. The calculated values of autogenous shrinkage and capillary depression are also close to the experiments and literature values, respectively.

Table 2. **The case of w/c = 0.25**

Age (h)	α	IRH (calculated)	*E* (GPa)	ν (Stefan et al., 2010)	*T* (K)	σ (MPa) (calculated)	ε (μm/m) (calculated)	ε (μm/m) (measured)
0	0	100	0	0.4	273.15	0	0	0
10.5	0.25	98	19	0.235	293.12	2.73	73	100
21	0.39	93	26	0.225	304.41	10.19	202	200
42	0.48	88	29	0.225	311.73	18.39	330	300
84	0.53	85	30	0.22	315.72	23.67	415	400

Table 3. **The case of w/c = 0.3**

Age (h)	α	IRH (calculated)	*E* (GPa)	ν (Stefan et al., 2010)	*T* (K)	σ (MPa) (calculated)	ε (μm/m) (calculated)	ε (μm/m) (measured)
0	0	100	0	0.4	273.15	0	0	0
10.5	0.2	99.93	13	0.265	289.15	0.13	3	75
21	0.4	96	23	0.235	305.15	5.75	133	150
42	0.51	93	26	0.23	313.95	10.51	217	230
84	0.55	90	27	0.225	317.15	15.42	313	300

Table 4. **The case of w/c = 0.35**

Age (h)	α	IRH (calculated)	*E* (GPa)	ν (Stefan et al., 2010)	*T* (K)	σ (MPa) (calculated)	ε (μm/m) (calculated)	ε (μm/m) (measured)
0	0	100	0	0.4	273.15	0	0	0
10.5	0.2	100	7	0.28	289.15	0.09	6	5
21	0.4	99	14	0.25	305.15	1.41	50	75
42	0.51	97	16	0.24	313.95	4.41	140	150
84	0.58	95	18	0.234	319.55	7.56	229	230

Table 5. **The case of w/c = 0.4**

Age (h)	α	IRH (calculated)	*E* (GPa)	ν (Stefan et al., 2010)	*T* (K)	σ (MPa) (calculated)	ε (μm/m) (calculated)	ε (μm/m) (measured)
0	0	100	0	0.4	273.15	0	0	0
10.5	0.27	100	6	0.33	294.37	0.002	11	25
21	0.43	99.5	10	0.275	307.47	0.71	45	60
42	0.55	99	12	0.25	316.80	1.47	88	90
84	0.62	98	13	0.24	322.38	3.01	159	150

Conclusion

In conclusion, this study proposes a model for predicting the variation of internal relative humidity (IRH) with the progression of hydration in cement pastes. The proposed model was validated using the data from previous studies and showed good agreement with the experimental results.

Moreover, the study shows that there is a direct relationship between the decrease in IRH and the increase in autogenous shrinkage. This finding is important for the design of concrete structures, as it highlights the importance of controlling internal humidity in order to avoid excessive autogenous shrinkage.

The proposed IRH model can predict the decrease of IRH at both early and late ages, and it can be used to calculate the capillary depression and the meniscus radius using Laplace–Kelvin equation. Additionally, the proposed method of calculating autogenous shrinkage at early ages gives significant results, and the calculated values are close to the experimental data.

In summary, this study provides a comprehensive understanding of the relationship between IRH and autogenous shrinkage in cement pastes, and offers a practical model for predicting IRH and autogenous shrinkage at early and late ages. These findings are useful for the design and maintenance of concrete structures.

Reference

Arps, J. J. (1945). Analysis of decline curves. *Transactions of the AIME*, Vol. 160, Issue 01, pp. 228–247. DOI: 10.2118/945228-G.

Bažant, Z. P. and Prasannan, S. (1989). Solidification theory for concrete creep. I: Formulation. *Journal of Engineering Mechanics*, Vol. 115, Issue 8, pp. 1691–1703.

Bentz, D. P. and Aïtcin, P.-C. (2008). The hidden meaning of water-to-cement ratio. *Concrete International*, Vol. 30, No. 5, pp. 51–54.

Bentz, D. P., Garboczi, E. J., Jennings, H. M., and Quenard, D. A. (1994). Multi-scale digital-image-based modelling of cement-based materials. *MRS Online Proceedings Library*, Vol. 370, pp. 33–41. DOI: 10.1557/PROC-370-33.

Bentz, D. P., Jensen, O. M., Hansen, K. K., Oleson, J. F., Stang, H., and Haecker, C.J. (2004). Influence of cement particle size distribution on early age autogenous strains and stresses in cement-based materials. *Journal of the American Ceramic Society*, Vol. 84, Issue 1, pp. 129–135. DOI: 10.1111/j.1151-2916.2001.tb00619.x.

Cervera, M., Oliver, J., and Prato, T. (1999). A thermo-chemo-mechanical model for concrete. I: Hydration and aging. *Journal of Engineering Mechanics*, Vol. 125, Issue 9, pp.1018–1027. DOI: 10.1061/(ASCE)0733-9399(1999)125:9(1018).

Davis, H. E. (1940). Autogenous volume changes of concrete. *Proceedings of ASTM*, Vol. 40, pp. 1103–1110.

Eguchi, K. and Teranishi, K. (2005). Prediction equation of drying shrinkage of concrete based on composite model. *Cement and Concrete Research*, Vol. 35, Issue 3, pp. 483–493. DOI: 10.1016/j.cemconres.2004.08.002.

Ferdinand P. Beer, E. Russel Johnson, Jr. John T. DeWolf, David F. Mazurek. (2012) Mechanics of materials. 6th edition. McGraw-Hill, 758 p.

Haecker, C.-J., Garboczi, E. J., Bullard, J. W., Bohn, R. B., Sun, Z., Shah, S. P., and Voigt, T. (2005). Modeling the linear elastic properties of Portland cement paste. *Cement and Concrete Research*, Vol. 35, Issue 10, pp. 1948–1960. DOI: 10.1016/j.cemconres.2005.05.001.

Hansen, P. F. and Pedersen, E. J. (1977). Maturity computer for controlled curing and hardening of concrete. *Nordisk Betong*, Issue 1, pp. 21–25.

Hua, C., Acker, P., and Ehrlacher, A. (1995). Analyses and models of the autogenous shrinkage of hardening cement paste: I. Modelling at macroscopic scale. *Cement and Concrete Research*, Vol. 25, Issue 7, pp. 1457–1468. DOI: 10.1016/0008-8846(95)00140-8.

Hua, C., Ehrlacher, A., and Acker, P. (1997). Analyses and models of the autogenous shrinkage of hardening cement paste II. Modelling at scale of hydrating grains. *Cement and Concrete Research*, Vol. 27, Issue 2, pp. 245–258. DOI: 10.1016/S0008-8846(96)00202-5.

Huang, H. and Ye, G. (2016). Use of rice husk ash for mitigating the autogenous shrinkage of cement pastes at low water cement ratio. *4th International Symposium on Ultra-High-Performance Concrete and High-Performance Construction Materials, Kassel, Germany, March 09–11, 2016*.

Koenders, E. A. B. and van Breugel, K. (1997). Numerical modelling of autogenous shrinkage of hardening cement paste. *Cement and Concrete Research*, Vol. 27, Issue 10, pp. 1489–1499. DOI: 10.1016/S0008-8846(97)00170-1.

Kumarappa, D. B., Peethamparan, S., and Ngami, M. (2018). Autogenous shrinkage of alkali activated slag mortars: Basic mechanisms and mitigation methods. *Cement and Concrete Research*, Vol. 109, pp. 1–9. DOI: 10.1016/j.cemconres.2018.04.004.

Lu, T., Li, Z., and van Breugel, K. (2020). Modelling of autogenous shrinkage of hardening cement paste. *Construction and Building Materials*, Vol. 264, 120708. DOI: 10.1016/j.conbuildmat.2020.120708.

Lura, P., Jensen, O. M. and van Breugel, K. (2003). Autogenous shrinkage in high-performance cement paste: an evaluation of basic mechanisms. *Cement and Concrete Research*, Vol. 33, Issue 2, pp. 223–232. DOI: 10.1016/S0008-8846(02)00890-6.

Mabrouk, R., Ishida, T., and Maekawa, K. (2004). A unified solidification model of hardening concrete composite for predicting the young age behavior of concrete. *Cement and Concrete Composites*, Vol. 26, Issue 5, pp. 453–461. DOI: 10.1016/S0958-9465(03)00073-8.

Mounanga, P. (2003).*Étude expérimentale du comportement de pâtes de ciment au très jeune âge : hydratation, retraits, propriétés thermophysiques*.PhD Thesis in Civil Engineering, University of Nantes.

Neubauer, C. M., Jennings, H. M., and Garboczi, E. J. (1996). A three-phase model of the elastic and shrinkage properties of mortar. *Advanced Cement Based Materials*, Vol. 4, Issue 1, pp. 6–20. DOI: 10.1016/S1065-7355(96)90058-9.

Paulini, P. (1994). A through solution model for volume changes of cement hydration. *Cement and Concrete Research*, Vol. 24, Issue 3, pp. 488–496. DOI: 10.1016/0008-8846(94)90137-6.

RILEM TC 119-TCE (1997). Recommendations of TC 119-TCE: Avoidance of thermal cracking in concrete at early ages. *Materials and Structures*, Vol. 30, Issue 202, pp. 451–464.

Schindler, A. and Folliard, K. (2005). Heat of hydration models for cementitious materials. *ACI Materials Journal*, Vol. 102, Issue 1, pp. 24–33. DOI: 10.14359/14246.

Shen, D., Zhou, B., Wang, M., Chen, Y., and Jiang, G. (2018). Predicting relative humidity of early-age concrete under sealed and unsealed conditions. *Magazine of Concrete Research*, 1800068. DOI: 10.1680/jmacr.18.00068.

Shimomura, T. and Maekawa, T. (1997). Analysis of the drying shrinkage behavior of concrete using a micromechanical model based on the micropore structure of concrete. *Magazine of Concrete Research*, Vol. 49, Issue 181, pp. 303–322. DOI: 10.1680/macr.1997.49.181.303.

Song, C., Hong, G., and Choi, S. (2020). Modeling autogenous shrinkage of hydrating cement paste by estimating the meniscus radius. *Construction and Building Materials*, Vol. 257, 119521. DOI: 10.1016/j.conbuildmat.2020.119521.

Stefan, L., Benboudjema, F., Torrenti, J.-M., and Bissonnette, B. (2010). Prediction of elastic properties of cement pastes at early ages. *Computational Materials Science*, Vol. 47, Issue 3, pp. 775–784. DOI: 10.1016/j.commatsci.2009.11.003.

Xi, Y. and Jennings, H. M. (1997). Shrinkage of cement paste and concrete modelled by a multiscale effective homogeneous theory. *Materials and Structures*, Vol. 30, Issue 6, pp. 329–339. DOI: 10.1007/BF02480683.

Ulm, F.-J., Constantinides, G., and Heukamp, F. H. (2004). Is concrete a poromechanics material? – A multiscale investigation of poroelastic properties. *Materials and Structures*, Vol. 37, Issue 1, pp. 43–58. DOI: 10.1007/BF02481626.

van Breugel, K. (2001). Numerical modelling of volume changes at early ages-Potential, pitfalls and challenges.*Materials and Structures*, Vol. 34, Issue 5, pp. 293–301. DOI: 10.1007/BF02482209.

Wei, Y., Wang, Y., and Gao, X. (2015). Effect of internal curing on moisture gradient distribution and deformation of a concrete pavement slab containing pre-wetted lightweight fine aggregates. *Drying Technology*, Vol. 33, Issue 3, pp. 335–364. DOI: 10.1080/07373937.2014.952740.

Wyrzykowski, M. and Lura, P. (2013). Moisture dependence of thermal expansion in cement-based materials at early ages. *Cement and Concrete Research*, Vol. 53, pp. 25–35. DOI: 10.1016/j.cemconres.2013.05.016.

К ВОПРОСУ ОБ АУТОГЕННОЙ УСАДКЕ ЦЕМЕНТНОГО ТЕСТА

Абдельгафур Саади*, Абдельмалек Брахма

Университет Саад Дахлаб Блида 1, Алжир

*E-mail: Saadi.abdelghafour@yahoo.fr

Аннотация
Введение: Данное исследование посвящено исследованию процессов развития аутогенной усадки цементных паст и представляет новый метод расчета, учитывающий изменения внутренней относительной влажности. Внутренняя относительная влажность существенно влияет на аутогенную усадку, и ее эволюция моделируется на основе кривых снижения. Предложенный метод точно оценивает аутогенную усадку и хорошо согласуется с экспериментальными данными. Кроме того, по уравнению Лапласа-Кельвина были рассчитаны капиллярная депрессия и радиус мениска. **Методы:** Чтобы предотвратить развитие ранней аутогенной усадки строительных материалов, был разработан новый метод расчета, который учитывает изменение внутренней относительной влажности. Проанализированы кривые снижения, использованные для моделирования изменения внутренней относительной влажности, и подтверждена достоверность новой модели на основе анализа эмпирических данных, представленных в других исследованиях. **Результаты:** Новая модель прогнозирования изменения внутренней относительной влажности и аутогенной усадки в портландцементных пастах, основанная на степени гидратации цемента, соотношении воды и цемента (в/ц) и критической степени гидратации (αcr), согласуется с экспериментальными данными и существующими моделями. Это исследование подчеркивает важность контроля внутренней влажности для уменьшения аутогенной усадки в бетонных конструкциях.

Ключевые слова: цементное тесто, аутогенная усадка, внутренняя относительная влажность, прогнозирование, моделирование, кривые снижения.

DOI: 10.23968/2500-0055-2023-8-3-23-31

EVALUATION OF ENERGY-COST-EFFICIENT DESIGN ALTERNATIVES FOR RESIDENTIAL BUILDINGS IN KARNATAKA'S TROPICAL WET AND DRY CLIMATIC ZONES

Darshini Shekhar*, Jagdish Godihal

Presidency University, Bengaluru, Karnataka, India

*Corresponding author's e-mail: darshinis@presidencyuniversity.in

Abstract

Introduction: The existing building construction techniques in India account for increased operating energy consumption. Due to this, there is a need to apply sustainable construction methods by including passive design techniques. In accordance with the local climatic condition, a good passive design not only maintains a comfortable environment in the house, but also consumes less energy all the while performing the same basic functions as the traditional structures. **Purpose of the study:** The present research focuses on residential villas by analyzing parameters such as illuminance, energy, and cost consumption using Revit (Insight 360) software with two different cases. **Methods:** Considering Case 1 as an existing villa of conventional design and Case 2 presenting a proposed villa, a remodeling of the existing villa with an increased window wall ratio (WWR), different fenestration designs, and a new building plan. The authors followed the Indian Green Building Council (IGBC) guidelines relating to illuminance and generated an analytical energy model using Insight 360 to compare the energy consumption and cost efficiency of the cases. **Results:** The effectiveness of various fenestration types related to direct heat gain, window orientation that would provide more natural light, total operating energy consumption and costs of two different cases of villas are investigated in this paper.

Keywords: Energy and cost consumption, Sustainable architecture, Window wall ratio, Fenestration design.

Introduction

Climate-responsive architecture is defined as building design that is responsive to the local climatic condition. Windows, walls, roofs, and doors are examples of building components. Windows are the only transparent parts of a structure that allow natural light to enter the building. Sunlight is more compatible with the human vision compared to all other forms of lighting since it offers a better lighting environment than electrical lighting sources (Kralj et al., 2019). Building occupants spend more than 90% of their time inside the structure. Interaction between the exterior world and the building interior is thus necessary to increase the cognitive performance of building inhabitants (Jamrozik et al., 2019). Daylight is beneficial to one's health, consciousness, productivity, and sense of comfort, and it plays an important part in the construction. An illumination level of 110 to 2200 lux is adequate lighting to be provided to ensure visual comfort for the occupants, thereby reducing strain on the eyes and associated health impacts (IGBC, 2017). The proximity to any obstruction that may shadow the structure, such as nearby buildings and trees, creates the most difficult design and may have an impact on the distribution of light and solar heat gain in structures. Sustainable building design includes the orientation of a building and the placement of its windows, roofs, and other fenestrations at the site (Baruah and Sahoo, 2020).

Autodesk Revit has applications for architects, drafters, mechanical, structural, and MEP engineers and designers. It is an easy-to-follow tool for enhancing a building's life cycle energy and environmental efficiency. Insight 360 visualizes and interacts with critical performance data, benchmarks, variables, ranges, and criteria for whole-building energy, heating, cooling, daylighting, and solar radiation simulations. This software is a dependable market-leading simulation engine that combines cutting-edge parallel cloud computing techniques that simultaneously simulate multiple potential outcomes. Windows, especially external windows, are irreplaceable building components. People want windows primarily for daylight and secondarily for the view. They have the function of linking indoor and outdoor environments, introducing fresh air and providing better daylight through transparency and openness. It has been reported that energy loss through external windows amounts to 57–63% of total building energy loss (Liu et al., 2019). To reduce such a high energy loss, the application of window shades is essential for fenestration systems to reduce the heating load of buildings as well as daylight discomfort due to glare. Well-arranged window shades could protect the window from excessive solar radiation in summer and allow maximum solar heat gain in winter (Ghosh and Neogi, 2018). A comparison of the performance results of indoor and outdoor

shading devices via Energy Plus software showed that using window shades always improves thermal comfort and affects energy consumption (Atzeri et al., 2014). Window shades could effectively reduce the annual air conditioning energy consumption, and the opening mode of window shades also impacts annual air conditioning energy consumption (Tan et al., 2020). Small window sizes ranging between 10% and 20% WWR with the installation of triple-glazed windows are recommended for residential buildings based on design optimization analysis of an apartment building located in a hot and dry region of India (Chaturvedi et al., 2020). Test results on occupant satisfaction concerning the sense of inner space and visual comfort for different window size results showed that participants tend to perceive good visual comfort when the WWR is within 15–30% (Hong et al., 2019). Window features, such as frame and glass options, area, thermal transmittance value, solar factor, and orientation of windows, need to be selected at an early stage of a building design, as they highly influence the environmental and cost performance of buildings (Souviron et al., 2019).

BIM methodology is a project technique that views information as a key relevant factor throughout the project life cycle (Boton et al., 2015). The digital revolution of the built environment and construction sectors is driven by the BIM approach. The importance of BIM as a strategic component for cost, social, and environmental quality, as well as for establishing growth and competitiveness policies in the sector, is recognized by governments and public advocates throughout Europe and the rest of the world (Hermoso-Orzáez et al., 2019; Tang et al., 2019). The standards for designing sustainable buildings include implementing passive design techniques such as building orientation according to site topography, and good fenestration design for reduced heat gain and glare, while increasing natural illumination (Shekhar and Godihal, 2023). An ideal daylighting solution is consistent with careful consideration of the local climate; several authors have focused on room geometry and orientation as the design's first step (Baker, N. and Steemers, 2002; Nardi et al., 2018). Satisfaction with a daylighting design is a complicated subject that is affected by numerous factors such as facade orientation, obstructions, and window direction. When windows are properly oriented, they allow maximum daylight penetration while reducing the need for external lighting systems and introducing complex shading devices (Freewan et al., 2020). Regarding educational spaces, a study has examined light shelves, upper windows, and reflectors in Jordanian educational buildings. The study results showed that by using light shelves or skylights, electricity consumption was reduced in classrooms by an average of 40–50%, and light shelves or rear windows improved uniformity and illuminance levels considerably (Sedaghatnia et al., 2021).

Investigation on optimizing window design decisions to maximize daylighting while minimizing glare and energy use is done by means of Ladybug and Honeybee, Grasshopper plugins for Rhinoceros software; Energy Plus and Dayism engines allow analyzing daylighting and energy performance. A window with no shading consumes more energy per year than a window with light shelves and louvers. Overall, the best shading systems for any climatic building differ depending on the WWR, orientation, and design initiatives (Xing et al., 2022). 40% WWR in a south-facing building facade in a humid subtropical climate setting provides the best energy performance of electrochromic (EC) smart window glazing among other configurations tested with different WWR and orientation. South-facing windows in a hot climate are the best option for reducing total energy loads while maintaining visibility, natural lighting, and comfort (ISHRAE, 2018–2019). The threshold illuminance level for a living room, bedroom, and kitchen is 300 lux, 100 lux, and 500 lux, respectively, according to the second version of ISHRAE (2018–2019).

Hassan is located in Karnataka's tropical wet and dry climate zones. Throughout the year, Hassan city receives an average of 2718.97 hours of sunlight. The city's lowest and highest temperatures are respectively 20.1 and 25 degrees Celsius (en.climate-data.org, 2019). Appropriate use of building energy-saving strategies has a significant influence on building energy efficiency and the socio-economic growth of our current civilization. As a result, it may save a significant amount of building energy, which would be much appreciated in order to reduce GHG emissions and protect the environment from anthropogenic climate change (Akram et al., 2023). An overview of the literature devoted to the topics on energy scenario, green building and retrofitting, and cases of awarded green buildings in Malaysia revealed that buildings were designed taking climate into account in an effort to use less energy overall. The use of passive structural devices and the integration of advanced technologies are strong building characteristics that have their origins in proactive strategies to address environmental and energy conservation problems as well as consideration of sustainability (Mohd-Rahim et al., 2017). One of the elements that must be taken into account when planning a building is energy-efficient building design models. Buildings can use sunlight as a source of natural light from early in the morning until late at night. Utilizing natural light will lower the amount of energy used by buildings. The level of illumination in the workspace has been determined using quantitative statistical descriptive analysis. The distribution of natural light with the building's orientation towards the east was found to

be greater than with the orientation towards the south (Jamala et al., 2021).

The accompanying investigation and analysis in this paper are based on a case study of a three-bedroom residential corner villa built using traditional construction techniques. The Revit Insight 360 program was used to evaluate the building's lighting performance including its operating energy and cost consumption. Based on the results of the analysis, the paper proposes a framework for the construction of a single-story residential building based on the chosen locality to maximize illuminance and reduce operating power and cost consumption. The study's criteria include the observation of building residents based on daylight illuminance, a survey of nearby building characteristics, setback distance, and the physical attributes of existing buildings. The following objectives directed the study's implementation:

- To find the ideal plan typology for delivering optimized daylighting through the use of sustainable design techniques by changing the building floor plan, window wall ratio (WWR), and fenestration design.
- To give detailed optimal daylight performance, cost-effective and energy-efficient design standards for the hypothetically modeled single-story residential villa.

Methodology

To validate and apply the recommended sustainable design approach, the authors initially chose a real case study of a 3BHK residential villa building. The structure of this paper has the following three sections. Section 1: three-dimensional (3D) modeling of the existing villa using Revit as per the architecture design and building components. Section 2: the existing villa was remodeled to the advanced design by modifying the building plan, increasing the WWR, and introducing different fenestration designs. Section 3: daylight, energy, and cost consumption of the existing building and remodeled building were analyzed and compared under four different contexts using Revit Insight 360. The analysis was performed under clear skies conditions and at 12 p.m. in the month of September, as recommended by the IGBC. The methodology adopted in this study is shown in Fig. 1.

Fenestrations in the building envelope here are referred to as window shading types. In the context of sustainable design, the choice of fenestration design affects the lighting and energy performance of buildings, as well as the economic aspects of sustainability. Fig. 2 depicts several types of fenestration designs examined for the present research.

Results and Discussion

Existing villa (EV): Case 1

The existing villa has a built-up area of 1650 m^2 encircled by two single-story buildings with two elevations facing the main road and the main entrance door towards the west as shown in Fig. 3.

The villa has been constructed maintaining a minimum setback distance of 1.5 feet as per Hassan City Corporation's recommendation. Table 1 presents the given window wall ratio for each side of the Case 1 structure. Three-dimensional modeling of the clay brick structure and type 1 fenestration design was performed using Revit 2020. The villa's floor-to-floor height is 10 feet; sill height of 3 feet, lintel height of 7 feet, and 200 mm RCC roof were input while designing in Revit based on the survey done by the researchers.

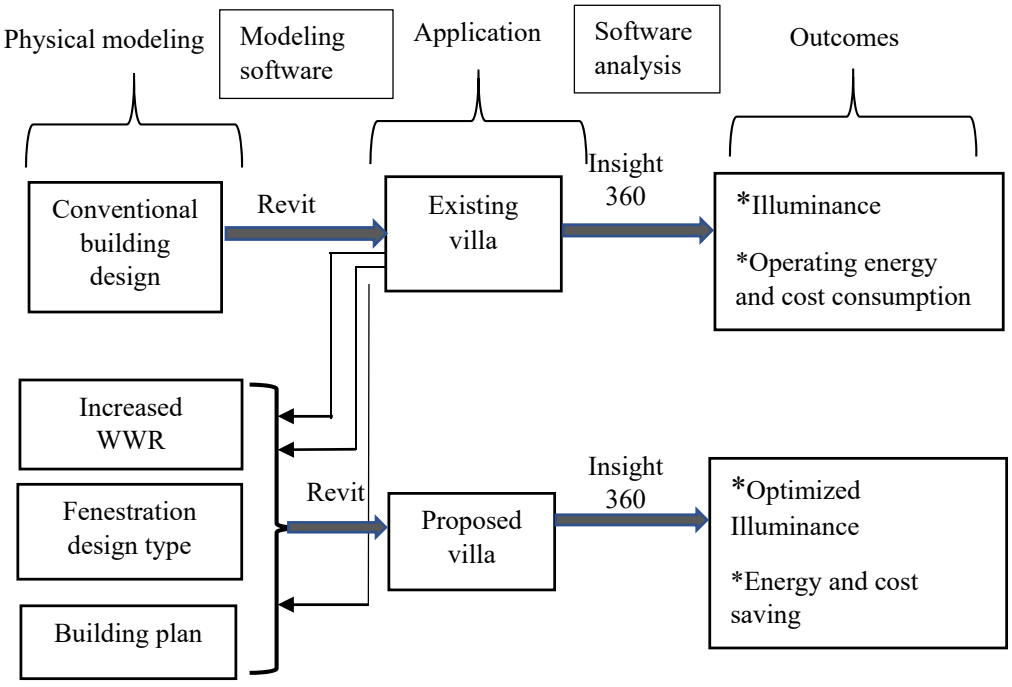

Fig. 1. Methodology adopted for the study

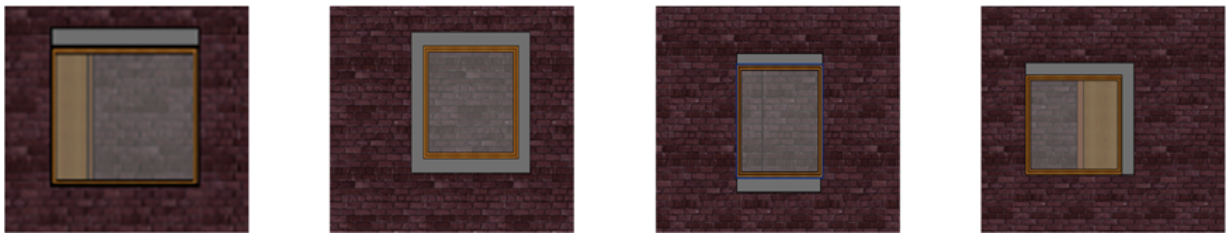

Fig. 2. Fenestration shading types

In the owner-occupied conventional villa, the building envelope includes wall assembly and roof assembly with the values of thermal conductivity and SHGC of glass as shown in Table 2. These building factors control the building energy consumption as a secondary source through heat transfer into the building.

Proposed villa (PV): Case 2

The proposed building design is propounded for the same area of the existing villa while keeping the other design specifications the same. The results are compared in terms of daylight illuminance, operating energy, and cost per square meter per year. Window orientation (WO) and WWR were altered and new fenestration types were introduced in a new villa. Fig. 4 shows a two-dimensional architectural design of a renovated villa with modifications to the building's geometry and window orientation in accordance with Case 1.

The current study suggests a larger WWR for a proposed villa so as to gain more natural daylight and reduce operating energy consumption, and eventually cut the costs. To enable the heat loss via the window to be greater than the heat gain from solar radiation, a mix of different fenestration designs for varying window orientation and dimensions was contemplated while remodeling EV into PV. Under the Case 2 condition, four different contexts with various fenestration types, window orientation, and WWR were considered as indicated in Table 3.

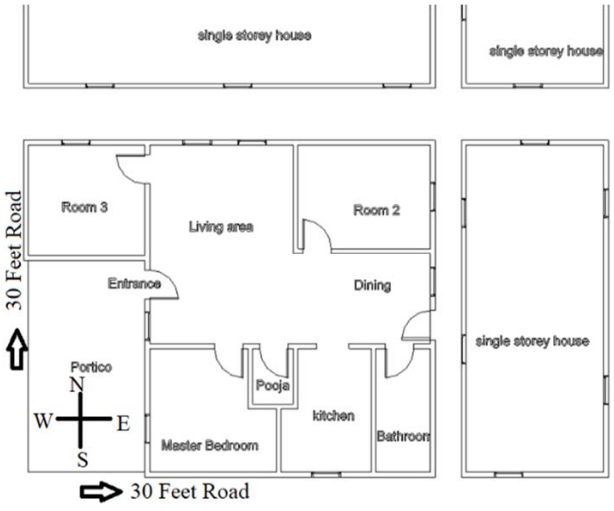

Fig. 3. Existing villa floor plan

Table 1. **Window wall ratio of Case 1**

Window orientation	Window wall ratio
East side	11%
West side	12%
North side	7%
South side	4%
Mean WWR	8.5%

Table 2. **Thermo-physical characteristics of case study building**

Property	***Values***	***Abbreviation***
Location	Hassan 24.9025° N, 67.0729° E	R= Thermal resistivity SHGC= Solar heat gain coefficient U=Thermal conductivity
Clay brick	U=3.543W/m^{2}K, R=0.382m^{2}K/W	
Plane glass	SHGC=0.78	
RCC roof	U=2.61 W/m^{2}K, R=0.282 m^{2}K/W	

Daylight characteristics

Case 1: Illuminance

The luminous flux per unit area in Case 1 was found to be less than the illuminance threshold of 110 lux. The grouping of lux at different parts of the house is shown in Fig. 5. Since the portico is open, it receives up to 800 lux, which is more sunlight than in any other part of the house. A portion of room 2 and the dining area, which are located behind a one-story building, receive up to 2200 lux. It is observable that designing windows in the south is more effective than planning openings in other directions. Fig. 6 depicts the range of illuminance per unit area characteristic of the case study villa. Illuminance evaluation using Insight 360 is done following the steps below:

Case 2: Illuminance

The authors remodeled Case 1 by changing the house floorplan, installing larger windows, and combining four different fenestration types. Thus, the proposed villa would receive illuminance greater than the existing villa ranging from 107 to 2200 lux of total natural light. The luminous flux per unit area (lux) in Case 2 in all four contexts is shown in Figs. 7–10.

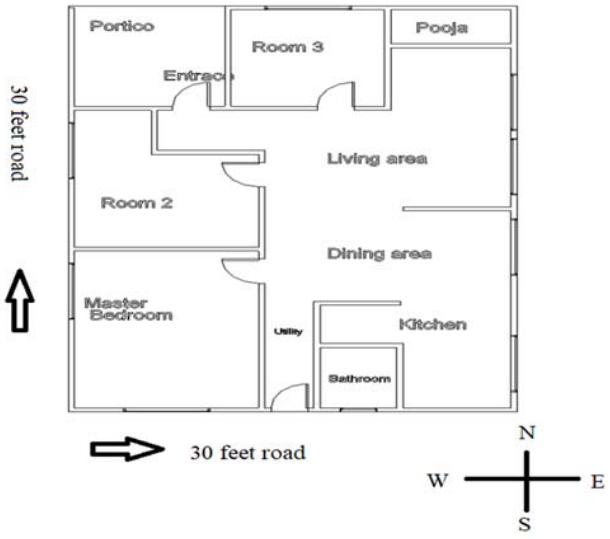

Fig. 4. Proposed villa floor plan

Contexts 3 and 4 provide greater illuminance than Contexts 1 and 2, but they fail to meet the IGBC criteria for visual comfort due to glare. In case of Context 1, about 50% of the modeled area receives up to 2071 lux.

Fenestration type attributes — energy consumption

Aside from maximizing daylight penetration, a good fenestration design is required to reduce the energy demand of buildings by dissipating the direct heat gain and giving glare-free light. Window orientation, WWR, and fenestration design type factors play important roles in limiting the potential heat gain by any structure, hence energy consumption related to fenestration is proportionate to these three factors. Operating energy consumption for a combination of window direction, area, and fenestration design type in Case 2 compared to Case 1 is expressed in Fig. 11.

For all four of the investigated fenestration types and as demonstrated in Table 3 and Fig. 10, energy consumption is considerably lower in the south direction up to 12.5% WWR than in the other three directions. Despite the fact that the WWR is relatively lower, type 2 fenestration is a worse combination for the north side. Larger windows (up to 20%) in the east direction and west-orientated windows with >10% WWR should be installed with type 3 fenestration for the ideal

Table 3. **Details on Case 1 and Case 2**

		Case 1	Case 2 Proposed villa				Case 2 Mean WWR
Direction	**Variants**	**Existing villa**	**Context 1**	**Context 2**	**Context 3**	**Context 4**	
East	Fenestration	Type 1	Type 1	Type 3	Type 2	Type 4	
	WWR (%)	11	13	20	12	10	13.75%
West	Fenestration	Type 1	Type 4	Type 1	Type 3	Type 2	
	WWR (%)	12	9	10	15	16	12.5%
North	Fenestration	Type 1	Type 2	Type 4	Type 1	Type 3	
	WWR (%)	7	11	12	10	13	11.5%
South	Fenestration	Type 1	Type 3	Type 2	Type 4	Type 1	
	WWR (%)	4	12	7	14	18	12.75%
Mean WWR		8.5%	11.25%	12.25%	13.25%	14.25%	

Fig. 5. Existing building illuminance

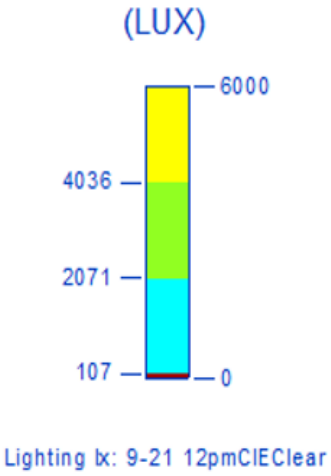

Fig. 6. Lux range

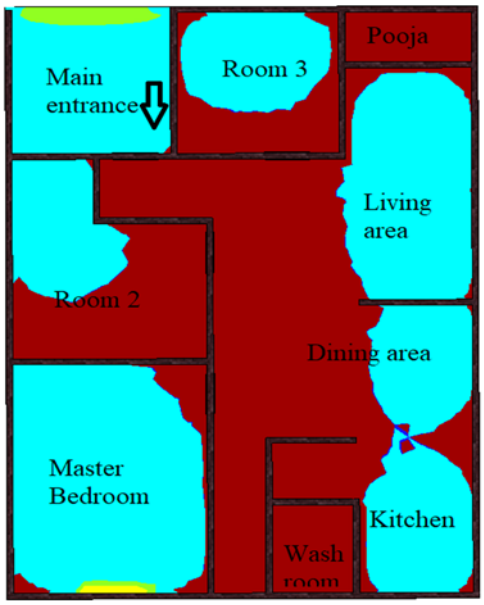

Fig. 7. Case 2 — Context 1

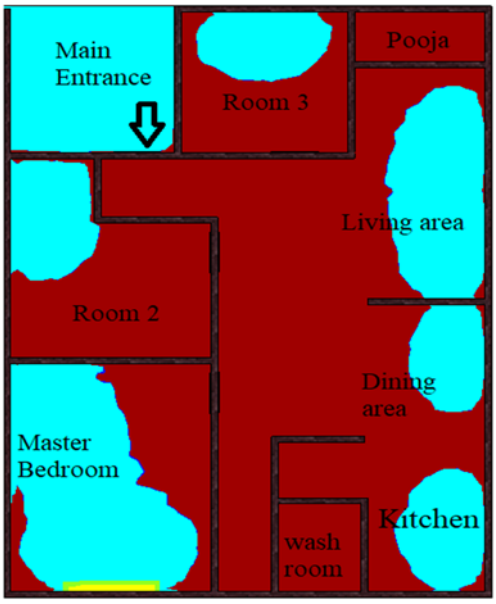

Fig. 8. Case 2 — Context 2

solution of gaining maximum illuminance and reduced heat transfer.

Window orientation attributes — energy demand

As the WWR increases from Case 1 to Case 2 in different contexts, energy consumption is decreasing as seen in Fig. 12. South-facing windows are the most preferable in terms of saving energy followed by north and east orientation. In the case of west-facing windows, energy demand increases as the heat gain through west windows is considerably higher than in the other three directions. For substantially identical WWR, windows on the north side of the building will use more energy and have high potential of transmitting heat than those in the east. Large south-facing windows are more energy-efficient with respect to daylight, heat, and cooling effect compared to other window orientations.

Behavior of Case 1 and Case 2

A comparison of relative cost and energy consumption between conventional method and sustainable construction technique is presented in Table 4 by taking a building case study. The operating energy cost estimated by Insight 360 is described in terms of cost per unit area per year. The cost and energy accredited to Case 1 and Case 2 imply that adopting the sustainable construction method like the efficient design of a building according to its geographical condition would help in the natural

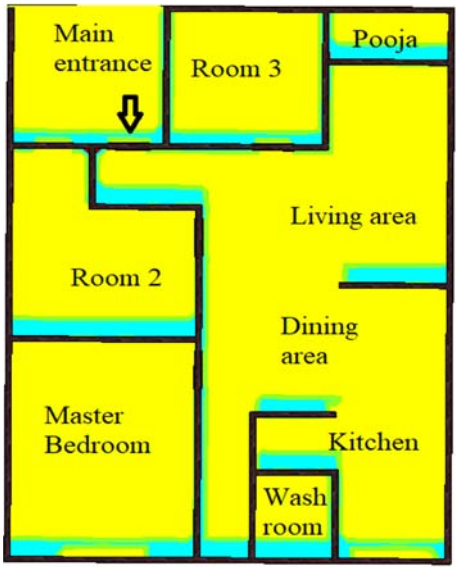

Fig. 9. Case 2 — Context 3

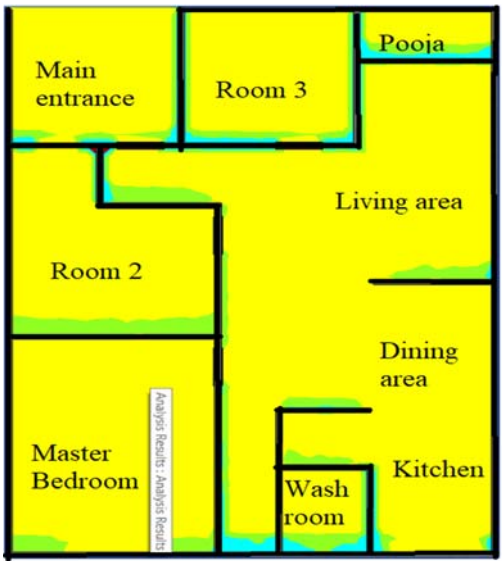

Fig. 10. Case 2 — Context 4

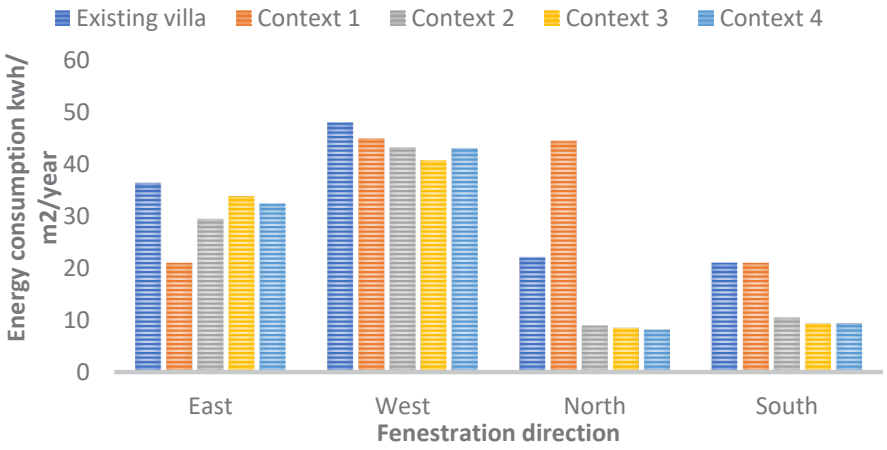

Fig. 11. Energy pattern of EV and PV as for fenestration

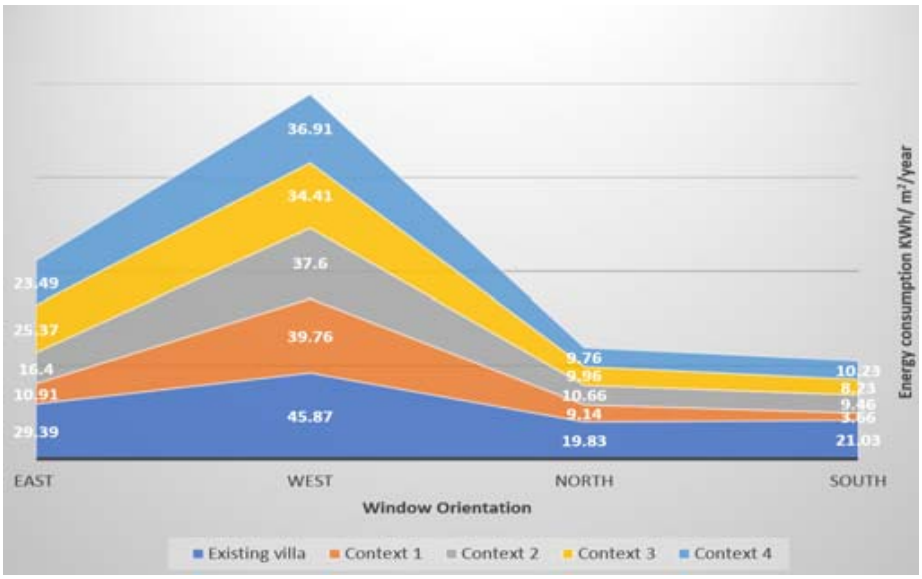

Fig. 12. Energy pattern of EB and NB as for window orientation

energy utilization of the building rather than getting energy using an external source.

Conclusions

Revit and Insight 360 will aid in creating cost-effective and energy-efficient building designs for specific locations and designing energy-efficient structures. The existing villa was designed for 8.5% WWR and is receiving 108 lux of natural light within the building. As the Green Rating for Integrated Habitat Assessment (GRIHA, India) suggests a minimum of 10% WWR provided in building design, the authors propose an increase in WWR, which increased the intensity of light in a range of 108–2200 lux in the majority of the residential area. Context 1 of the proposed villa design has optimal daylight illuminance ranging within 108–800 lux and approximately 10% energy saving is achieved thanks to the increased WWR and unique shade type. Type 3 fenestration is revealed to be a powerful design maximizing illuminance, which nonetheless requires additional adaptation to satisfy subjective criterion of visual comfort of the occupants. A switch to south-facing windows is also a beneficial solution to counter heat gain.

Table 4. **Comparison of energy consumption for EV and PV**

Building variants	Study contexts	Cost INR/m²/year	Energy KWh/m²/year
Case 1	Existing villa	1653	293
Case 2	Context 1	1479	258
	Context 2	1510	265
	Context 3	1520	270
	Context 4	1542	267

References

Akram, M. W., Hasannuzaman, M., Cuce, E., and Cuce, P. M. (2023). Global technological advancement and challenges of glazed wi

ndow, facade system and vertical greenery-based energy savings in buildings: A comprehensive review. *Energy and Built Environment*, Vol. 4, Issue 2, pp. 206–226. DOI: 10.1016/j.enbenv.2021.11.003.

Atzeri, A., Cappelletti, F., and Gasparella, A. (2014). Internal versus external shading devices performance in office buildings. *Energy Procedia*, Vol. 45, pp. 463–472. DOI: 10.1016/j.egypro.2014.01.050.

Baker, N. and Steemers, K. (2002). *Daylight design of buildings: A handbook for architects and engineers*. London: Routledge, 260 p.

Baruah, A. and Sahoo, S. (2020). Energy efficiency performance analysis of a residential building for the effects of building orientations, types of roof surfaces, walls and fenestrations at different locations in the Himalayan terrain of India. *AIP Conference Proceedings*, Vol. 2273, Issue 1, 050061). DOI: 10.1063/5.0024245.

Boton, C., Kubicki, S., and Halin, G. (2015). The challenge of level of development in 4D/BIM simulation across AEC project lifecyle. A case study. *Procedia Engineering*, Vol. 123, pp. 59–67. DOI: 10.1016/j.proeng.2015.10.058.

Chaturvedi, S., Rajasekar, E., and Natarajan, S. (2020). Multi-objective building design optimization under operational uncertainties using the NSGA II algorithm. *Buildings*, Vol. 10, Issue 5, 88. DOI: 10.3390/buildings10050088.

en.climate-data.org (2019). *Climate data for cities worldwide*. [online] Available at: https://en.climate-data.org/ [Date accessed September,9,2023].

Freewan, A. A. Y. and Al Dalala, J. A. (2020). Assessment of daylight performance of advanced daylighting strategies in large university classrooms; case study classrooms at JUST. *Alexandria Engineering Journal*, Vol. 59, Issue 2, pp. 791–802. DOI: 10.1016/j.aej.2019.12.049.

Ghosh, A., and Neogi, S. (2018). Effect of fenestration geometrical factors on building energy consumption and performance evaluation of a new external solar shading device in warm and humid climatic condition. *Solar Energy*, Vol. 169, pp. 94–104. DOI: 10.1016/j.solener.2018.04.025.

Hermoso-Orzáez, M. J., Lozano-Miralles, J. A., Lopez-Garcia, R., and Brito, P. (2019). Environmental criteria for assessing the competitiveness of public tenders with the replacement of large-scale LEDs in the outdoor lighting of cities as a key element for sustainable development: case study applied with Promethee methodology. *Sustainability*, Vol. 11, Issue 21, 5982. DOI: 10.3390/su11215982.

Hong, T., Lee, M., Yeom, S., and Jeong, K. (2019). Occupant responses on satisfaction with window size in physical and virtual built environments. *Building and Environment*, Vol. 166,106409. DOI: 10.1016/j.buildenv.2019 106409.

IGBC (2017). *IGBC health and well-being rating for occupants*. [online] Available at: https://igbc.in/assets/html_pdfs/IGBC%20Health%20and%20Well-being%20Rating%20System.pdf [Date accessed September,9,2023].

ISHRAE (2018–2019). *Indoor Environmental Quality Standard*. [online] Available at: https://ishrae.in/Content/Download/ISHRAE_IEQ_Feb_26_2019_public_draft.pdf [Date accessed September,9,2023].

Jamala, N., Rahim, R., Ishak, T., and Shukri, S. M. (2021). The analysis of the illuminance level in the workspace, using natural and artificial lighting in Graha Pena Building in Makassar, Indonesia. *Journal of Design and Built Environment*, Vol. 21 (1), pp. 1–12.

Jamrozik, A., Clements, N., Hasan, S. S., Zhao, J., Zhang, R., Campanella, C., Loftness, V., Porter, P., Ly, S., Wang, S., and Bauer, B. (2019). Access to daylight and view in an office improves cognitive performance and satisfaction and reduces eyestrain: A controlled crossover study. *Building and Environment*, Vol. 165, 106379. DOI: 10.1016/j.buildenv.2019.106379.

Kralj, A., Drev, M., Žnidaršič, M., Černe, B., Hafner, J., and Jelle, B. P. (2019). Investigations of 6-pane glazing: Properties and possibilities. *Energy and Buildings*, Vol. 190, pp. 61–68. DOI: 10.1016/j.enbuild.2019.02.033.

Liu, Z., Liu, Y., He, B.-J., Xu, W., Jin, G., and Zhang, X. (2019). Application and suitability analysis of the key technologies in nearly zero energy buildings in China. *Renewable and Sustainable Energy Reviews*, Vol. 101, pp. 329–345. DOI: 10.1016/j.rser.2018.11.023.

Mohd-Rahim, F. A., Pirotti, A., Keshavarzsaleh, A., Zainon, N., and Zakaria, N. (2017). Green construction project: A critical review of retrofitting awarded green buildings in Malaysia. *Journal of Design and Built Environment*, 2017: Special Issue: Livable Built Environment, pp. 11–26. DOI: 10.22452/jdbe.sp2017no1.2.

Nardi, I., Lucchi, E., de Rubeis, T., and Ambrosini, D. (2018). Quantification of heat energy losses through the building envelope: A state-of-the-art analysis with critical and comprehensive review on infrared thermography. *Building and Environment*, Vol. 146, pp. 190–205. DOI: 10.1016/j.buildenv.2018.09.050.

Sedaghatnia, M., Faizi, M., Khakzand, M., and Sanaieian, H. (2021). Energy and daylight optimization of shading devices, window size, and orientation for educational spaces in Tehran, Iran. *Journal of Architectural Engineering*, Vol. 27, Issue 2, 04021011. DOI: 10.1061/(ASCE)AE.1943-5568.0000466.

Shekhar, D. and Godihal, J. (2023). Sustainability assessment methodology for residential building in urban area — a case study. In: Pal, I. and Shaw, R. (eds.). *Multi-Hazard Vulnerability and Resilience Building: Cross Cutting Issues*, Bangkok, pp. 45–59. DOI: 10.1016/B978-0-323-95682-6.00013-9.

Souviron, J., van Moeseke, G., and Khan, A. Z. (2019). Analysing the environmental impact of windows: a review. *Building and Environment*, Vol. 161, 106268. DOI: 10.1016/j.buildenv.2019.106268.

Tan, Y., Peng, J., Curcija, C., Yin, R., Deng, L., and Chen, Y. (2020). Study on the impact of window shades' physical characteristics and opening modes on air conditioning energy consumption in China. *Energy and Built Environment*, Vol. 1, Issue 3, pp. 254–261. DOI: 10.1016/j.enbenv.2020.03.002.

Tang, S., Shelden, D. R., Eastman, C. M., Pishdad-Bozorgi, P., and Gao, X. (2019). A review of building information modeling (BIM) and the internet of things (IoT) devices integration: Present status and future trends. *Automation in Construction*, Vol. 101, pp. 127–139. DOI: 10.1016/j.autcon.2019.01.020.

Xing, W., Hao, J., Ma, W., Gong, G., Nizami, A.-S., and Song, Y. (2022). Energy performance of buildings using electrochromic smart windows with different window-wall ratios. *Journal of Green Building*, Vol. 17, Issue 1, pp. 3–20. DOI: 10.3992/jgb.17.1.3.

ОЦЕНКА ЭНЕРГЕТИЧЕСКОЙ И ЭКОНОМИЧЕСКОЙ ЭФФЕКТИВНОСТИ АЛЬТЕРНАТИВНЫХ ДИЗАЙНОВ ЖИЛЫХ ЗДАНИЙ В ТРОПИЧЕСКИХ ВЛАЖНЫХ И СУХИХ КЛИМАТИЧЕСКИХ ЗОНАХ ШТАТА КАРНАТАКА

Даршини Шекхар[1]*, Джагдиш Годихал[2]

Президентский университет, Бангалор, Карнатака, Индия

*E-mail: darshinis@presidencyuniversity.in

Аннотация
Введение: Существующие технологии строительства зданий в Индии приводят к увеличению энергопотребления. Это вызывает необходимость применения методов устойчивого строительства, в том числе пассивных методов проектирования. Соответствуя местным климатическим условиям, хорошая пассивная конструкция не только поддерживает комфортную среду в доме, но и потребляет меньше энергии, при этом выполняя те же основные функции, что и традиционные конструкции. **Цель исследования:** Данная работа посвящена исследованию жилых вилл путем анализа таких параметров, как освещенность, энергопотребление, экономическая эффективность с использованием программного обеспечения Revit (Insight 360) на примере двух кейсов. **Методы:** Кейс 1 представляет собой реально существующую виллу традиционного дизайна, а Кейс 2 предлагает модель реконструкции существующей виллы с увеличенным соотношением площади окон к площади стен, различными конструкциями окон и новым планом здания. Авторы следовали рекомендациям по освещенности Индийского совета по экологическому строительству (IGBC) и создали аналитическую энергетическую модель с помощью Insight 360 для сравнения энергопотребления и экономической эффективности кейсов. **Результаты:** В этой статье исследуется эффективность различных типов окон, связанная с прямым притоком тепла, ориентацией окон, обеспечивающей больше естественного освещения, общим эксплуатационным потреблением энергии и затратами в двух разных случаях вилл.

Ключевые слова: энергопотребление и затраты, устойчивая архитектура, соотношение площади окон к площади стен, проектирование окон.

DOI: 10.23968/2500-0055-2023-8-3-32-44

STUDY ON WATER LEAKAGE DETECTION AND TREATMENT IN METRO STATION STRUCTURES

Qiaofeng Shen*[1], Chen Shen[1], Xun Liu[1], Wuxiang Sun[1], Luning Shi[2], Ting Chen[2]

[1]Beijing Subway Construction Facilities Maintenance Co., Ltd, Beijing, China

[2]Zhongke Jiantong Engineering Technology Co., Ltd, Beijing, China

*Corresponding author's e-mail: 18813094515@163.com

Abstract

Introduction: Considering the condition of water leakage at metro stations and the availability of various leakage detection methods, studying combination detection methods suitable for various working conditions can serve as the basis for leakage treatment. **Purpose of the study:** We aimed to use a number of leakage detection methods that can complement and verify each other in terms of accuracy and depth of detection, improve the identification of defects, and ensure precise grouting. **Methods:** In the course of the study, model tests and field application of detection methods were used. **Results:** Using an infrared detector and a water leakage detection instrument, it is possible to identify leakage points on the surface of both the non-decorative layer and the wet-sticking decorative layer more accurately. By combining a ground penetrating radar and an ultrasonic cross-section scanner, it is possible to better identify internal structural defects within both the non-decorative layer and the wet-sticking decorative layer. If the decorative layer is not dismantled, an air-coupled radar based on an industrial endoscope and a specially developed camera system can effectively detect the leakage path in concrete as well as surface leakage points.

Keywords: subway, station design, water leakage, comprehensive inspection, grouting repair.

Introduction

The increased groundwater level, combined with more precipitation during flood and rainy seasons, and the issue of waterproof failure in older metro structures lead to more severe cases of water leakage. According to the statistical analysis of data ion water leakage at 19 underground line structures in Beijing in recent five years, the structural leakage shows an upward trend. The number has grown from 2,226 in 2017 to 3,505 in 2021, which is a 57.5% increase. The leakage point statistics are shown in Fig. 1.

The existing water leakage remedial effect is generally poor. The main reason is that the location of the water leakage disease in the concrete structure is not clear before remediation. Blind remediation, which only relies on superficial symptoms, cannot achieve the purpose of treating both the symptoms and root causes of water leakage. As a result, this leads to the recurring issues of "treating water leakage wherever it occurs" and "treating water leakage only for it to occur again after the remediation". This not only requires a significant amount of manpower and resources, but also does not ensure the desired remedial effect. Due to the presence of a decorative floor and the impact of train operation, it becomes challenging to determine the exact location of the leakage point at a metro station. Through systematic investigation and analysis of water leakage defects in existing stations, three specific defects were identified as research objects: groundwater return, water accumulation in straight ladder wells, and side wall leakage. Method for rapid detection of water leakage defects were studied with regard to three complex concrete structures in order to quickly locate water leakage and assess the internal condition of the concrete, thus elucidating the causes of water leakage defects. Based on the main structure and zoning of metro stations, and taking into account functional zoning and decorative layers, five different conditions related to water leakage were identified in three types of concrete structures: leakage from the side walls of dry-hanging decorative layers, leakage from the side walls of non-decorative layers, groundwater return in wet-sticking decorative layers, groundwater return in non-decorative layers, and water accumulation in straight ladder wells.

Gong and Guo (2021) discussed the types and causes of water leakage, the methods and principles of detecting leakage during operation, the concepts and technical measures for preventing water leakage during design and construction, and the meaning and methods of water leakage remediation during construction and operation. Asakura and Kojima (2003) introduced the maintenance methods for tunnels in Japan during operation. Sandrone and Labiouse (2011) addressed the analysis and identification of defects related to highway tunnels in Switzerland. Shi and Li (2015) studied the mechanisms of tunnel defects and

For citations: Shen, Q., Shen, C., Liu, X., Sun, W., Shi, L., Chen, T. (2023). Study on water leakage detection and treatment in metro station structures. Architecture and Engineering, No 3 (8), pp. 32-44. DOI: 10.23968/2500-0055-2023-8-3-32-44.

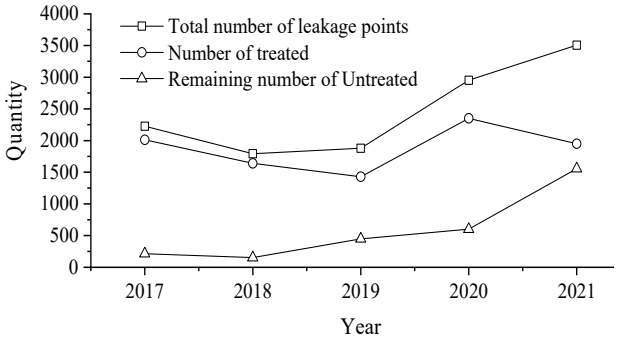

Fig. 1. Statistical chart of structural leakage data

structural deterioration in soft soils. Montero et al. (2015) introduced the use of a robot for tunnel detection. Clark et al. (2003), Ma et al. (2022), and Yu et al. (2016) studied the application of infrared thermography in tunnel leakage detection. Musolino et al. (2007) investigated the feasibility of a diagnostic method for non-destructive testing (NDT) of concrete structures based on ultrasonic wave propagation. Jiang et al. (2020) discussed the application of the impact elastic wave method in detecting areas of low density and voids in concrete. Cheng et al. (2021), Feng et al. (2011), Han et al. (2012), Kashani et al. (2015), and Liu et al. (2009) analyzed the effects of GPR application in detecting tunnel leakage defects. A new method was proposed for underground water leakage detection in tunnels using corrected intensity data and a 3D point cloud of a terrestrial laser scanning (TLS) sensor (Xu et al., 2018). Liu et al. (2012) developed a set of digital image processing algorithms to detect tunnel lining water leakage defects, which include denoising, sharpening, segmentation, and correction. Lam (2006) explained the process of choosing an appropriate laser scanner, calibrating it, acquiring survey data in the field, and using computational algorithms for image registration, fusion, and error analysis. These advancements enable the effective use of point clouds in evaluating the geometric tolerances of tunnel structures during as-built survey.

However, most of the existing detection studies are aimed at concrete structure defects rather than water leakage defects. Most of the existing studies focus on one detection method, and there is no comprehensive application of various detection methods to enhance detection accuracy and efficiency. The current specification (Chinese State Standard, 2010, 2022) for detection methods and conditions for detection objects is somewhat limited, which is not suitable for complex station conditions. There are very few specific or inherent specifications for detecting structural leakage. Therefore, it is necessary to study a detection method for identifying leakage points and leakage paths in metro stations. This will help determine the causes of the leaks, pinpoint the exact location of the problem, and facilitate accurate grouting.

Research on Combined Detection Technology

After conducting an investigation, the characteristics and advantages of various concrete leakage disease detection equipment and detection methods are analyzed. In order to accurately detect internal defects in concrete, it is necessary to comprehensively utilize the advantages of various equipment. This allows for the combined detection of different depths and different types of defects. Ultimately, a solution can be formed for accurately locating leakage points in concrete structures and detecting various internal disease forms.

Based on the conditions of water leakage in metro stations and the applicability of various detection methods, appropriate detection methods for different conditions are proposed. The corresponding detection equipment is selected according to the detection methods, as shown in Table 1.

The proposed combined detection method utilizes video imaging technology to detect water leakage points on the back surface of the dry-hanging decorative layer. It specifically aims to improve the video imaging and image mosaic technology for blocks and partitions. In cases where the surface leakage cannot be captured in a single panoramic shot, the software can stitch and merge multiple images taken in blocks to create a complete detection area image. This allows for accurate positioning of leakage points and identification of the type of disease. With the combination of the infrared thermal imaging technology and leakage detection technology, it is possible to detect surface leakage points of side wall seepage, groundwater return, and elevator shaft leakage without a decorative layer. In terms of detecting internal concrete disease leakage paths, detection accuracy and efficiency are improved by utilizing the ultrasonic cross-section scanning technology and radar detection technology, which enable combined detection, data complementarity, and interactive verification. Additionally, the grid detection technology is employed to achieve a 3D representation of the morphology of internal concrete defects.

Model Test Analysis

In order to simulate the application effect of the detection method and verify the accuracy of the detection results for various types of defects, a concrete block with 0.5 m × 0.5 m × 1.5 m dimensions was made. This block contained an empty bottle, a bottle with water, an earth bag, a stone bag, and linoleum paper to simulate a cavity, water content, slag inclusion, porosity, and cracks, respectively. After the curing of concrete specimens under standard conditions was completed, the detection method was adopted to locate simulated disease. The simulated disease location and concrete specimens are shown in Fig. 2. The internal defects of concrete specimens were detected using

Table 1. **Detection methods under different conditions**

No.	Conditions	Detection method
1	Groundwater return without a decorative floor	Combined detection of surface leakage points: infrared thermal imaging method and water leakage detection method. Combined detection of structural internal defects: GPR method, ultrasonic 3D scanning method, and concrete perspective instrument method.
2	Groundwater return in the wet-sticking decorative layer	Combined detection of surface leakage points: infrared thermal imaging method and water leakage detection method. Combined detection of structural internal defects: GPR method, ultrasonic 3D scanning method, and concrete perspective instrument method.
3	Side wall leakage without a decorative layer	Combined detection of surface leakage points: infrared thermal imaging method and water leakage detection method. Combined detection of structural internal defects: GPR method, ultrasonic 3D scanning method, and concrete perspective instrument method.
4	Side wall leakage in the dry-hanging decorative layer	Combined detection of surface leakage points: endoscope, specially developed camera system; Combined detection of structural internal defects: air-coupled ground penetrating radar.
5	Water accumulation in straight ladder wells	Combined detection of surface leakage points: infrared thermal imaging method and water leakage detection method. Combined detection of structural internal defects: GPR method, ultrasonic 3D scanning method, and concrete perspective instrument method.

a ground penetrating radar and an ultrasonic 3D scanner. Based on the model size, five radar survey lines were arranged, with two on the front side, two on the back side, and one on the top. The survey line arrangement is shown in Fig. 3.

Since a 900 MHz radar antenna was used for detection, the theoretical resolution was 2.8 cm. However, due to the influence of instruments and the detection environment, the actual resolution was about 4 cm. Therefore, the radar could not detect a cavity with a diameter of 1 cm. Due to the pre-existing water storage in the borehole, the radar wave was sensitive to water. As a result, there was a prominent reflection point on the survey line result map that corresponded to the borehole position. It is inferred that this reflection point indicates a leakage point in the borehole. The detection results for the survey lines are shown in Fig. 4.

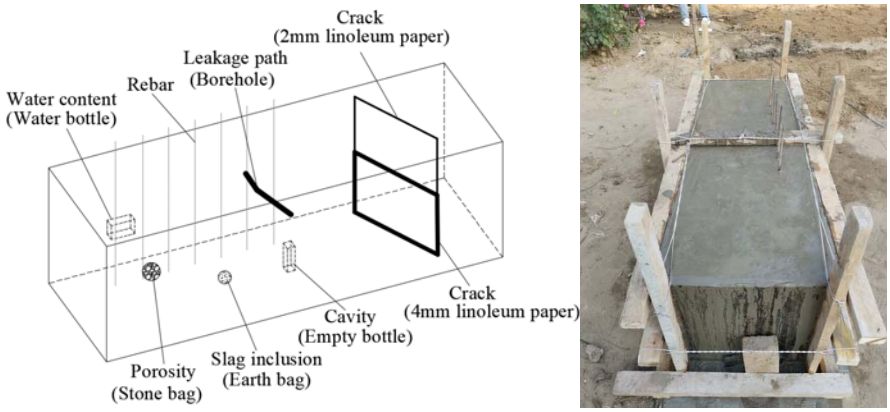

Fig. 2. Schematic diagram of disease location and concrete specimen

Fig. 3. Survey line arrangement of defects location on concrete specimen

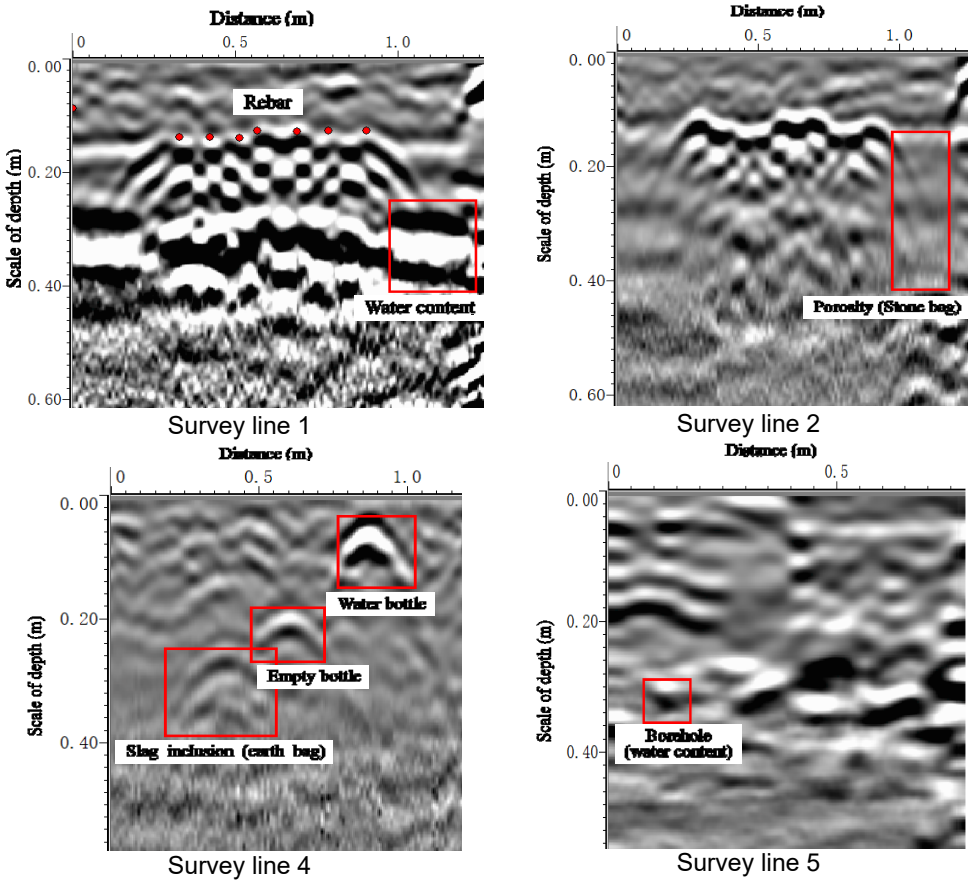

Fig. 4. Map with the radar detection results for each survey line

The ultrasonic 3D scanner was used to detect the shape of a concrete specimen, and the results of the detection in different display modes can be seen in Fig. 5. Due to its high precision, the ultrasonic 3D scanner can identify more abnormal areas and encounter interference if the concrete is unevenly poured. When the size of the disease is small, other methods are needed to verify and enhance accuracy.

Through model tests, the standard GPR waveform diagram of the disease was summarized, and the reliability of the detection method was verified. This provides a reference for applications in engineering detection.

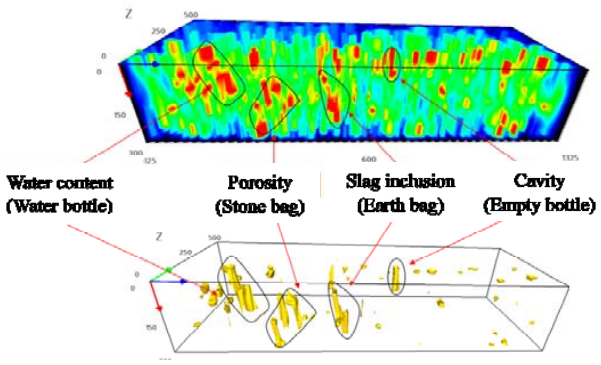

Fig. 5. Map with the detection results from the ultrasonic 3D scanner

Analysis of Detection Method Engineering Application

According to the five conditions of the metro station, namely: groundwater return without a decorative layer, groundwater return with a wet-sticking decorative layer, side wall leakage without a decorative layer, side wall water accumulation with a dry-hanging decorative layer and straight ladder wells, corresponding test points were selected for combined detection.

1. Groundwater return without a decorative floor

According to the detection method proposed in Table 1, an infrared detector and a water leakage detection instrument were used to detect the leakage point under the condition of groundwater return without a decorative layer. A ground penetrating radar (900 MHz and 400 MHz), an ultrasonic 3D scanner, and a concrete steel bar perspective instrument were used to detect internal defects in the concrete. The detection lines are arranged in a grid of 30cm x 30cm (Fig. 6), the leakage point detection results are shown in Fig. 7, and the results of internal structural defects detection are shown in Fig. 8.

As can be seen from Fig. 7, the blue area in the infrared thermal image represents the area with low temperature abnormalities. The value measured at the same position by the water leakage detection instrument can be inferred as the point of water leakage.

As can be seen from Fig. 8, the ultrasonic 3D scanning map, along with the infrared thermal image and the water leakage detection instrument, shows that there is a disease in the concrete of the bottom slab at this location. It was verified through drilling that this position is indeed a point of leakage.

After a comprehensive inspection, both the infrared thermal imager and the leakage water detection instrument detected abnormalities at the same location. This confirms that there is a surface leakage point in that area. Furthermore, the ultrasonic 3D scanner, which has an accuracy of 1 cm, was utilized to identify concrete quality issues

Fig. 6. Layout drawing of the groundwater return condition detection line without a decorative floor

Fig. 7. Results for the groundwater return condition detection line without a decorative floor for leakage point detection

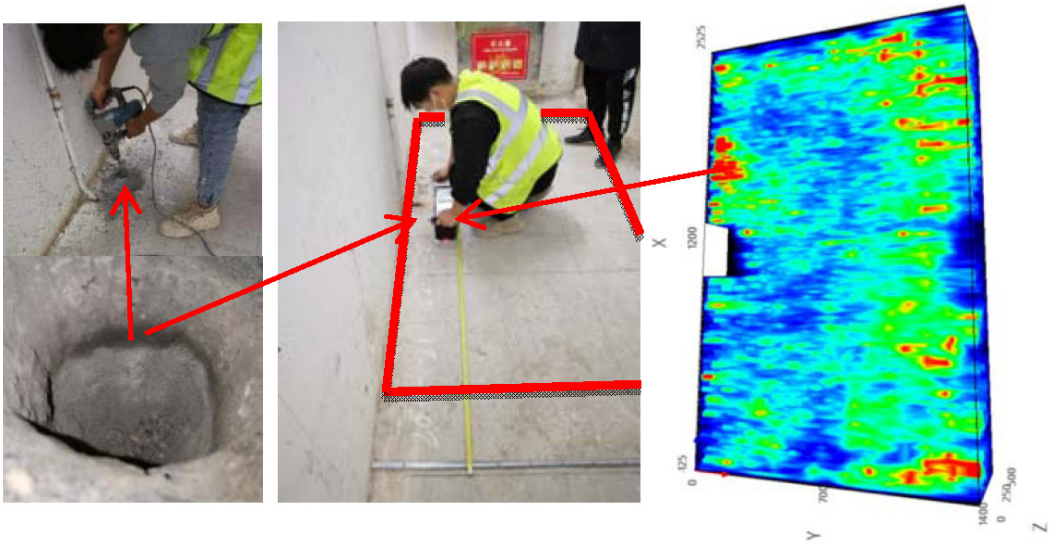

Fig. 8. Results of the detection of internal defects in the structure for the groundwater return condition detection line without a decorative floor

at the same point. The results from the surface detection were also supported by the findings from the ultrasonic scanner. The ground penetrating radar did not detect any abnormality here because the size of the disease is small. The ground-penetrating radar can distinguish defects of 3 cm minimum.

2. Groundwater return in the wet-sticking decorative layer

The infrared thermal imager and water leakage detection instrument were used to detect the leakage point for the groundwater return condition in the wet-sticking decorative layer. Additionally, the ground penetrating radar (900 MHz and 400 MHz), ultrasonic 3D scanner, and concrete steel bar perspective instrument were used to detect the leakage path.

The leakage point detection results are shown in Fig. 9, and the results of internal structural defects detection are shown in Fig. 10.

As can be seen from Fig. 9, the red area in the infrared thermal image represents the area with high temperature abnormalities. The value measured at the same position by the water leakage detection instrument can be inferred as the point of water leakage. As can be seen from Fig. 10, the ultrasonic 3D scanning map, at the same position

Fig. 9. Leakage point detection results for groundwater return in the wet-sticking decorative layer

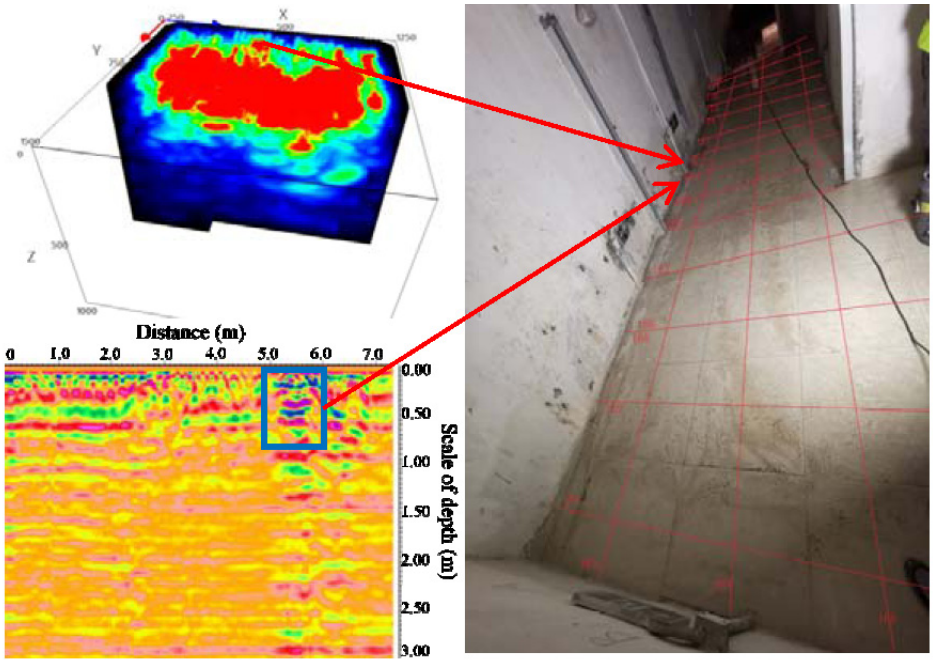

Fig. 10. Results of internal structural defects detection for groundwater return in the wet-sticking decorative layer

as the infrared thermal image and the water leakage detection instrument, shows that there are defects in the bottom slab's concrete. These defects were also detected by the GPR.

After conducting the combined detection, both the infrared thermal imager and the water leakage detection instrument detected abnormalities at the same location, indicating that this area is the source of surface leakage. Additionally, the ultrasonic 3D scanner, with a precision of 1 cm, was used to identify concrete quality issues at the same spot, confirming the results of the surface detection. Furthermore, the ground penetrating radar also identified an abnormality in this area, with the size of the disease being approximately 1 m in length.

3. Side wall leakage without a decorative layer

The infrared thermal imager and water leakage detection instrument were used to detect the leakage point in the side wall without a decorative layer. Additionally, the ground penetrating radar (900 MHz and 400 MHz), ultrasonic 3D scanner, and concrete steel bar perspective instrument were used to detect the leakage path. The diagram in Fig. 11 shows the implementation of combined field detection at test points.

The results of identifying leakage points and internal structural defects are displayed in Fig. 12. As shown in Fig. 12, the blue area in the infrared thermal image represents the area with low temperature abnormalities. The water leakage detection instrument reveals a high reading in this area, indicating that it may be the point of surface leakage. Moreover, the blue abnormality area in the ground penetrating radar map denotes a crack, which is consistent with the actual situation on site. The position highlighted by the black box in the ultrasonic 3D scanning image coincides with the location of the surface leakage point detected by the infrared thermal imager and water leakage detection instrument.

4. Side wall leakage in the dry-hanging decorative layer

The back side of the decorative layer can only be detected using an industrial endoscope. However, the flexible measuring line of the industrial endoscope cannot effectively detect behind the top plate and the long-distance side wall. Moreover, the flexible measuring line cannot accurately pinpoint the source of leakage. The invention includes a device and a method for identifying and locating leakage points behind the decorative layer of metro stations. The detection method can not only determine the leakage point behind the decorative layer but also grasp the surrounding environment and coordinate the positioning of the leakage point behind the decorative layer. The equipment is not subjected to the height of the roof decorative layer, as shown in Fig. 13.

The surface leakage point of the side wall with the dry-hanging decorative layer was detected using an industrial endoscope and a specially developed camera system. The leakage path was identified using an air-coupled ground penetrating radar (400 MHz). The diagram in Fig. 14 shows the implementation of combined field detection at test points.

The results of identifying leakage points and internal structural defects are displayed in Fig. 15.

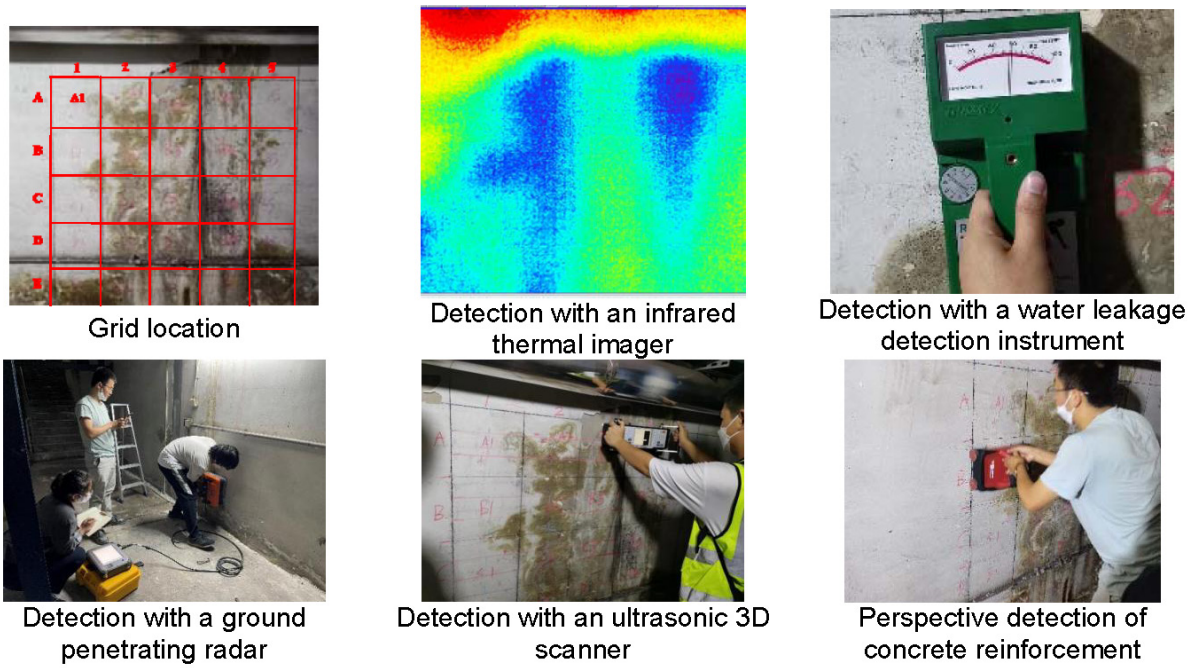

Fig.11. Diagram for implementing combined detection of side wall leakage without a decorative layer

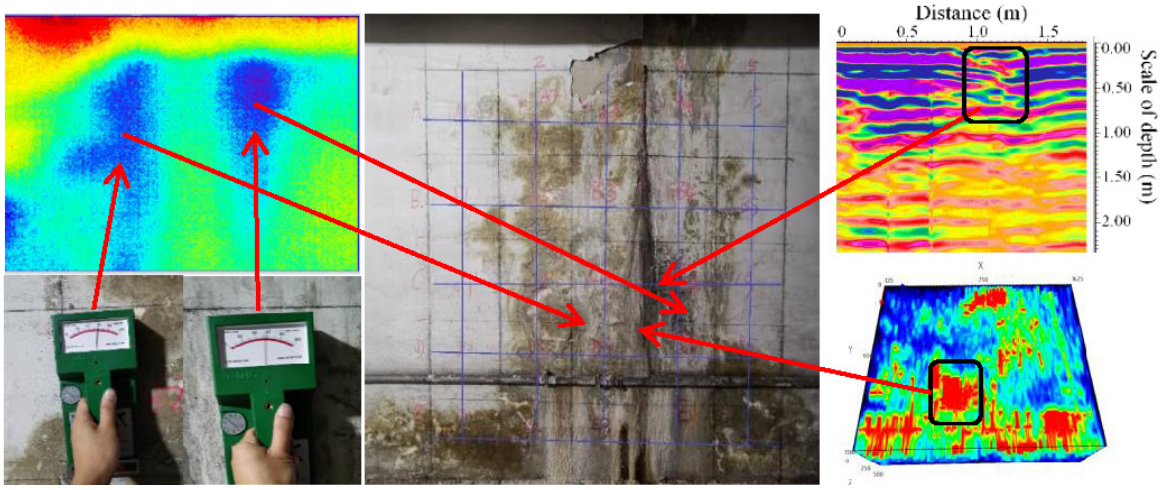

Fig. 12. Results of combined detection of side wall leakage without a decorative layer

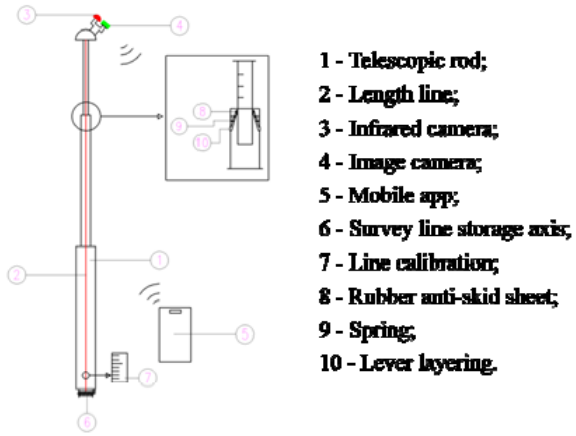

Fig. 13. Schematic diagram of a combined detection device for identifying leakage points behind the decorative layer

As can be seen from Fig. 15, the combination of an industrial endoscope, a specially developed camera system, and a ground penetrating radar can be used to detect the leakage condition of the side wall with the dry-hanging decorative layer. It can determine the location of the leakage point, reduce the need for demolition of the decorative layer, and improve remedial efficiency. In the figure, the red numbers represent the location of the survey line, and the yellow numbers represent the location of the ceramic tile in the decorative layer.

5. Water accumulation in straight ladder wells

The infrared thermal imager and water leakage detection instrument were used to detect the surface leakage points in straight ladder wells under water accumulation conditions. Additionally, the ground penetrating radar (900 MHz and 400 MHz), ultrasonic 3D scanner, and concrete steel bar perspective instrument were used to detect the leakage path. The combined detection results are shown in Fig. 16.

As shown in Fig. 16, due to the recent removal of the accumulated water, the temperature of the bottom plate is fairly even, and the infrared thermal imager cannot detect any areas with abnormal temperatures. Although the accumulated water was removed, the amount of water within 10 cm of the surface layer can still be detected using the water leakage detection instrument. The ground penetrating radar and ultrasonic 3D scanner can essentially identify abnormalities at the same location, which can be basically classified as structural defects.

When the detection method was used for on-site detection, it was found that the infrared thermal imager and water leakage detection instrument were affected by the detection environment and did not function effectively under all conditions. When the

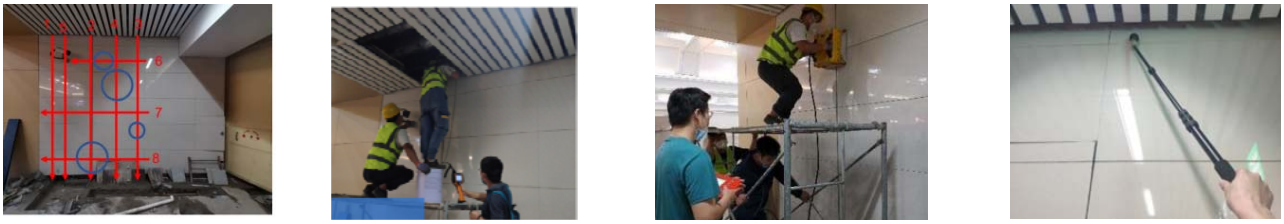

Grid location | Inspection with an industrial endoscope | Detection with a ground penetrating radar | Detection with a specially developed camera system

Fig. 14. Diagram for implementing combined detection of side wall leakage in the dry-hanging decorative layer

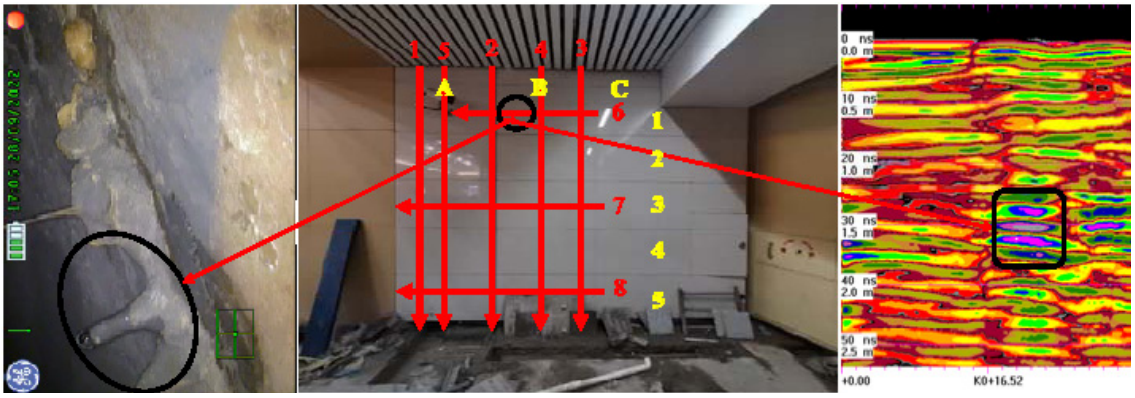

Fig. 15. Results of combined detection of side wall leakage with the dry-hanging decorative layer

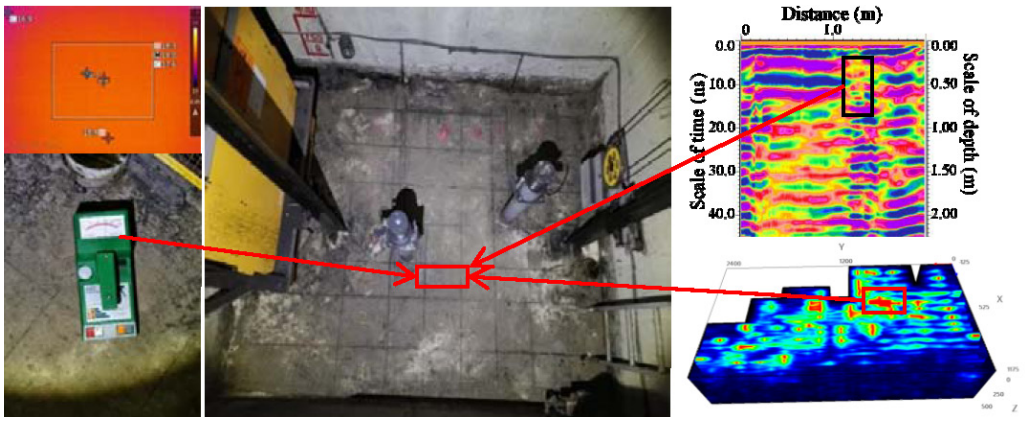

Fig. 16. Combined detection results for water accumulation in the straight ladder wells

concrete defects are small, the detection by GPR and ultrasonic 3D scanning methods is not obvious. However, the detection effect of an infrared thermal imager and a water leakage detection instrument on shallow water enrichment can be used as an important reference. The ground penetrating radar has a high detection efficiency and is suitable for large-scale detection. The ultrasonic 3D scanner has a higher detection accuracy than the ground penetrating radar, but its detection efficiency is low, making it suitable for small-scale detection.

According to the analysis of the combined detection results, it can be seen that:

(1) With the combined detection technology of “infrared detector + water leakage detection instrument”, a more accurate preliminary identification of leakage points on the surface of the non-decorative and wet-sticking decorative layers can be achieved.

(2) With the combined detection technology of “GPR + ultrasonic section scanner”, the internal defects of the non-decorative layer and wet-sticking decorative layer can be detected more effectively.

(3) Under the condition of not removing the decorative layer, the detection of leakage points in the side wall with the dry-hanging decorative layer mainly depends on the industrial endoscope and specially developed camera system. The leakage path in the concrete can be effectively detected using the air-coupled radar.

Grouting Remediation and Effect Evaluation

Based on the combined detection results for each test point, grouting remediation is carried out at the disease location related to the test point. After grouting remediation, the evaluation of grouting effect mainly includes the following: 1. whether there is still water leakage; 2. geophysical prospecting determines if the leakage path of defects (porosity, cavity, slag inclusion, etc.) is tightly sealed; 3. check the compactness of the grouting through drilling and coring. This paper only offers the grouting remediation solution for groundwater return condition with regard to the wet-sticking decorative layer. Based on the combined detection results, acrylate and modified epoxy resin grouting is performed on the leakage points on the bottom plate surface of the evacuation passageway and in areas with concrete quality issues (leakage paths). The grouting remediation site is shown in Fig. 17, whereas the apparent effect after remediation can be seen in Fig. 18. The ground penetrating radar detection result is displayed in Fig. 19. To ensure more accurate verification of the

Fig. 17. On-site grouting remediation for groundwater return condition with regard to the wet-sticking decorative layer

grouting effect, drilling and coring were performed in the B10 area (Fig. 20).

Conclusions

During the field implementation process, leakage points and types of leakage defects were initially investigated using engineering experience. Afterwards, the combined detection was conducted to accurately locate and determine the types of leakage defects. Based on the model tests and field tests, the following conclusions were drawn:

(1) At the initial stage of leakage, there was a significant temperature difference (greater than 0.08°C) between the leaking water and the surrounding environment. The infrared thermal imaging method proved to be effective in locating the points of leakage.

(2) The water leakage detection instrument can detect the water content in a depth of 0 to 10 cm. It is sensitive to the area with water content, but this method requires that the detection surface be flat and free from any water accumulation.

(3) The resolution of the ground penetrating radar is less than 3 cm, and the detection depth is 3 m, while the resolution of the ultrasonic 3D scanner is 1 cm, and the detection depth is 0.5 m. The ground penetrating radar and ultrasonic 3D scanner can verify each other while detecting internal defects in concrete, thereby improving the rate and accuracy of disease recognition.

(4) When the concrete defects are small or greatly affected by the environment, the detection using the ground penetrating radar and ultrasonic 3D scanner. is not obvious. In such cases, the detection of water content in the shallow layer using the infrared thermal imager and water leakage detection instrument can

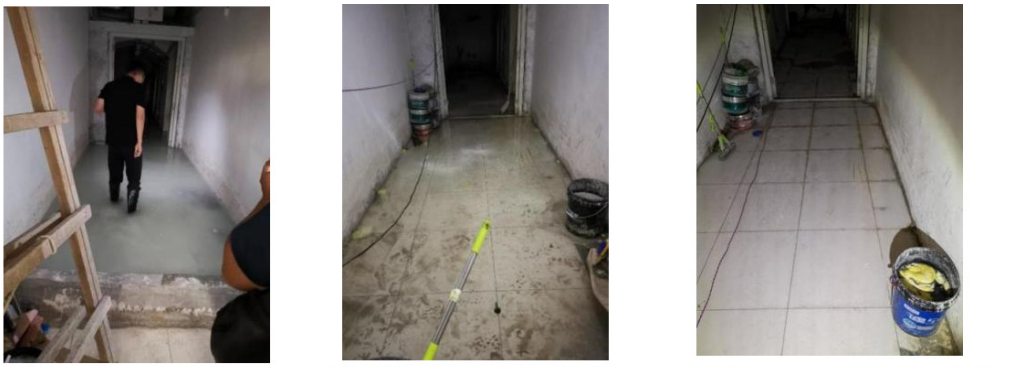

Fig. 18. Apparent effect after remediation for groundwater return condition with regard to the wet-sticking decorative layer

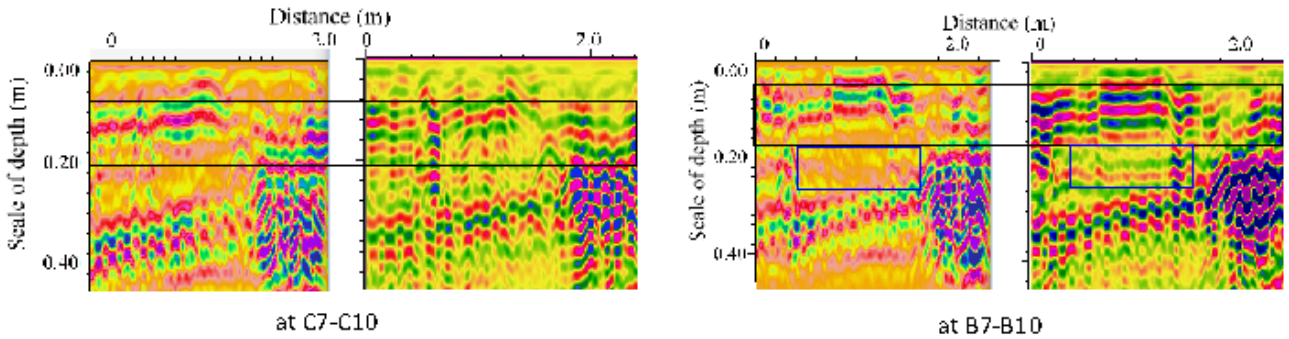

Fig. 19. Ground penetrating radar detection results before and after remediation (before remediation — on the left and after remediation — on the right)

Fig. 20. Borehole coring at B10 after remediation for ground water return condition with regard to the wet-sticking decorative layer

serve as an important reference for identifying the leakage path.

(5) The ground penetrating radar has a high detection efficiency and is suitable for large-scale detection. The ultrasonic 3D scanner has a higher detection accuracy than the ground penetrating radar, but its detection efficiency is low, making it suitable for small-scale detection.

(6) Water leakage is influenced by various defects and the actual environment, and a single method often cannot accurately detect the points and paths of leakage. Different detection methods can complement and verify each other in terms of accuracy and depth of detection as well as objects they detect. This helps enhance disease identification and accuracy, ultimately achieving the goal of precise grouting.

The combined detection device for detecting leakage points behind the decorative layer proposed herein is the subject of a patent application (#ZL 2022 2 2739345.1).

References

Asakura, T. and Kojima, Y. (2003). Tunnel maintenance in Japan. *Tunnelling and Underground Space Technology*, Vol. 18, Issues 2–3, pp. 161–169. DOI: 10.1016/S0886-7798(03)00024-5.

Cheng, X., Hu, X., Tan, K., Wang, L., and Yang, L. (2021). Automatic detection of shield tunnel leakages based on terrestrial mobile LiDAR intensity images using deep learning. *IEEE Access*, Vol. 9, pp. 55300–55310. DOI: 10.1109/ACCESS.2021.3070813.

Clark, M. R., McCann, D. M., and Forde, M. C. (2003). Application of infrared thermography to the non-destructive testing of concrete and masonry bridges. *NDT & E International*, Vol. 36, Issue 4, pp. 265–275. DOI: 10.1016/S0963-8695(02)00060-9.

Feng, D.-S., Chen, C.-S., and Yu, K. (2011). Signal enhancement and complex signal analysis of GPR Based on Hilbert-Huang transform. In: Wan, X. (ed.). *Electrical Power Systems and Computers, Lecture Notes in Electrical Engineering*, Vol. 99, pp. 375–384. DOI: 10.1007/978-3-642-21747-0_46.

Gong, X.-N. and Guo, P.-P. (2021). Prevention and mitigation methods for water leakage in tunnels and underground structures. *China Journal of Highway and Transport*, Vol. 34, Issue 7, pp. 1-30. DOI: 10.19721/j.cnki.1001-7372.2021.07.001.

Han, S., Cho, H., Kim, S., Jung, J., and Heo, J. (2012). Automated and efficient method for extraction of tunnel cross sections using terrestrial laser scanned data. *Journal of Computing in Civil Engineering*, Vol. 27, Issue 3, pp. 274–281. DOI: 10.1061/(ASCE)CP.1943-5487.0000211.

Jiang, Y., Wu, J., Ma, Y., and Huang, B. (2020). Research and application of detection technology of tunnel lining concrete strength based on impact elastic wave. *Railway Engineering*, Vol. 60, Issue 6, pp. 1–5, 11. DOI: 10.3969/j.issn.1003-1995.2020.06.01.

Kashani, A. G., Olsen, M. J., Parrish, C. E., and Wilson, N. (2015). A review of LIDAR radiometric processing: From *ad hoc* intensity correction to rigorous radiometric calibration. *Sensors*, Vol. 15, Issue 11, pp. 28099–28128. DOI: 10.3390/s151128099.

Lam, S. Y. W. (2006). Application of terrestrial laser scanning methodology in geometric tolerances analysis of tunnel structures. *Tunnelling and Underground Space Technology*, Vol. 21, Issues 3–4, p. 410. DOI: 10.1016/j.tust.2005.12.057.

Liu, B., Li, S.-C., Li, S.-C., Zhang, Q. S., Xue, Y. G., and Zhong, S. H. (2009). Study of application of complex signal analysis to predicting karst-fractured ground water with GPR. *Rock and Soil Mechanics*, Vol. 30, Issue 7, pp. 2191–2196. DOI: 10.1016/S1874-8651(10)60073-7.

Liu, X., Sang, Y., and Su, Y. (2012). Detection technology of tunnel leakage disaster based on digital image processing. *Chinese Journal of Rock Mechanics and Engineering*, Vol. 31, Issue S2, pp. 3779–3786.

Ma, X., Duan, P., and Li, J. (2022). Water leakage detection technology for tunnel lining of Shuozhou-Huanghua Railway based on infrared thermal imaging. *Railway Engineering*, Vol. 62, Issue 8, pp. 126–129. DOI: 10.3969/j.issn.1003-1995.2022.08.28.

Montero, R., Victores, J. G., Martínez, S., Jardón, A., and Balaguer, C. (2015). Past, present and future of robotic tunnel inspection. *Automation in Construction*, Vol. 59, pp. 99–112. DOI: 10.1016/j.autcon.2015.02.003.

Musolino, A., Raugi, M., Tucci, M., and Turcu, F. (2007). Feasibility of defect detection in concrete structures via ultrasonic investigation. In: *Progress in Electromagnetic Research Symposium*, Prague, Czech Republic, August 27–30, 2007, pp. 371–375.

Sandrone, F. and Labiouse, V. (2011). Identification and analysis of Swiss National Road tunnels pathologies. *Tunnelling and Underground Space Technology*, Vol. 26, Issue 2, pp. 374–390. DOI: 10.1016/j.tust.2010.11.008.

Shi, P. and Li, P. (2015). Mechanism of soft ground tunnel defect generation and functional degradation. *Tunnelling and Underground Space Technology*, Vol. 50, pp. 334–344. DOI: 10.1016/j.tust.2015.08.002.

State Standard of China (2010). *JGJ/T 212-2010*. *Technical specification for remedial waterproofing of the underground works*. Beijing: Standardinform, pp. 79.

State Standard of China (2022). *DB32/T 4283-2022*. *Technical standard for leakage detection of building engineering*. Nanjing: Standardinform, pp. 15.

Xu, T., Xu, L., Li, X., and Yao, J. (2018). Detection of water leakage in underground tunnels using corrected intensity data and 3D point cloud of terrestrial laser scanning. *IEEE Access*, Vol. 6, pp. 32471–32480. DOI: 10.1109/ACCESS.2018.2842797.

Yu, T., Zhu, A., and Chen, Y. (2016). Efficient crack detection method for tunnel lining surface cracks based on infrared images. *Journal of Computing in Civil Engineering*, Vol. 31, Issue 3, 04016067. DOI: 10.1061/(ASCE)CP.1943-5487.0000645.

ИССЛЕДОВАНИЕ ОБНАРУЖЕНИЯ И УСТРАНЕНИЯ ПРОТЕЧЕК В КОНСТРУКЦИИ СТАНЦИИ МЕТРОПОЛИТЕНА

Цяофэн Шэнь[1]*, Чэнь Шэнь[1], Сюнь Лю[1], Усян Сунь[1], Лунин Ши[2], Тин Чэнь[2]

[1] Beijing Subway Construction Facilities Maintenance Co., Ltd, Пекин, Китай

[2]Zhongke Jiantong Engineering Technology Co., Ltd, Пекин, Китай

*E-mail: 18813094515@163.com

Аннотация

Введение: Принимая во внимание протечки на станциях метрополитена и различные методы обнаружения протечек, изучение методов комбинированного обнаружения, подходящих для различных эксплуатационных условий, может послужить основой для устранения протечек. **Цель:** Применение различных взаимодополняющих методов обнаружения протечек, обеспечивающее более тщательный контроль в отношении точности обнаружения и глубины расположения объектов, совершенствование процедуры обнаружения и повышение точности выявления дефектов, а также обеспечение точного цементирования. **Методы:** В ходе исследования были использованы модельные испытания и применение методов обнаружения протечек в условиях эксплуатации. **Результаты:** С помощью инфракрасного детектора и прибора для обнаружения протечек воды можно более точно определить место протечки на поверхности недекоративного слоя и «мокрого» декоративного слоя. С помощью подповерхностного радиолокатора и ультразвукового сканера поперечного сечения можно лучше определить внутренние дефекты структуры недекоративного слоя и «мокрого» декоративного слоя. При условии, что декоративный слой не демонтируется, путь протечки в бетоне, а также места протечки на поверхности могут быть эффективно обнаружены с помощью радиолокатора с воздушной связью на базе промышленного эндоскопа и специально разработанной системы камер.

Ключевые слова: метрополитен, конструкция станции, протечка, комбинированное обнаружение, восстановление цементирования.

DOI: 10.23968/2500-0055-2023-8-3-45-52

RESTORATION COMPOUNDS FOR TERRAZZITE PLASTER ON THE EXAMPLE OF CULTURAL HERITAGE SITES OF THE 20TH CENTURY (RUSSIA)

Lyubov Zakrevskaya, Galina Maslova, Elizaveta Repina*

Vladimir State University named after Alexander and Nikolay Stoletovs (VLSU), Vladimir, Russia

*Corresponding author's e-mail: elizavetarepina64@gmail.com

Abstract

Inroduction: Gradual destruction of buildings or structures of historical significance is a natural process that cannot be stopped. Therefore, preservation of architectural monuments is one of the most important areas of restoration activity. Complete replacement of damaged building materials of architectural monuments changes the historical appearance, and thus cultural sites are stripped of their original look. Innovations in the re-creation of historical building materials and technologies help preserve historical continuity. **The purpose of the study** was to develop a number of compounds of terrazzite plaster mixtures for cultural heritage sites of the 20th century, which, from an aesthetic point of view, will not allow the loss of the natural and picturesque appearance of the monument, and will be able to preserve the "patina of time". **As a result** of the research, the authors studied the compositions of the selected samples, proposed restoration compounds of terrazzite plaster, and determined the algorithm for applying an analogue of the historical plaster. In terms of technical and economic indicators, the developed restoration compounds are effective and make it possible to return architectural monuments to their original appearance with minimal costs. Based on the results obtained, conclusions were drawn about the feasibility of using the proposed new components in terrazzite plaster mixtures to increase strength and ensure high-quality adhesion of the old and new plaster layers. The proposed technology contributes to the return of architectural monuments to their original appearance without losing the historical authenticity of the buildings.

Keywords: terrazzite plaster, restoration of building facades, cultural heritage sites.

Introduction

The modern construction market offers a large number of different materials, not only for high-quality work meeting customer needs, but also for restoring any coatings and surfaces to maintain the proper appearance of buildings or structures (Subbotin, 2019).

One of the important problems that arise during restoration is the issue of low-quality restoration of plaster facades, which is primarily associated with an unreasonable and even erroneous choice of mixtures for renovation. It is possible to use materials close to historical ones, but in the case of problematic foundations (e.g., with a high water or salt load), it is quite difficult to achieve a positive result, since corrosive environment can cause damage (Hoła et al., 2017; Knyazeva and Koroleva, 1998; Makarov and Shpolyansky, 2015; Vozniuk et al., 2013).

Many building facades in large cities were made using terrazzite plaster. This is a decorative dry mixture based on lime-cement binder, the main purpose of which is the finishing of facades, walls, columns, and architectural elements. It is used for concrete or brick surfaces.

The terrazzite plaster compounds currently used in construction mainly include the following components: calcium hydroxide (slaked lime), quartz sand, Portland cement, fillers (chips of artificial or natural stone, marble, etc.), mica, and may also contain mineral dyes.

Several types of terrazzite plaster can be distinguished depending on the size of the aggregate corresponding to a certain size grade: K — large chips, granule size 4–6 mm, C — medium chips, granule size 2–4 mm, and M — small chips, granule size 1–2 mm (Blumberga et al., 2016; Kamendere et al., 2016; Khan et al., 2017). In construction, terrazzite plaster is supplied in the form of ready-made dry mixtures and is prepared for application immediately before use (Pastukh et al., 2020).

We examined several historical sites, where construction and restoration included the use of terrazzite plaster mixture.

The construction of the Soviet era building of the State Bank in Yaroslavl was carried out in 1918–1936, as the southern building of Gostiny Dvor was completely destroyed during the Yaroslavl Uprising of 1918 (Dergunov et al., 2021; Panasyuk et al., 2018; Ventolà et al., 2011). Gostiny Dvor consisted of two parts: the northern and southern buildings, which were identical in their layout and located symmetrically. After the end of the Uprising in 1918, the damage was so significant that it was decided to completely dismantle the building.

According to the State Historical and Cultural Expertise, the building dates back to the construction

period of 1929–1936. In 1928, the building was designed by I. I. Knyazev and G. P. Goltz. The architects managed not only to harmoniously fit the building into the surrounding space, but also add some novelty to it (Pastukh et al., 2020; Safonova, 2017).

The State Bank became the first building of neo-Renaissance constructivism style on Komsomolskaya Street (Fig. 1).

The main architectural theme was a heavy rusticated wall with widely spaced windows in the style of Florentine architects. The windows were designed as high and rectangular with arched frames in the form of small niches. The only volumetric element of the flat facade was the entrance made in the form of a four-arched portico (Figs. 2, 3).

According to the design, the building included not only administrative and technological premises, but also residential ones. The architectural rational solution was based on the flexible use of space.

It was decided to use the southern part of the building as a living area of six apartments. Also, service buildings were provided on the territory adjacent to the building. Construction of the main building of the State Bank was completed in 1936. With minor changes, the interior of the building has been preserved to this day (Fierascu et al., 2020; Yevseyev, 2016).

In February 1995, the entire State Bank complex was declared a cultural heritage site, and by order of the Department of Cultural Heritage Site Protection of the Yaroslavl Region, the building was given the status of a cultural heritage site of federal significance.

In 2021, it was decided to restore the facade, interior, and also organize access for people with limited mobility to the building.

The second site under study is the building of the Main Treasury in St. Petersburg (Fig. 4). The building was designed in the neoclassical style by architects D. M. Iofan and S. S. Serafimov and built by civil engineer S. S. Korvin-Krugovsky in the period from 1913 to 1915. The building consists of four parts: the main facade building, the central part of the building, and two wings adjacent to the central part on both sides. The central part of the facade building is adorned with decorative pilasters and

Fig. 1. Fragment of a drawing from the newspaper “Severny Rabochiy”, 1929. Design of a new building of the State Bank

Fig. 2. Fragment of the main facade of the State Bank, Yaroslavl

Fig. 3. Fragment of the north-eastern facade of the State Bank, Yaroslavl

Fig. 4. View of the main facade of the Main Treasury, St. Petersburg

columns, and an attic runs above the cornice. The central part of the building is covered with a dome (Chainikova, 2022; Crinson, M. and Williams, 2019; Saifullina, 2014; Šahmenko et al., 2015).

The internal space of the building consists of not only administrative premises, including a spacious lobby and operating room (with an area of more than 3000 m^2), offices, cash desks, but also residential premises, for example, managers' apartments.

During the Great Patriotic War, a bomb hit the building and destroyed the interior, but later it was restored.

In 2022, it was decided to restore the facade building.

Materials and methods

In our work we used the following methods and equipment: scanning electron microscope (SEM), material moisture meter VIMS-2.12 and strength meter for building materials IPS-MG4.03, diffractometer Bruker AXS D8 ADVANCE (model D8, manufacturer: Bruker Optik GmbH, Germany).

To study the composition and physical and technical properties, the customer provided samples of building materials selected at the sites.

Fig. 5 indicates the location for sampling the material from the building of the Yaroslavl Central Bank, and Fig. 6 shows a sample of terrazzite plaster on the facade of the said bank.

Fig. 7 shows the sampling location of the Main Treasury building in St. Petersburg, and Figs. 8–11 show samples of terrazzite plaster of the same facade.

The study of the SEM microstructure and X-ray phase analysis of the presented terrazzite plaster samples allows us to conclude that at the research site during construction, as well as during further

Fig. 5. Location of material sampling from the building of the Yaroslavl Central Bank

Fig. 6. Sample No. 1 of the plaster of the facade of the Yaroslavl Central Bank building

Fig. 7. Location of material sampling from the Main Treasury building in St. Petersburg

Fig. 8. Sample No. 2 of the plaster of the Main Treasury building in St. Petersburg

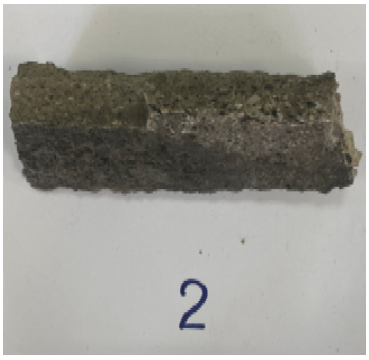

Fig. 9. Sample No. 3 of the facade plaster of the Main Treasury building in St. Petersburg

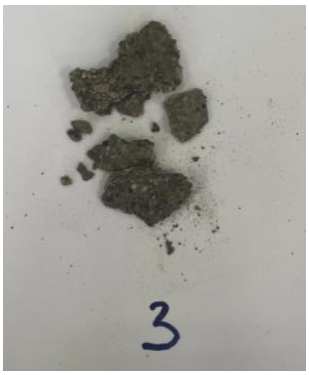

Fig. 10. Sample No. 4 of the facade plaster of the Main Treasury building in St. Petersburg

Fig. 11. Sample No. 5 of the facade plaster of the Main Treasury building in St. Petersburg

reconstruction of the building, the composition used contained lime, dolomite, sand and clay as the main components.

Results

Fig. 12 shows the results of X-ray phase analysis of sample No. 1 of terrazzite plaster on the facade of the Yaroslavl Central Bank building.

Table 1 presents a number of developed terrazzite plaster compounds for the restoration of the facade of the Yaroslavl Central Bank building.

Table 2 presents the compounds of terrazzite plaster for the restoration of the facade of the Main Treasury building in St. Petersburg.

Results and discussion

The results of studying the macrostructure of terrazzite plaster samples using scanning electron microscopy (SEM) are presented in Figs. 14–16:

The structure of sample No. 3 of the Main Treasury building in St. Petersburg is a porous material with cavities from 50 to 100 microns (Fig. 14).

The macrostructure of sample No. 4 of the Main Treasury building in St. Petersburg is homogeneous, with inclusions of metallurgical slag up to 1 mm in size (Fig. 15).

The macrostructure of sample No. 5 (Fig. 16) of the Main Treasury building in St. Petersburg is heterogeneous, characterized by strongly open cracks and voids [Khan et. al., 2017].

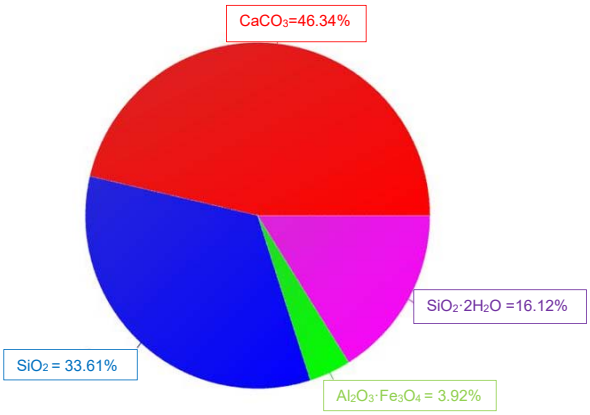

Fig. 12. Results of X-ray phase analysis of sample No. 1 of terrazzite plaster on the facade of the Yaroslavl Central Bank building

Table 1. **Compounds of terrazzite plaster mixtures for restoration of the facade of the Yaroslavl Central Bank building**

No.	Composition / Components	R_1	R_2	R_3	R_4	R_5
		Components, wt%				
1	Super white cement CEM I 52.5 R ADANA OYAK CIMENTO	16	12	13	14	15
2	Slaked lime	25	24	24	25	20
3	Quartz sand	7.5	7.5	7.5	7.5	7.5
4	Foam glass microgranules fraction 0.25–1.0 mm Density 400 kg/m^3 Strength 2.5 MPa	7.5	7.5	7.5	7.5	7.5
5	Granite chips d=6–8 mm	20	25	26	16.5	24.5
6	Mica GOST 10698-80	6	5	4	2	3
7	Plasticizer P-17	5	7.5	5	6	5
	Pigment					
8	Minium	1.5	-	0.5	1	0.5
9	Fired clay (ochre)	10	-	10	15	10
10	Soot	1.5	-	-	-	-
11	Umber	-	10	2.5	5	5.5
12	Manganese dioxide	-	1.5	-	0.5	1.5
Strength (MPa)		10–12				
Water absorption (%)		4–6				
Porosity (%)		8–10				

The technology for preliminary surface preparation consists of the following operations:

1) Removal of loose and exfoliated destruction products.

2) Cleaning of the restored surface with hard brushes without leveling.

3) Dust removal of the area where the renovation compound is applied.

4) Thorough rinsing of the surface under restoration with water.

5) Spraying the terrazzite compound before applying the plaster mixture to the prepared and primed surface.

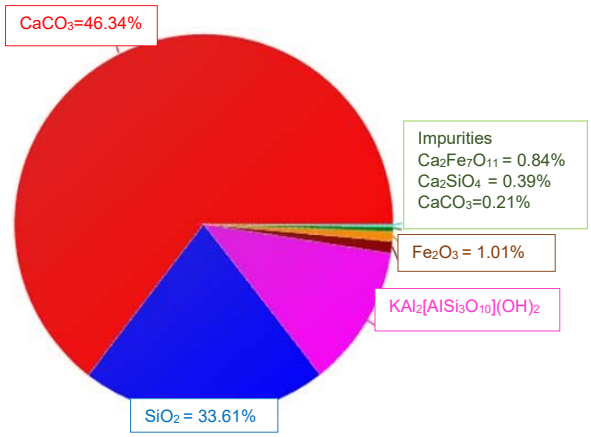

Fig. 13. Results of X-ray phase analysis of sample No. 2 of terrazzite plaster of the Main Treasury building in St. Petersburg

Table 2. **Compositions of mixtures for terrazzite plaster of the Main Treasury building in St. Petersburg**

No.	Composition / Components	R_1	R_2	R_3	R_4	R_5
		Components, wt%				
1	Super white cement CEM I 52.5 R ADANA OYAK CIMENTO	16	12	13	14	15
2	Slaked lime	25	24	24	25	20
3	Quartz sand	7.5	7.5	7.5	7.5	7.5
4	Foam glass microgranules fraction 0.25–1.0 mm Density 400 kg/m^3 Strength 2.5 MPa	7.5	7.5	7.5	7.5	7.5
5	Granite chips d=6–8 mm	20	25	26	16.5	24.5
6	Mica GOST 10698-80	6	5	4	2	3
7	Plasticizer P-17	5	7.5	5	6	5
	Pigment					
8	Minium	1.5	-	0.5	1	0.5
9	Fired clay (ochre)	5	-	5	5	3.5
10	Soot	6.5	4	5	10	6.5
11	Umber	-	6	2.5	5	5.5
12	Manganese dioxide	-	1.5	-	0.5	1.5
Strength (MPa)		7–11				
Water absorption (%)		5–6				
Porosity (%)		8–10				

The technology for applying terrazzite plaster includes the following steps:

1) Spraying the surface to be restored with the terrazzite compound. Exposure for 1–5 hours.

2) Applying a given number of primer layers to the area under restoration taking fillers into account. Leveling and compacting the resulting surface with the impact of a trowel.

3) Preparing the renovation compound from dry fillers and a cement-pigment mixture, and mixing it thoroughly.

4) Adding the required amount of water while constantly stirring the mixture.

5) Forming a given texture and appearance of the surface by processing it with various tools.

6) Protecting the surface under renovation with covering material from precipitation, dirt, etc., within 24 hours, starting from the moment of applying the

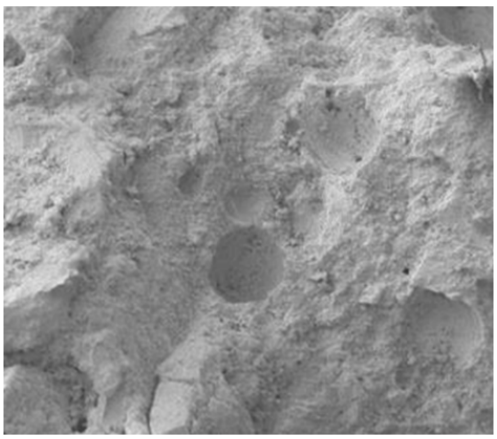

Fig. 14. Structure of plaster sample No. 3 of the Main Treasury building in St. Petersburg

Fig. 15. Structure of plaster sample No. 4 of the Main Treasury building in St. Petersburg

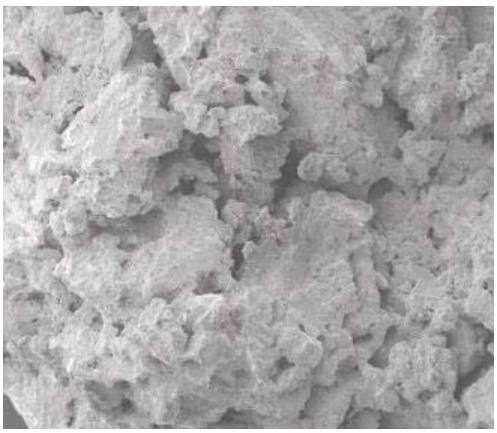

Fig. 16. Macrostructure of plaster sample No. 5 of the Main Treasury building in St. Petersburg

renovation compound. During hot periods, protection of the surface from exposure to direct sunlight for 48 hours and wetting of the surface with water.

7) After the final setting of the compound, rinsing the surface with water to reveal significant texture elements (grains, stone).

In the process of the work, we studied selected samples of historical plaster and, on their basis, developed authentic restoration compositions of terrazzite plaster mixtures.

A step-by-step technology for restoration work on the historical facade was developed.

As a result of the research, a conclusion was made about the effectiveness of using the proposed new components in the composition of terrazzite plaster to increase strength (up to 7–12 MPa) and ensure high-quality adhesion of the old and new plaster layers. Thus, it is possible for an architectural monument to look authentic again without losing its historical appearance. One of the main goals of this work was to create a color scheme for historical sites. Therefore, as a result of the variability of pigments, the optimal amount of processing was achieved to form a palette of unique shades.

References

Blumberga, A., Kass, K., and Kamendere, E. (2016). A review on Latvian historical building stock with heavy walls. *Energy Procedia*, Vol. 95, pp. 17–21. DOI: 10.1016/j.egypro.2016.09.004.

Chainikova, O. O. (2022). *Reconstruction of architectural monuments in modern restoration practice (case study of the Saint Petersburg region)*. PhD Thesis in Architecture. Saint Petersburg State University of Architecture and Civil Engineering.

Crinson, M. and Williams, R. J. (2019). *The architecture of art history: a historiography*. London: Bloomsbury, 185 p.

Dergunov, S. A., Serikov, S. V., Satyukov, A. B., and Serikova, O. V. (2021). *Dry construction repair mix*. Patent RU2751180C1.

Fierascu, R. C., Doni, M., and Fierascu, I. (2020). Selected aspects regarding the restoration/conservation of traditional wood and masonry building materials: a short overview of the last decade findings. *Applied Sciences*, Vol. 10, Issue 3, 1164. DOI: 10.3390/app10031164.

Hoła, A., Matkowski, Z., and Hoła, J. (2017). Analysis of the moisture content of masonry walls in historical buildings using the basement of a medieval town hall as an example. *Procedia Engineering*, Vol. 172, pp. 363–368. DOI: 10.1016/j.proeng.2017.02.041.

Kamendere, E., Grava, L., Zvaigznitis, K., Kamenders, A., and Blumberga, A. (2016). Properties of bricks and masonry of historical buildings as a background for safe renovation measures. *Energy Procedia*, Vol. 95, pp. 119–123. DOI: 10.1016/j.egypro.2016.09.032.

Khan, M. I., Abbas, Y. M., and Fares, G. (2017). Review of high and ultrahigh performance cementitious composites incorporating various combinations of fibers and ultrafines. *Journal of King Saud University - Engineering Sciences*, Vol. 29, Issue 4, pp. 339–347. DOI: 10.1016/j.jksues.2017.03.006.

Knyazeva, V. P. and Koroleva, T. V. (1998). *Actual trends in the development of quality management systems for restoration design (based on the system of ISO-9000 standards)*. Moscow: Department of State Control for Protection and Use of Monuments, 134 p.

Makarov, N. A. and Shpolyansky, S. V. (eds.) (2015). *Archaeology of the Vladimir–Suzdal Land: Proceedings of the Research Workshop*. Issue 5. Moscow: Institute of Archaeology of the Russian Academy of Sciences, 288 p.

Panasyuk, V. V., Marukha, V. I., and Sylovanyuk, V. P. (2018). Efficient injection materials and the technologies of restoration of the serviceability of damaged building structures intended for long-term operation. *Materials Science*, Vol. 54, No. 2, pp. 154–162. DOI: 10.1007/s11003-018-0169-0.

Pastukh, O., Gray, T., Golovina, S. (2020). Restored layers: reconstruction of historical sites and restoration of architectural heritage: the experience of the United States and Russia (case study of St. Petersburg). *Architecture and Engineering*, Vol. 5, No. 2, pp. 17–24. DOI: 10.23968/2500-0055-2020-5-2-17-24.

Safonova, T. R. (2017). Change of the functional purpose as an alternative method of preserving fragments of archtectural monuments. *Austrian Journal of Humanities and Social Sciences*, No. 3–4, pp. 3–8. DOI: 10.20534/AJH-17-3.4-3-8.

Šahmenko, G., Aispurs, S., and Krasnikovs, A. (2015). The use of high performance cement composite in renovation and restoration of architectural elements of buildings facades. *Procedia Engineering*, Vol. 117, pp. 317–324. DOI: 10.1016/j.proeng.2015.08.256.

Saifullina, L. S. (2014). History and methodics of restorations. Some problems of modern theory and practice. *News of the Kazan State University of Architecture and Engineering*, No. 2 (28), pp. 70–77.

Subbotin, O. S. (2019). Features of the building materials use in architectural and urban heritage restoration. *IOP Conference Series: Materials Science and Engineering*, Vol. 698, Issue 3, 033045. DOI: 10.1088/1757-899X/698/3/033045.

Ventolà, L., Vendrell, M., Giraldez, P., and Merino, L. (2011). Traditional organic additives improve lime mortars: New old materials for restoration and building natural stone fabrics. Construction and *Building Materials*, Vol. 25, Issue 8, pp. 3313–3318. DOI: 10.1016/j.conbuildmat.2011.03.020.

Vozniuk, G., Kavalerova, E., Kryvenko, P. V., and Petropavlovsky, O. (2013). Physical and chemical properties of adhesives based on geocement for restoration and rehabilitation of building materials. *Advanced Materials Research*, Vol. 688, pp. 123–129. DOI: 10.4028/www.scientific.net/AMR.688.123.

Yevseyev, E. (2016). Evolution of construction technologies in the context of the 19th century architecture history: restoration aspect. *The World of Art: Bulletin of the International Institute of Antiques*, No. 3 (15), pp. 86–92.

РЕСТАВРАЦИОННЫЕ СОСТАВЫ ДЛЯ ТЕРРАЗИТОВОЙ ШТУКАТУРКИ НА ПРИМЕРЕ ОБЪЕКТОВ КУЛЬТУРНОГО НАСЛЕДИЯ XX ВЕКА (РОССИЯ)

Любовь Владимировна Закревская, Галина Юрьевна Маслова, Елизавета Анатольевна Репина

Владимирский государственный университет им. А. Г. и Н. Г. Столетова, Владимир, Россия

*E-mail: elizavetarepina64@gmail.com

Аннотация

Введение: Постепенное разрушение зданий или сооружений исторического значения – это естественный процесс, который остановить, к сожалению, невозможно. Но инновационные материалы способны в значительной степени этот процесс замедлить. Сохранение памятников архитектуры – одно из важнейших направлений реставрационной деятельности. Замена подвергнувшихся разрушениям строительных материалов памятников архитектуры снижает их историческую значимость, происходит утрата культурных ресурсов. Современные строительные материалы и технологии помогают сохранить историческую преемственность. **Цель исследования** состояла в разработке сеток составов смесей терразитовой штукатурки для объектов культурного наследия XX века. **В результате** проведенных исследований были определены составы отобранных образов и составлены сетки составов смесей терразитовой штукатурки, а также определена технологическая последовательность выполнения нанесения терразитовой штукатурки для реставрации фасада здания. По своим технико-экономическим показателям разработанные реставрационные составы позволяют с минимальными затратами вернуть памятникам архитектуры первозданное состояние. Сделаны выводы на основе полученных результатов о значимости для строительной отрасли разработок в области реставрационных строительных материалов, позволяющих вернуть памятникам архитектуры первозданный вид без потери исторической значимости.

Ключевые слова: терразитовая штукатурка, реставрация фасада зданий, объекты культурного наследия.

DOI: 10.23968/2500-0055-2023-8-3-53-59

MODELING OF SNOW LOAD ON ROOFS OF UNIQUE BUILDINGS

Olga Poddaeva

Moscow State University of Civil Engineering (MGSU), Moscow, Russia

E-mail: poddaevaoi@gmail.ru

Abstract

Introduction: The purpose of the work is to study the processes of snow transfer and snow deposition on the roofing of a unique building. Currently, the problem of assigning snow loads to the roofs of buildings and structures remains relevant, since cases of roof collapses in winter are still recorded annually, including those in the Russian Federation. A circus building with the roof in the form of a suspended reinforced concrete shell was chosen as the object of study. **Methods:** The design diagram for this type of roof is contained in SP 20.13330.2016; the snow load distribution diagrams for this roof were adopted according to Appendix B to SP 20.13330.2016. The author considered several options of snow load distribution and chose the most unfavorable one, when an increased value of the snow load is observed on one half of the roofing. During one winter period, field measurements of the thickness of the snow cover were carried out at the site. **Results:** It was established that in general, with the exception of local zones, the actual distribution of snow cover coincides with the adopted design solution, while the actual value of the weight of the snow cover for the current winter season was significantly lower than the calculated one. **Discussion:** The obtained result demonstrates that when developing design solutions for certain types of suspended roofing, it is permissible, without conducting specialized experimental studies, to use the data given in the scientific and technical literature, based on the results of monitoring the thickness of the snow cover on the roofing of the building.

Keywords: snow load, validation, snow deposits, snow transfer.

Introduction

The main task of designing building structures is to ensure their safety. In recent years, the Russian Federation has seen an increase in technogenic emergency failures of buildings and structures (Gar'kin and Gar'kina, 2014). Snow loads are the most common cause of roofing collapses (Lobkina, 2012). Roof collapses of buildings and structures are recorded annually in the territory of the Russian Federation. In the vast majority of cases, underestimation of the snow load at the design stage is what causes such accidents (Lobkina, 2012).

A number of works are devoted to the issues of modeling snow impacts and taking into account snow loads on the roofing of buildings and structures (Bang et al., 1994; Belostotsky et al., 2021; Delpech et al., 1997; Ellingwood and O'Rourke, 1985; Giever and Sack, 1990; Meløysund et al., 2007; O'Rourke and Wrenn, 2004; Poddaeva, 2021; Popov et al., 2001; Scarascia-Mugnozza et al., 2000). Domestic regulatory document SP 20.13330.2016 contains diagrams of snow deposits for typical roof shapes.

In this paper, snow load distribution diagrams are adopted on the basis of the regulatory document SP 20.13330.2016, which is currently in force. The purpose of this work is to assess the possibility of using the specified snow cover distribution diagrams when designing a circus building with a unique roof shape without conducting specialized experimental studies.

Methods

The method for determining snow load is based on the assumption that snow deposits form on the roofing as a result of precipitation and further wind transfer of snow. Fallen snow covers the roof with a uniform layer with a thickness equivalent to the layer on a flatland. During a snowfall, snow may slide off the inclined surfaces of the roof forming snow bags in the proximity of these roof design features. Due to the influence of wind, snow deposits are redistributed, thus forming a general pattern.

Wind transfers the snow particles. The uneven structure of the wind flow over the roofing determines the pattern of snow deposits. The design features of the roofing shape lead to the formation of the zones of low wind speed and the zones of strong wind, which blows snow particles off the surface of the snow cover, and carries them along or off the roof. There are studies that determine the wind speed at which snow is blown off the surface of the snow cover and carried by the wind flow. It is known that when the wind speed decreases, the raised snow falls again on the roof forming an uneven layer of snow deposits. For a given wind direction, a certain vortex structure is formed above the roof, which uniquely determines the redistribution pattern of

snow deposits. A change in wind direction changes the pattern of wind flows over the roof and leads to the formation of new zones with increased snow deposits. During the cold period of the year, when precipitation in the form of snow falls in a given area, the intensity of the snowfall changes randomly, the direction of the wind changes and, as a result, it is impossible to predict what form of snow deposits is expected in the coming winter. The random nature of the atmospheric influence on a building structure requires assigning the load value with a certain margin. At the same time, the roof structure may contain elements of such wind characteristics that the snow cover does not linger there, which allows assigning snow load with a reduction factor. To model snow transfer, different authors use different materials. A common property of the model material is the ability to move it along the roofing under the influence of wind flow. Modeling of snow deposits requires choosing such a flow velocity at which the particles rise from the layer of the fallen model powder and are further transferred along the roofing.

When choosing a model powder, the desire to simulate the microstructure of individual snowflakes is justified. The retention of the model powder on the roofing under study should be identical to natural conditions. At the same time, the range of changes in the physical parameters of natural snow is so wide that the main property of the model powder is the ability to move it with the wind flows. Thus, for identical roof structures, identical snow deposit patterns should be expected for a given wind direction. This criterion can be considered as a parameter for comparing the results of a model experiment performed in different wind tunnels. Based on the results of circular blowing with a certain step along the angle of attack, the snow load on the roof is modeled. When assigning a snow load, the prevailing wind direction, determined in accordance with the methodology outlined above, is taken into account. There may be structural elements on the roofing that can be interpreted as standard shapes reflected in building regulations. When assigning a snow load, “standard” elements are identified and the results of the assigned load are checked with the recommendations of the standard. Wood flour manufactured in accordance with GOST 16361-87 is used as a model material. The moisture content of wood flour in the experiment was no more than 8%, particle size was 0.2 mm.

The process of the experimental research on snow transfer was carried out in three stages:

• Applying a uniform thin layer of wood flour to the roof of the facility.

• Blowing the model with a wind flow at a speed when powder particles begin to fall off the roofing. The typical speed was 2–5 m/s. Exposure for sufficient time until significant transfer of model powder ceased.

• Increasing the flow speed by 2–3 m/s for a few seconds and stopping the blowing.

At the end of the blowing, photographic recording of the results of model snow transfer was carried out. The surface of the model was cleared and the model was rotated to a different angle of attack. The experiment repeated. The number of angles at which blowing was performed was regulated by the technical specifications. In some cases, blowing was carried out in detailed steps in case other structures could interfere with the flow.

Based on the results of the experiment, as well as engineering analysis of regulatory diagrams for snow load distribution, which represent a more conservative approach based on field observations, the snow load was assigned taking into account the prevailing wind directions in the construction area. For buildings and structures, the shape of which differs significantly from the primitives considered in the regulatory documents, developing of recommendations should include the use of the data on similar facilities obtained as a result of monitoring or from published scientific and technical sources.

A circus building with a suspended reinforced concrete shell as its roofing was chosen as the object of study (Fig. 1).

According to clause 10.1 of SP 20.13330.2016 “Loads and actions”, the standard value of the snow load on the horizontal plan of the roofing is determined by the following equation:

$$S_0 = c_e\, c_t\, \mu\, S_g, \quad (1)$$

where c_e is the coefficient that takes into account the removal of snow from building roofing under the influence of wind or other factors, taken equal to one for a given roofing; c_t is the thermal coefficient taken equal to one; m is the coefficient of transition from the weight of snow cover of the ground to the snow load on the roofing, taken in accordance with the SP 20.13330.2016 diagrams; S_g is the weight of snow cover per 1 m^2 of horizontal ground surface. According to clause 10.2 of SP 20.13330.2016, the calculated value of the weight of snow cover per 1 m^2 of horizontal ground surface should be taken as S_g = 245 kgf/m^2.

As a rule, the snow load on the roofs of single-span buildings is distributed unevenly, since the snow deposits on double-slope roofs are blown off the roofing. This phenomenon is reflected in the standards of most countries by means of special coefficients m depending mainly on the roofing incline and elevation differences.

The structural elements located on the roof of the facility under study, as well as the shape of the roofing correspond to the diagrams given in Appendix

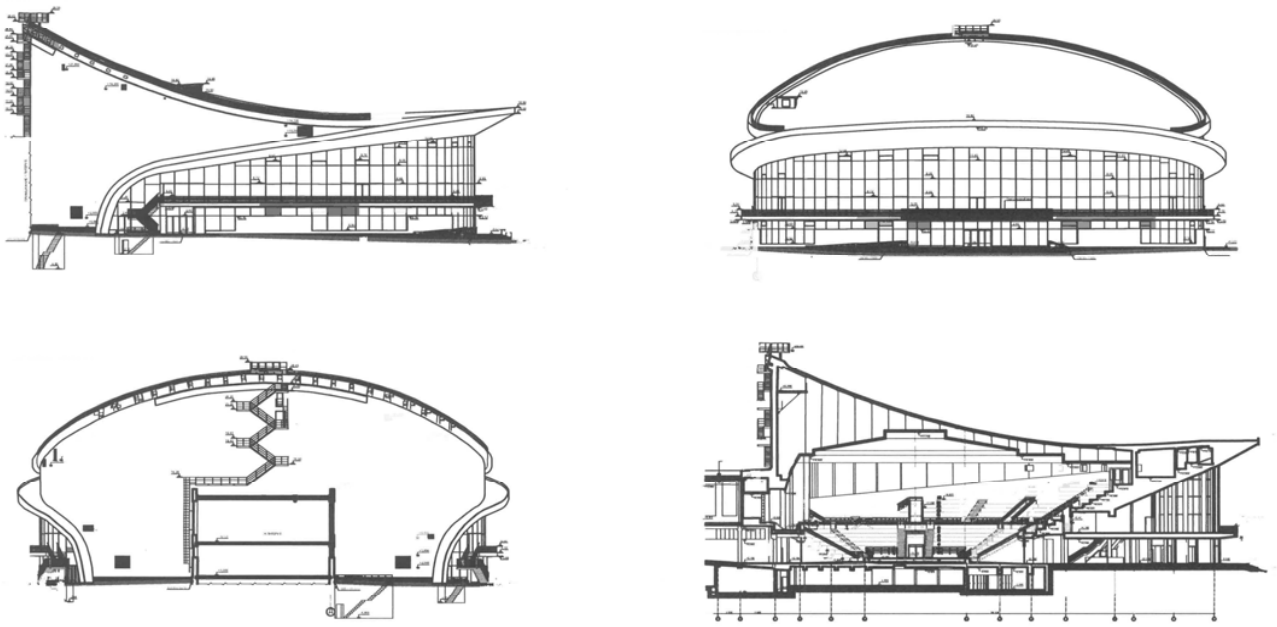

Fig. 1. Facility under study

B to SP 20.13330.2016 “Loads and actions". Updated edition of SNiP 2.01.07-85* permits using the diagrams given in the scientific and technical literature without conducting additional specialized experimental studies when assigning the transition coefficient μ and calculating the snow load.

The distribution of snow load in a section perpendicular to the longitudinal one is assumed to be the same as for a flat surface. Additionally, it is necessary to take into account the diagrams with partial loading of the roofing in both longitudinal and transverse directions. It is precisely these snow load diagrams that make it possible to take into account the most unfavorable operating conditions of the sagging shell.

Diagram B.10 is the closest shape in the longitudinal direction to the considered version of the suspended roof according to SP 20.13330. The standard view of this diagram is shown in Fig. 2.

This diagram takes into account the uniform loading of the roofing over the entire area of the horizontal plan, as well as uneven loading while

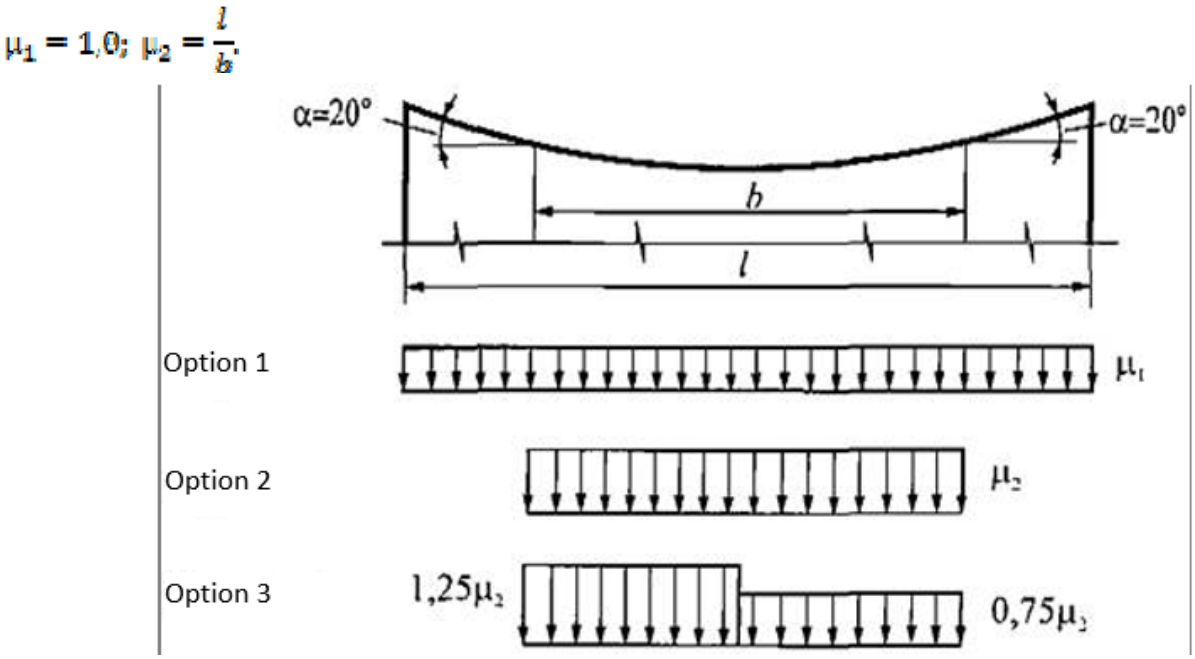

Fig. 2. Diagrams for snow load distribution on suspended cylindrical roofs

considering the possible accumulation of snow in the lower (sagging) part of the roofing and partial snow transfer with a stable wind direction.

Based on the SP Appendix, various options of snow load distribution on the roof of the facility were obtained. The most unfavorable loading option that must be taken into account during design is the diagram shown in Fig. 3. The diagrams show an increased value of the snow load on one half of the roofing as a result of transfer under a stable wind direction.

Results and Discussion

To compare the obtained data, photographic recording (Fig. 4) and field measurements of the thickness of the snow cover on this roof in the winter were carried out.

The measurements were carried out five times during the winter period. The snow load values obtained by taking a snow core were: 12/02/2022 – 16.8 kgf/m^2; 12/09/2022 – 54.3 kgf/m^2; 12/16/2022 – 49.7 kgf/m^2; 12/29/2022 – 76.7 kgf/m^2; 01/13/2023 – 113.8 kgf/m^2.

Snow thickness was measured at various points located according to the diagram in Fig. 5a, and the results of field measurements of the layer thickness at the indicated points are in Fig. 5b.

In general, the results of the field measurements indicate significant uneven distribution of snow cover on the roofing under study. It is not possible to directly compare field measurements and results obtained through analytical calculations even at a qualitative level, primarily due to the fact that the regulatory documents consider an idealized situation when the wind flow is directed strictly along the main coordinate axes of the roof. In our case, the most common direction of wind flow recorded on the dates of field measurements is at an angle to the coordinate axes. This condition explains the difference between the analytical diagrams and monitoring data; quantitative comparison requires a significantly longer observation time. However, the local nature of snow deposits corresponds to the analytical diagrams; zones with snow removal on the leeward part of the roofing (points 15, 17, 19, 25) and a fairly uniform distribution of snow cover in its central part are observed.

In general, the obtained results indicate that when developing design solutions for certain types of suspended roofing, it is permissible to use the data given in the scientific and technical literature, as well as the results of field observations without conducting additional specialized experimental studies. If necessary, one can adjust the snow load distribution diagrams based on the quantitative data from ongoing monitoring.

Conclusions

Comparing the diagrams obtained from the SP with the data of field measurements, it is clear that as a whole, the facility roofing under study corresponds to the diagram of uneven snow cover close to option 1 taking into account the direction of the wind flow (Fig. 3). Obviously, the data from five measurements of snow cover during one season are not enough to draw final conclusions. However, comparison of computational research data (as well as the results of numerical and experimental research) with field observation data is an important direction for ensuring the safety of buildings and structures, especially in matters of assigning snow loads, which have a significant impact on the stress-strain state of building structures.

Funding

All tests were carried out with the use of equipment of the Head Regional Shared Research Facilities and the Large Gradient Wind Tunnel, courtesy of the National Research Moscow State University of Civil Engineering.

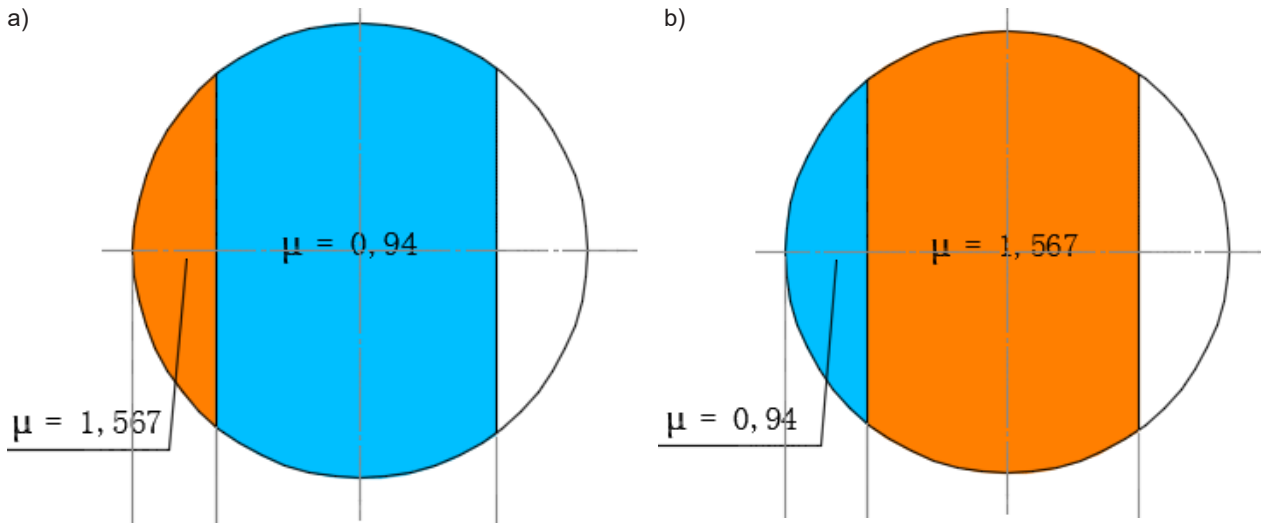

Fig. 3. Options of snow load distribution: a) option 1; b) option 2

Fig. 4. Photo recording of snow transfer on a full-scale facility

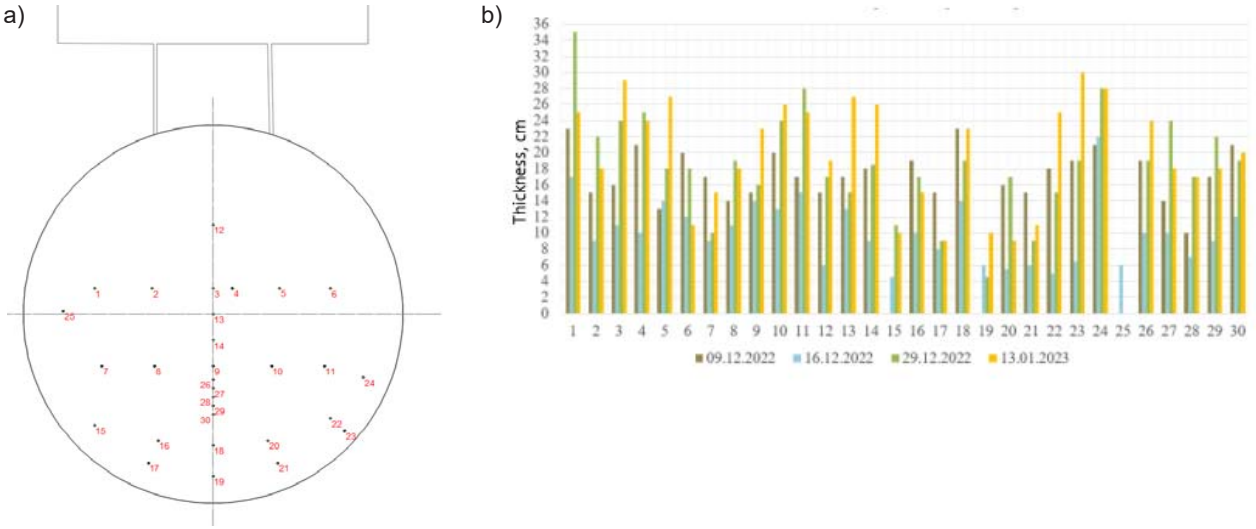

Fig. 5. Diagram of the points located on the roof of the facility (a) and the thickness of the snow cover on the facility roof at the points (b)

References

Bang, B., Nielsen, A., Sundsbø, P. A., and Wiik, T. (1994). Computer simulation of wind speed, wind pressure and snow accumulation around buildings (SNOW-SIM). *Energy and Buildings*, Vol. 21, Issue 3, pp. 235–243. DOI: 10.1016/0378-7788(94)90039-6.

Belostotsky, A., Britikov, N., and Goryachevsky, O. (2021). Comparison of determination of snow loads for roofs in building codes of various countries. *International Journal for Computational Civil and Structural Engineering*, Vol. 17, No. 3, pp. 39–47. DOI: 10.22337/2587-9618-2021-17-3-39-47.

Delpech, Ph., Pailer, P., and Gandemer, J. (1997). Snowdrifting simulation around Antarctic buildings. In: Solari, J. (ed.). *Proceedings of the Second European and African Conference on Wind Engineering*. Padova: SGE, pp. 903–910.

Ellingwood, B. and O'Rourke, M. (1985). Probabilistic models of snow loads on structures. *Structural Safety*, Vol. 2, Issue 4, pp. 291–299. DOI: 10.1016/0167-4730(85)90015-3.

Gar'kin, I. N. and Gar'kina, I. A. (2014). Analysis of collapse causes of industrial buildings structures from the point of view of system approach. *Almanac of Modern Science and Education*, No. 5-6 (84), pp. 48–50.

Giever, P. M. and Sack, R. L. (1990). Similitude considerations for roof snow loads. *Cold Regions Science and Technology*, Vol. 19, Issue 1, pp. 59–71. DOI: 10.1016/0165-232X(90)90018-R.

Lobkina, V. A. (2012). Damage from snow loads in the Russian Federation. Causes and consequences. *GeoRisk*, No. 1, pp. 50–53.

Meløysund, V., Lisø, K. R., Hygen, H. O., Høiseth, K. V., and Leira, B. (2007). Effects of wind exposure on roof snow loads. *Building and Environment*, Vol. 42, Issue 10, pp. 3726–3736. DOI: 10.1016/j.buildenv.2006.09.005.

O'Rourke, M. and Wrenn, P. D. (2004). *Snow loads. A guide to the use and understanding of the snow load provisions of ASCE 7-02*. Reston, VA: American Society of Civil Engineers, 133 p.

Poddaeva, O. (2021). Experimental modeling of snow action on unique construction facilities. *Architecture and Engineering*, Vol. 6, No. 2, pp. 45–51. DOI: 10.23968/2500-0055-2021-6-2-45-51.

Popov, N. A., Otstavnov, V. A., and Berezin M. A. (2001). Wind tunnel investigations of wind and snow loads acting on long-span roofs. In: Wisse, J. A., Kleinman, C. S., Geurts, C. P. W., and de Wit, M. H. (eds.). *Proceedings of the Third European & African Conference on Wind Engineering*. Eindhoven: Technische Universiteit Eindhoven, pp. 115–118.

Scarascia-Mugnozza, G., Castellano, J., Roux, P., Gratraud, J., Palier, P., Dufresne de Virel, M., and Robertson, A. (2000). Snow distributions on greenhouses. In: Hjorth-Hansen, E., Holand, I., Løset, S., and Norem, H. (eds.). *Snow Engineering 2000: Recent advances and developments*. London: Routledge, pp. 265–274.

МОДЕЛИРОВАНИЕ СНЕГОВОЙ НАГРУЗКИ НА ПОКРЫТИЯХ УНИКАЛЬНЫХ ЗДАНИЙ

Ольга Игоревна Поддаева

НИУ МГСУ, Москва, Россия

E-mail: poddaevaoi@gmail.ru

Аннотация
Введение: Целью работы является исследование процессов снегопереноса и снегоотложений на кровельном покрытии уникального здания. В настоящее время проблема назначения снеговой нагрузки на покрытия зданий и сооружений остается актуальной, поскольку случаи обрушения кровель в зимний период по-прежнему ежегодно фиксируются, в том числе на территории РФ. В качестве объекта исследования было выбрано здание цирка с покрытием в виде висячей железобетонной оболочки. **Методы:** Расчетная схема для данного типа кровли содержится в СП 20.13330.2016, схемы распределения снеговой нагрузки для данной кровли были приняты по приложению Б СП 20.13330.2016. Рассмотрены несколько вариантов распределения снеговой нагрузки, выбран самый неблагоприятный, когда наблюдается повышенное значение снеговой нагрузки на одной половине покрытия. В течение одного зимнего периода были проведены натурные замеры толщины снежного покрова на данном объекте. **Результаты:** Установлено, что в целом, за исключением локальных зон, реальное распределение снежного покрова совпадает с принятым проектным решением, при этом реальное значение веса снежного покрова для текущего зимнего сезона существенно ниже расчетного. **Обсуждения:** Полученный результат демонстрирует, что при разработке проектных решений для отдельных типов висячих кровельных покрытий допустимо без проведения специализированных экспериментальных исследований использовать данные, приведенные в научно-технической литературе, базирующиеся на результатах мониторинга толщины снежного покрова на поверхности покрытия здания.

Ключевые слова: снеговая нагрузка, валидация, снегоотложение, снегоперенос.

DOI: 10.23968/2500-0055-2023-8-3-60-76

ENERGY PERFORMANCE-BASED RETROFIT OF APARTMENT BUILDINGS IN ALBANIA USING MASS-HOUSING TYPOLOGIES AS CASE STUDIES

Anna Yunitsyna*, Ilda Sadrija

Epoka University, Tirana, Albania

*Corresponding author′s e-mail: ayunitsyna@epoka.edu.al

Abstract

Introduction: The study is focused on the analysis of the energy performance of mass-housing residential buildings in Albania and further evaluation of the opportunities for energy retrofit of these buildings. Currently, in Albania, energy performance evaluation is mandatory for newly constructed buildings, but there are no approaches that would address the existing building stock. **Methods:** The goal of this study is to evaluate apartment buildings of the communist period in Tirana and Shkodra and apply a number of passive and active retrofit strategies, which are appropriate in the Mediterranean climate conditions. **Results and Discussion:** Improvement of thermal conductivity and energy balance can be achieved through the additional insulation of the buildings' walls and roofs and window replacement, installation of photovoltaic panels and energy-efficient lighting. The application of passive strategies reduces energy losses in Tirana by 56% and in Shkodra — by 57%. **Conclusions:** Installation of photovoltaic panels can meet cooling and lighting demands during the warm period; however, their contribution during the wintertime is insufficient to satisfy heating demands.

Keywords: apartment building retrofit, building energy performance, energy efficiency, photovoltaic systems, energy balance.

Introduction

Energy performance of buildings is critical for the community. In Europe, urban areas account for 80% of carbon emissions. Industries, buildings, and transport increase the overall pollution (Harmathy et el., 2019). Residential areas account for 30–40% of the overall energy consumption (Huovila et al., 2007). In Albania, 60% of electricity is consumed by residential buildings (Struga and Marko, 2019). Renovating a building to reduce its energy consumption is quite important during the energy crisis. According to EUROSTAT (2020), the first global decrease in energy use was caused by the global financial crisis in 2009. In 2010, energy consumption recovered, however during COVID-19 it decreased again. Currently, European countries are forced to reduce energy use due to high prices and shortage of available fossil fuel sources. In the EU, residential buildings are the main target for the investments aiming to save energy by increasing passive energy gains, minimizing the use of fossil fuels, and reducing the overall energy use and energy consumption by residents (Botta, 2005). The EU building stock is extremely diverse and includes historic, prefabricated, and modern buildings of different heights and sizes, which requires the development of a large number of renovation scenarios.

This study is focused on the evaluation of the energy efficiency of brick residential buildings of the communist period in Tirana and Shkodra. It includes a renovation proposal using passive and active strategies to improve energy balance. The retrofit scenario includes improvement of the thermal performance of buildings and generation of renewable energy using photovoltaic panels. The goal of this study is to develop a renovation technique that could improve energy performance with moderate intervention in the Mediterranean climate conditions.

New knowledge about the environmental performance of buildings led to the expansion of building environmental evaluation tools (Villegas, 2017). To make a building energy-efficient, it is necessary to analyze the dynamic thermal behavior of each of its elements, the climate and site conditions, and the behavior of its users (Yüksek and Karadayi, 2017). The general approach towards building retrofitting includes measures aimed to decrease energy consumption, reduce energy demand, control energy use, and use on-site-generated energy (Felius et al., 2020). Renovation with the use of passive house techniques is an effective strategy to reduce energy use, which goes along with the EU building energy standards (Figueiredo et al., 2020). Strategies to reduce energy demand include insulation of the building envelope, window retrofit, cold roof application, air exchange reduction, controlled ventilation, upgrade of household equipment and lighting, and thermal energy accumulation (Ma et al., 2012). Passive house design strategies are applied in the construction of new buildings all over the world. Due to low energy

For citations: Yunitsyna, A., Sadrija, I. (2023). Energy performance-based retrofit of apartment buildings in Albania using mass-housing typologies as case studies. Architecture and Engineering, No 3 (8), pp. 60-76. DOI: 10.23968/2500-0055-2023-8-3-60-76.

consumption, the performance of these buildings is not drastically affected by the behavior of residents, which makes it predictable in terms of energy needs (Pitts, 2017). In housing construction, renewable energy can be provided by solar water heaters, photovoltaic panels, wind power, geothermal power, and biomass power systems (Ma et al., 2012).

All retrofit measures can be divided into those related to the building envelope and installation improvements (Konstantinou and Knaack, 2011). Energy efficiency standards specify the thermal resistance of windows, doors, walls, roofs, balconies, and other exterior components, as well as cover heating, cooling, air conditioning, ventilation, lighting, controls, fans, and electricity for external lighting. The primary focus of an energy-efficient building is on the building envelope (Laustsen, 2008). Başarır et al. (2012) state that 40% of energy losses in a multi-story building are through the exterior walls, 30% — through the windows, and the rest is attributed to the roof, basement slab, and air leaks. Therefore, they find it feasible to apply retrofit strategies to the roof, windows, and walls.

In case of brick buildings, the use of the exterior layer of thermal insulation contributes to minimizing the influence of adverse weather conditions and reduces the impact of thermal bridges (Kass et al., 2015). In the UK, the application of the external insulation layer over the brick walls reduces the annual heat losses through the walls by 75% and has the 5–6.5-year investment payback period (Brannigan and Booth, 2013). The optimal thickness of the thermal insulation layer should be selected based on the balance between energy performance and cost-effectiveness (Bonakdar et al., 2017). The climate zone and annual energy consumption requirements established by national standards affect the selection of the material and thickness of the thermal insulation layer (Usta and Zengin, 2021).

Energy-efficient roofs are designed with the aim of minimizing energy losses by reflecting sunlight and absorbing less heat. A green roof can be a good decision for the improvement of the energy performance of urban buildings with flat roofs (Department of Energy, 2015). The cool roof application reduces cooling energy demands during the hot season; however, it increases energy consumption for heating in winter (Ganguly et al., 2016). A study from Sicily demonstrates that a cool roof with the adequate thermal insulation layer reduces cooling energy demands by 54% (Romeo and Zinzi, 2013). A Shanghai case shows 8.7–14.9% reduction in the heating loads depending on the thickness of roof insulation (Chen et al., 2019). Comparable results with 14–15% reduction in the heating loads of the insulated roof were achieved with the roof retrofit of a building in New Kensington, PA (Habibi et al., 2020).

Energy-efficient windows should be selected appropriately, with account for the climate zone. Glazing with the use of weather stripping as well as thermal treatment and coverings reduces cooling demands in warm climates by more than 40% (AboKhalil and Ahemd, 2013). In Hong Kong, in hot summer and warm winter, the application of low-e glazing ensures energy reduction by up to 10% (He et al., 2019), while in the colder climate of Berlin, the application of triple-glazed low-e windows reduces heating loads by up to 66% (Urbikain, 2019). Building energy performance depends on the window-to-wall ratio, the solar heat gain coefficient, and the U-value of the windows. A study from South Korea demonstrates that the change of the U-value affects the level of energy savings, while the larger size of the retrofitted windows may cause an increase in the cooling loads (Ahn et al., 2015).

Switching to LED light bulbs has relatively high initial costs but the owners of a building can recoup the extra cost through the reduced utility and maintenance expenses (Bertoldi et al., 2001). Replacement of incandescent light bulbs with LED lights without dimming results in 62% reduction in energy consumption for lighting (Gavioli et al., 2015). Advanced occupancy control lighting systems, such as movement sensors, and automated daylight and shading control systems have the potential to increase energy savings by up to 93% (Dubois et al., 2015).

Renewable energy systems bring a valuable contribution to the reduction of overall building energy consumption (de Almeida et al., 2017). Installation of photovoltaic panels can supply all the energy needs of a building, which include lighting, heating, cooling systems, hot water and appliances (Ray, 2010). PV systems can be installed both on the roofs and facades of multi-story residential buildings, however, their performance depends on the surface orientation and the roof angle (Fina et al., 2019). The Mediterranean countries have great potential for the use of renewable solar energy, however, currently, in the southern and eastern regions, the use of fossil fuels prevails (Ciriminna et al., 2019). A PV system applied on the roof of a detached building in Madrid generated energy that could supply 43% of the annual demands (Aldegheri et al., 2014). In the case of a detached passive building in Jordan, the roof-based solar system reduced up to 83.7% of annual electricity consumption (Jaber and Hawa, 2016).

The evaluation of housing retrofit strategies applied in the Mediterranean region demonstrates that modifications of the building envelope, such as the thermal insulation of the walls and the installation of energy-efficient windows, reduce the heat transfer coefficient by 50% (Carpino et al., 2017). The results of energy-efficient retrofit of a 7-story apartment building in Athens show 80.3% of energy savings. The

retrofit plan included extensive energy simulations, thermal insulation and installation of energy-efficient windows, energy-efficient lighting, smart coverings, and a night ventilation passive technique (Synnefa et al., 2017). Similar results of 80% savings were achieved in the renovation of an apartment building in Austria. The facade of the building was covered with large active and passive facade elements, the pitched roof was converted to a flat roof with arrays of photovoltaic panels, and a mechanical ventilation system with heat recovery was installed. In the case of a multi-family building in Denmark, the improvement of the R-value of the whole building envelope provided 31% energy savings (Höfler et al., 2014). The retrofit strategy used in a gated community in Egypt, based on the additional thermal insulation of the roof and walls, use of single-glazed windows with shading devices, installation of efficient lighting, and integration of PV panels, reduced the energy loads at the community level by up to 88.68%, which made the buildings nearly zero-energy (Adly and El-Khouly, 2022). In a case from Algeria, the use of passive strategies for the retrofit of a middle-story apartment building included the thermal insulation of the roof, exterior and, partially, interior walls, double-glazed windows, glazing of the verandas, and installation of shading devices, which resulted in a decrease in the annual energy loads. At the apartment level, its location, orientation, and total area affect its energy performance significantly (Djebbar et al., 2018). A retrofit case from Switzerland, with the replacement of the windows, modifications of the facade and roof, installation of mechanical ventilation and water heating systems, and improvement of lighting, shows reduction in the heating demand by 90% (Höfler et al., 2014). A combination of changes to the building envelope and installation of PV panels resulted in 70% reduction of energy consumption in Portugal (Höfler et al., 2014).

Housing stock and current retrofit strategies in Albania

The current residential architecture in Albania can be classified by year of construction and building size. The first period of housing construction started in 1929–1932 under the Austrian influence. The prevailing housing typology was represented by detached or semi-detached residential villas with one or two floors (Hoxha et al., 2018). During the period of the Italian influence (1939–1943), the first apartment buildings with a height of up to four floors were constructed. During the communist period, massive residential construction using prefabricated building typologies was performed in Albania. Urban development was strongly influenced by the theory and practice of architects from the Soviet Union. The residential neighborhoods were designed using repetitive housing units, which could be applied throughout the country. The multi-family buildings were designed as units of a simple shape with a height of up to five floors. The apartment solutions were simple and rational; nevertheless, all the standards of natural lighting and ventilation were implemented, and the minimum required sanitary equipment was installed (Ndreçka and Nepravishta, 2014). However, except for the case of the coldest mountainous regions, no measures were taken to implement central heating or cooling and water heating (Aliaj, 2003). The structural solutions were the same throughout the country, therefore, the regions with different climate conditions did not differ in terms of the amount of thermal insulation. More than half of the Albanian buildings, which were built from 1945 to 1990, have significant problems in relation to energy performance and indoor comfort of inhabitants. The apartment buildings constructed in 1960–1990 are characterized by significant energy losses due to low quality of construction, thermal bridges, uninsulated structures, single-glazed windows, and open staircases. During the last decade of the communist regime (1979–1990), a new prefabrication typology with the use of composite load-bearing panels was introduced. The 14 cm lightweight cellular concrete, which was used to produce the panels, served as thermal insulation. Bitumen paste was used for the water-proofing of the seams between the panels at the construction site. The same types of panels were applied throughout the country, however, in the cold regions, compact apartment blocks with a simple rectangular perimeter were mainly constructed, while in the warmer areas, more expressive structures with a complex perimeter were used (Abazaj, 2019).

During the transition period of the 1990s, the Albanian state had minimal control over the urban development, which resulted in the massive growth of unauthorized individual dwelling construction and the reduction of architectural and structural quality of multi-family apartment blocks. Due to the implementation of concrete frames, the height of the buidlings grew up to nine floors. The exterior walls were composed of 20 cm hollow bricks and a plaster layer without thermal insulation. A thin layer of thermal insulation was added to the roofs of the buildings, which was covered with water-proofing materials and gravel. Overall residential comfort in these buidlings is quite low due to significant heat losses and moisture inside the living space (Dobjani, 2020).

All buildings constructed in Albania after 2003 must meet the standards established in the Energy Building Code and the law on energy saving and conservation in buildings (EEA, 2016), but currently, most buildings need to be renovated with the application of energy efficiency standards. Law No. 116/2016 “On the energy performance of buildings” (Këshilli i Ministrave, 2016) stipulates the following to be taken into account during the evaluation of energy performance:

– thermal characteristics of the building structure including thermal capacity, insolation, passive heating, cooling elements, and thermal bridges;
– heating systems and hot water supply systems;
– air conditioning systems;
– natural and mechanical ventilation systems;
– lighting systems;
– design, location and orientation of the building;
– shading systems;
– interior air conditioning;
– internal loads.

According to Law No 124/2015 “On energy efficiency”, every renovated building in Albania needs to pass the energy audit in order to satisfy the minimum energy efficiency requirements (Këshilli i Ministrave, 2015). One of the parameters to be evaluated is the energy consumption of the building before and after the renovation. The national energy policies define the level of the energy performance of household appliances, such as fridges, stoves, washing machines, air conditioners, TV sets, and domestic lamps. The solar radiation values and the annual number of sunny days in the Mediterranean region are very high compared to other European countries (Buchinger et al., 2017), which makes it reasonable to use solar water heaters and photovoltaic panels for energy generation.

During the last decade, several studies on the improvement of energy performance in residential buildings in Albania were conducted. A study based on the estimation of the volume coefficient of global losses for 24 buildings shows that it is necessary to add a 5 cm thermal insulation layer in order to ensure the thermal performance of a building in accordance with the European standards (Simaku, 2017). In Tirana, adding a 6 cm external thermal insulation layer to a contemporary 9-story building reduces the heating costs by 49–54% depending on the building size (Dobjani, 2020). A general evaluation of the potential performance of the entire residential building stock in Tirana demonstrates 47% energy savings. In case of a brick building, the maximum contribution was provided by 5 cm wall and roof insulation (6% and 5%, respectively), glazing (6%), reduced infiltration (9%), and the installation of PV panels (8%) (Sherifi, 2017). A retrofit scenario in Kosovo, a neighboring Albanian-speaking country, includes the replacement of the windows as well as the roof and walls in a detached brick building. Due to the poor economic conditions, the residents prefer choosing 5 cm thermal insulation and double-glazed windows, while the optimal scenario including 15 cm roof and wall thermal insulation and triple-glazed windows demonstrates a significant reduction in energy costs for a 20-year period (Bajraktari et al., 2019). An analysis of retrofit scenarios for public buildings in Albania shows improvements in the energy efficiency, however, the resulting energy demands are higher due to poor indoor comfort and currently limited use of heating and cooling systems (Novikova et al., 2020).

Methods

The annual energy demand is the main parameter of energy efficiency (Glushkov et al., 2016). It is the amount of energy consumed per square meter of the building area, which can be compared with the standards established for different building typologies and different climate conditions. Low-energy design involves the inspection of heat transfer, energy supply, and energy consumption in buildings. Ahuja et al. (2015) state that a building’s orientation, materials and components, shape compactness, volume, and perimeter complexity affect energy performance. Djebbar et al. (2019) suggest studying the specifics of the building envelope, structural solutions, heating, cooling, water heating and ventilation systems before choosing retrofit strategies.

The evaluation of energy performance started from the selection of two brick buildings as case studies. During the archival research and field observations, general spatial and structural parameters, such as the building area and height, design solutions, type of the construction system, structure of the walls and roofs, types and dimensions of the windows and doors, as well as climate conditions were studied. Based on those parameters, Revit 3D models representing all the important features of the buildings were built. At the second stage, passive and active strategies for retrofit were selected, including thermal insulation of the walls and roofs, triple-glazed windows, energy-efficient lighting, and installation of photovoltaic panels. The energy consumption scenarios of the case studies were evaluated with simulation using various software, such as PV Watts, PV CAD calculator, Design Builder, EnergyPlus engine, and Revit. The annual energy balance was evaluated after the calculation of energy gains and energy losses during heating and cooling periods.

The study addresses two prefabricated brick buildings located in Tirana and Shkodra. These buildings are similar in terms of architectural layout, spatial distribution, construction materials and techniques. Fig. 1 shows the location of the two cities in Albania and the location of the two selected buildings in the urban context.

The capital city of Tirana is located in the central part of Albania on the Plain of Tirana and surrounded by Dajti Mountain from the east and a range of hills from the south-west. The distance from the Adriatic Sea is about 27 km. Tirana is one of the largest cities in the Balkans, and during the last century, it transformed from a small settlement to a large metropolis. The urban fabric of Tirana is very diverse, and it is composed of historical Ottoman neighborhoods, prefabricated residential

Fig. 1. Location of the selected cities in Albania and location of the selected buildings in the urban context (source: the authors, 2021)

blocks constructed during the communist regime, unauthorized detached residences as well as massive residential complexes and high-rise apartment buildings constructed during the transition and democracy periods.

The city of Shkodra is located in the northern part of Albania, and it ranks fifth in the country by population. It occupies the Plain of Mbishkodra and is surrounded by the Shkodra Lake from the north, the foothills of the Albanian Alps, and Buna, Drin and Kir rivers. The distance to the Adriatic coast is about 25 km. The urban fabric of Shkodra mainly consists of mid-rise buildings, including historical Ottoman districts, prefabricated blocks and detached houses as well as mid-scale and high-rise buildings of the recent periods. The prefabricated blocks located along all the main streets of Shkodra take the significant part of its housing stock.

Both cities are located in the Mediterranean climate zone based on the Köppen climate classification (Chen and Chen, 2013). This zone is characterized by mild temperate climate with hot, dry summer. Fig. 2 gives a general overview of the climate conditions of Shkodra and Tirana.

The climate conditions of the two cities are very similar, however, there are some differences due to the difference in the surrounding geographical features. In Tirana, the average temperature of the hot season is 24.6°C and the average temperature of the cool season is 6.1°C, the warmest month is July, and the coldest month is January (Weather Spark, 2021b). In Shkodra, the average temperature of the hot season is 26°C and the average temperature of the cool season is 5.8°C, the warmest month is August (Weather Spark, 2021b). The average wind speed during the warm season is 8.9 km/h for both cities, but during the cold season, the average wind speed in Shkodra is 15 km/h, which is higher than in Tirana — 13.4 km/h. The amount of precipitation in Shkodra and Tirana is similar, while the monthly rainfall is significantly higher in Shkodra during the cold season.

- **Case Study 1 (Tirana)**

Case study 1 (Fig. 3) is a former exhibit block built during the communist period in Albania and located in Tirana near the Kombinati neighborhood, known as Kompleksi Bushi. This four-floor building has a simple geometric shape and a flat roof. It is composed of eight apartments per floor, which can be accessed from two staircases. In the post-communist period, many individual household interventions were made, distorting the block's elevations and changing them in a non-uniform manner with uncontrolled additions. Some parts of the facades remained brick, while the others were plastered and painted according to the individual decisions of the inhabitants.

- **Case Study 2 (Shkodra)**

Case study 2 (Fig. 4) is a residential building in Shkodra located on the Daut Borici Road. This brick building with a flat roof is composed of two units connected with each other by an open staircase. This type of residential building has five floors. The first floor is of mixed use and includes apartments and various businesses, services, and shops, while other floors are composed of six apartments each. Similar to the Tirana case, the facades were plastered in a non-uniform manner by the inhabitants.

The key features of these two case studies are given in Table 1.

The two buildings are similar in the building scale, construction materials and techniques, and state of preservation. The design is not unique, since during

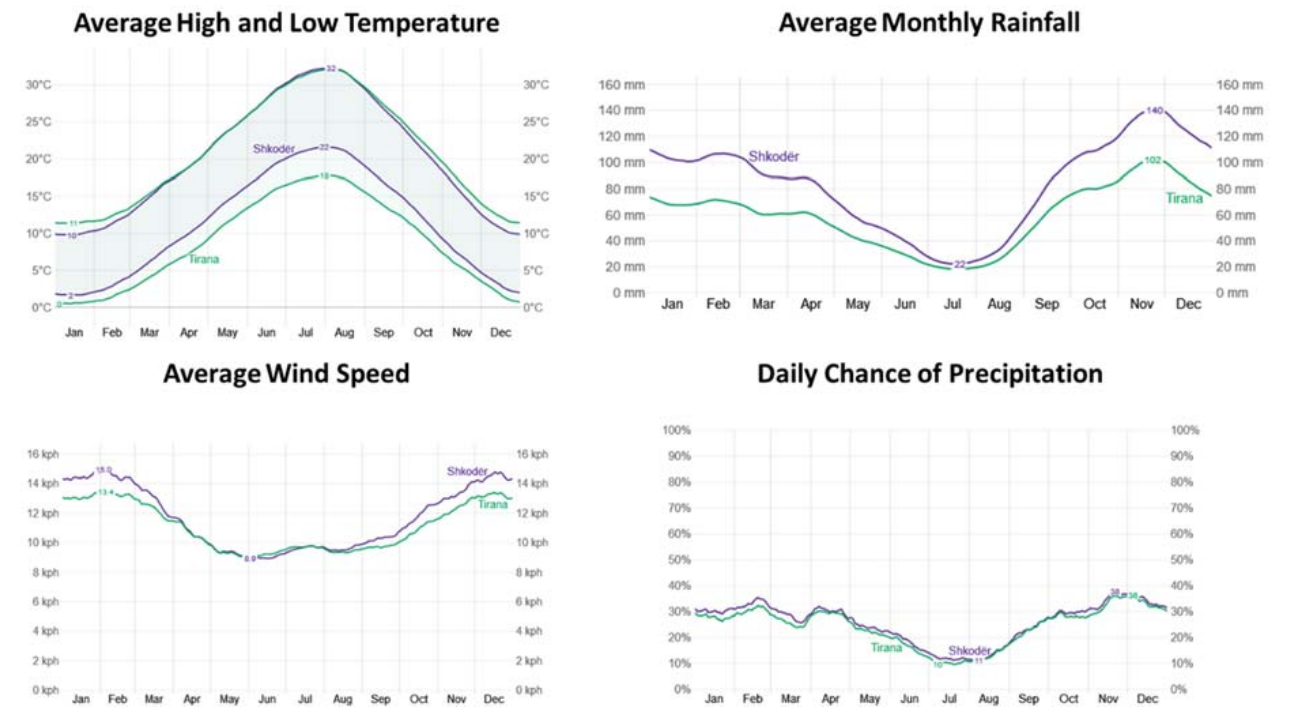

Fig. 2. Average high and low temperature, average monthly rainfall, average wing speed, and daily chance of precipitation in Tirana and Shkodra (Weather Spark, 2022)

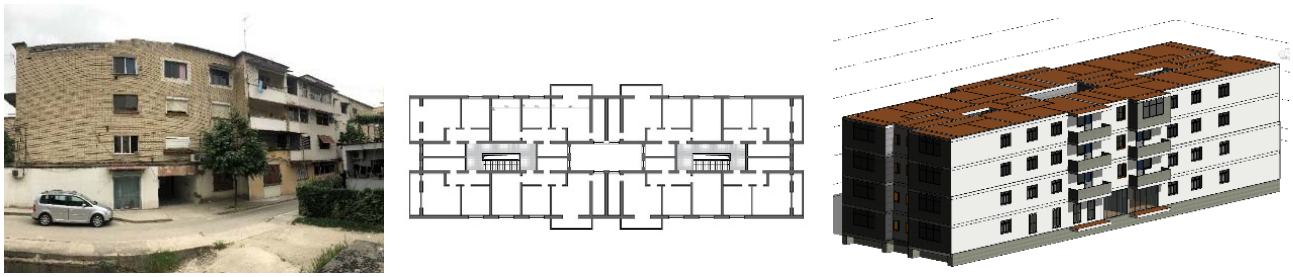

Fig. 3. Street view (photo by the authors), plan view, and 3D model of the Tirana case study (source: the authors, extracted from the Revit software, 2021)

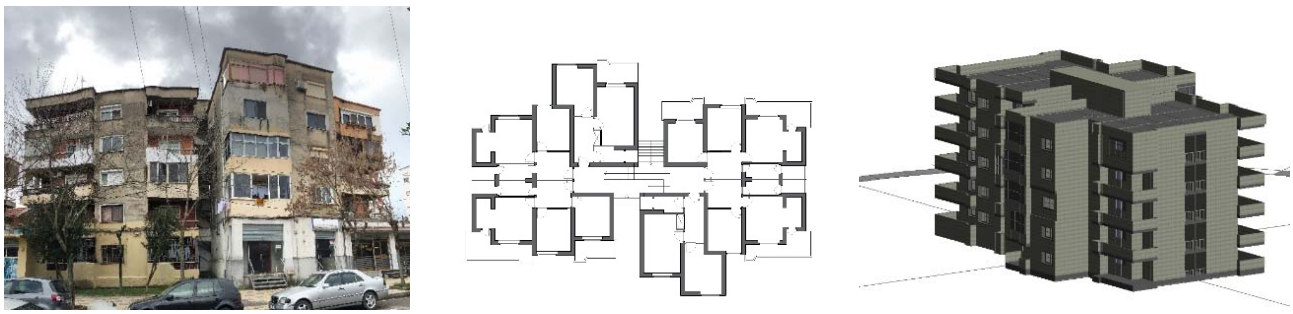

Fig. 4. Street view (photo by the authors), plan view, and 3D model of the Shkodra case study (source: the authors, extracted from the Revit software, 2021)

the communist period these dwelling typologies were repetitively built throughout the country. The apartment blocks were constructed with the use of load-bearing brick walls. The two buildings are also comparable by the number of apartments. There is no thermal insulation applied to the external walls and roofs. The existing windows and balconies are double-glazed, with wooden frames. There are no central heating and cooling systems, no central water heating. During the last decade, the residents were taking individual measures to improve the thermal performance of the buildings, including

Table 1. **Summary of two case studies**

	Case study 1. Tirana	**Case study 2. Shkodra**
Typology	Residential apartment building	Residential apartment building
No. of floors	4	5
No. of apartments	32	30
Construction year	1965–1975	1975–1980
Structural system	Load-bearing walls	Load-bearing walls
Object state	Degraded	Good
Facade	Windows, balconies	Windows, balconies
Facade extensions	Yes	No
Facade materials	Brick, partially plastered	Plaster
Windows	Single, partially double glazing	Single, partially double glazing
First floor	Services, bar, cafe, shops	Mixed use (apartments + businesses)
Footprint area, m²	765	523
Total area, m²	3060	2165
Perimeter, m	110	115
Total wall area, m²	1099	1491
Total window area, m²	221	234

the replacement of the old wooden windows with plastic ones, partial insulation and finishing of the facades, glazing of the balconies, and arrangement of additional rooms on the first floor. Heating and cooling is provided with air conditioners installed by the residents.

Results

– **Improvement of the thermal insulation of the building envelope**

The walls lose 19–20% of heat used to heat the apartments. The exterior walls of both case study buildings are composed of a double brick layer and a plaster layer. The renovation strategy includes the following changes: addition of a 5 cm exterior fiberglass batt layer; improvement of the interior plaster; and addition of a 3 cm exterior plaster layer (Fig. 5).

The roof construction (Fig. 6) is similar for the two case studies. The renovation strategy includes: addition of a polystyrene layer; addition of a vapor insulation membrane; water-proofing and a protective layer; and improvement of the interior plaster.

To find the heat conduction in the case of both the walls and roofs, the first step is to find the thermal resistance of each of the materials (R_i):

$$R_i = \frac{x_i}{k_i}, \quad (1)$$

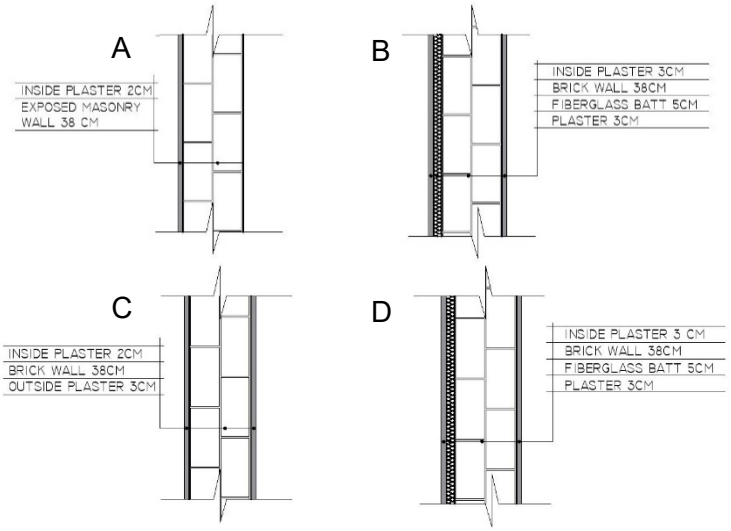

Fig. 5. Details of the existing wall in Tirana (A) and Shkodra (C) and the proposed new walls in Tirana (B) and Shkodra (D) (source: the authors, extracted from the AutoCAD software, 2021)

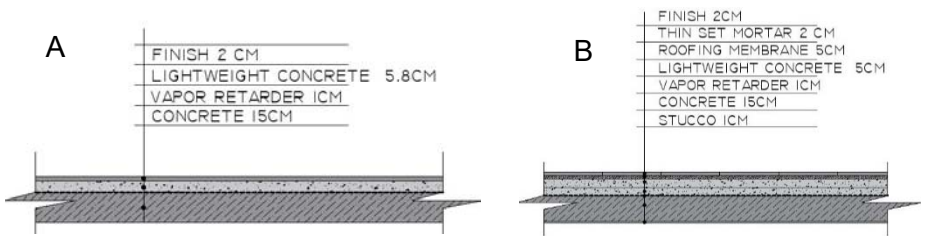

Fig. 6. Details of the existing roof (A) and the proposed roof (B) in Tirana and Shkodra (source: the authors, extracted from the AutoCAD software, 2021)

Table 2. **Material composition and thermal resistance of the existing and proposed walls and roofs in two case studies**

Materials	x exist., m	k, W/(mK)	R exist., m²K/W	x prop., m	k, W/(mK)	R prop., m²K/W
Case study 1. Tirana. Walls						
Interior plaster	0.03	0.42	0.071	0.03	0.42	0.071
Brick	0.38	0.9	0.422	0.38	0.9	0.422
Fiberglass wool	-	-	-	0.05	0.03	1.613
Exterior plaster	-	-	-	0.03	0.42	0.071
Total			0.494			2.178
Case study 2. Shkodra. Walls						
Interior plaster	0.03	0.42	0.071	0.03	0.42	0.071
Brick	0.38	0.9	0.422	0.38	0.9	0.422
Mineral wool	-	-	-	0.05	0.045	1.111
Exterior plaster	0.03	0.42	0.071	0.03	0.42	0.071
Total			0.565			1.676
Case study 1 and 2. Roof						
Interior plaster	0.02	0.41	0.488	0.02	0.41	0.488
Concrete	0.18	1.6	0.113	0.18	1.6	0.113
Polystyrene	-	-	-	0.05	0.8	0.063
Lightweight concrete	0.05	0.4	0.125	0.05	0.4	0.125
Bitumen	0.01	0.138	0.072	0.01	0.138	0.072
Total			0.798			0.860

where x_i is the thickness of the material and k_i is the thermal conductivity coefficient. The summary of the thermal resistance values of the walls and roofs before and after the retrofit is given in Table 2.

The second step is to calculate the heat conduction of multi-layered objects, which gives the total amount of heat losses during the heating or cooling period (Q).

$$Q = \frac{1}{\sum R} A\left(T_1 - T_2\right) 24\,\mathrm{HDD}, \qquad (2)$$

where $\sum R$ is the sum of all thermal resistance values of the layers; A is the surface of the material; $T_1 - T_2$ is the difference between the indoor and outdoor temperatures, and *HDD* is the amount of heating or cooling degree days in a season. The renovation strategy demonstrates 77% increase in the thermal resistance of the building walls in the case of Tirana and 66% increase in the case of Shkodra. For the roof, in both cases, an increase in the thermal resistance is 7% (Table 3). The retrofit strategy also includes the replacement of the double windows with high-performance windows with triple glazing, which increases thermal resistance by 78%.

Tirana and Shkodra are both located in a warm zone, and the two cities slightly differ in climate and in the duration of the heating and cooling seasons due to their location (climate-data.org, 2021a, 2021b; Weather Spark, 2021a, 2021b). Table 4 shows the average temperature and the duration of the hot and cold seasons in these two cities.

During the calculation of the annual energy losses, the heating loads during the cold season and the cooling loads for air conditioning during the hot season were evaluated. The indoor temperature was accepted at the level of 21°C. The energy losses for the different building envelope elements during the cooling and heating seasons calculated for the whole building and for the square meter of its area are shown in Table 5.

Based on the calculation, it can be seen that the energy consumed during the cooling period in summer is comparable to the energy needed to heat the building during the wintertime. The duration

Table 3. **Thermal resistance of the existing and proposed building elements in two case studies**

Building element	Case study 1. Tirana		Case study 2. Shkodra	
	R existing, m²K/W	R proposed, m²K/W	R existing, m²K/W	R proposed, m²K/W
Walls	0.494	2.178	0.565	1.676
Windows	0.260	1.200	0.260	1.200
Roof	0.798	0.860	0.798	0.860

Table 4. **Average temperature and duration of the heating and cooling seasons in Shkodra and Tirana**

	Case study 1. Tirana		Case study 2. Shkodra	
	Hot season	Cold season	Hot season	Cold season
Average temperature, C°	24.6	6.1	26	5.8
Duration, days	88	116	90	110

Table 5. **Energy losses during the heating and cooling seasons in Shkodra and Tirana**

Building element	Case study 1. Tirana				Case study 2. Shkodra			
	Q existing		Q proposed		Q existing		Q proposed	
	Whole building, kWh	Per m^2, kWh/m^2	Whole building, kWh	Per m^2, kWh/m^2	Whole building, kWh	Per m^2, kWh/m^2	Whole building, kWh	Per m^2, kWh/m^2
Heating season								
Walls	91,976	30.05	20,860	6.82	105,765	48.85	41,853	19.2
Windows	39,633	12.95	7614	2.49	36,069	16.66	9175	4.24
Roof	34,141	11.16	36,774	12.01	30,834	14.24	28,609	13.21
Cooling season								
Walls	16,999	5.56	3856	1.26	28,643	13.23	9656	4.46
Windows	6495	2.12	1407	0.46	9769	4.51	2117	0.98
Roof	7325	2.39	6797	2.22	7114	3.29	6601	3.05

of the two periods is almost equal, which can be explained by the Mediterranean location of the two case studies. Currently, a significant amount of energy is transferred through the building walls, but the proposed renovation measures make it possible to decrease energy losses. The selected measures are efficient for the building walls and windows, but the renovated roof demonstrates only minor energy savings. In the case of Tirana, the reduction of energy losses is significantly higher, which is explained by the compact shape of the building with a smaller surface to volume ratio and smaller windows. Due to the complex plan of the Shkodra building, each room has at least two external walls, which increases energy losses.

– **Application of energy-efficient lighting**

In residential buildings, lighting accounts for 11% of energy use. New lighting technologies are more efficient than traditional ones, such as incandescent bulbs. Switching to new light bulbs, such as LED lights, results in a considerable reduction in energy loads (Baggio et al., 2017). Alteration of lighting brings significant direct cost savings. In Albania, incandescent bulbs have been used from the 1990s, but recently LED lighting has become very common. Examination of energy consumption comparison for the LED light bulb and the incandescent light bulb is based on the data provided by the online LED Bulb Power Consumption Calculator (Electrical4u, 2021).

The Tirana building has eight apartments per floor; of them four apartments have five rooms each with one lamp per room, and other four have six rooms each with one lamp per room. The four-story building has 176 light bulbs in total. The Shkodra buiding has six apartments per floor, of them two apartments have five rooms each, two apartments have six rooms each, and two apartments have seven rooms each with one lamp per room. The five-floor building in Shkodra has 180 light bulbs in total. An incandescent light bulb consumes 60 W, while a LED bulb with the same light emission consumes 10 W. For the calculation, it was assumed that the lamps work on average for 6 hours per day. For the Tirana case, the installation of the LED lighting system showed a significant drop in annual energy consumption from 19,272 kWh/year to 3854 kWh/year; for the Shkodra case, the energy consumption lowered from 19,710 kWh/year to 3942 kWh/year.

– **Annual energy performance simulation**

The simulation of the annual energy consumption was completed to estimate the energy performance of the two case studies and understand the changes that occur after the application of the renovation strategy. Detailed 3D models of the two buildings were built using the Revit software. The models were based on the actual dimensions of the two case studies. All structures and materials of the exterior and interior walls and roofs as well as window and door typologies were reflected in the model. The 3D models of the existing and renovated buildings were imported into the Design Builder software in order to perform the simulation. First, the type of building was determined, which is the multi-family residential building. Based on the location of the building, the necessary climatic data was used for the calculation. The construction of the walls, floors, ceilings, terraces, and windows was imported from the Revit

Table 6. **Annual temperatures, heat gains, and energy consumption of the existing and proposed buildings in Shkodra and Tirana**

Parameter	Case study 1. Tirana		Case study 2. Shkodra	
	Existing building	Renovated building	Existing building	Renovated building
Air temperature, °C	19.44	21.45	19.45	22.76
Radiant temperature, °C	19.58	21.90	19.36	23.07
Operative temperature, °C	19.51	21.68	19.40	22.92
Outside dry-bulb temperature, °C	15.40	15.40	16.12	16.12
Lighting, Wh/m²	36,976	21,712	43,800	30,878
Occupancy, Wh/m²	2572	2260	2379	2007
External infiltration, Wh/m²	-25,224	-35,432	-17,031	-34,026
Solar gains through the windows, Wh/m²	17,024	44,552	31,549	62,524

model, and the type of lighting was defined within the software. The annual temperatures inside and outside of the buildings, lighting, occupancy, and solar gains through the windows were found using the EnergyPlus engine (Table 6).

The simulation results show 41% reduction in electricity consumption in the case of Tirana and 30% reduction in the case of Shkodra. The occupancy is insignificantly decreased, while the solar gains rose by 62% in the case of Tirana and doubled in case of Shkodra. The application of the passive strategies results in approximately 2°C rising of the indoor temperature in both buildings.

– **Installation of photovoltaic panels on the roof**

A general rule for the installation of a solar system is to provide the maximum solar power output and use all the opportunities to accommodate the maximum number of panels on a roof. It allows the inhabitants to maximize the savings and speed up the payback period of the solar energy system. For each of the case studies, the photovoltaic system was placed on the rooftops. The arrangement of the PV panels and their performance were calculated using the PVCAD and PV Watts software (NREL, 2021). PV Watts is a popular web application, which is used in combination with the PVCAD software to estimate the energy generation of a grid-connected photovoltaic system. The electricity generation of a solar photovoltaic system is evaluated by: its power output productivity also depending on some other features, such as panel efficiency; temperature compassion; shading degree; and azimuth and tilt angle of the photovoltaic panels. The PV panels were installed in a way to maximize their number and increase energy generation. The PV panels were arranged in a fixed open-rack array with the array tilt of 20° and the azimuths corresponding to the orientation of the roof, which is south-west. The inverter efficiency was taken as 96%, DC to AC size ratio — as 1.2, and the performance and capacity factor — as 16.4%.

Fig. 7 shows the arrangement of the photovoltaic panels on the roofs of the two buildings. In the case of Tirana, there are 220 modules organized into 4 strings of 10 series-connected micro-inverters and 15 strings of 12 series-connected micro-inverters. In the case of Shkodra, there are 127 modules organized into 2 strings of 9 series-connected micro-inverters, 3 strings of 10 series-connected micro-inverters, 5 strings of 11 series-connected micro-inverters, and 2 strings of 12 series-connected micro-inverters. Since the roof of the Tirana building has a simple rectangular shape, the PV panels can be arranged in rows, while due to the complex outline of the Shkodra building, the space is not used in an efficient way, and relatively fewer panels can be applied.

Fig. 8 shows the monthly distribution of the energy produced by the PV panels of the two buildings. Due to the greater roof surface, the monthly energy

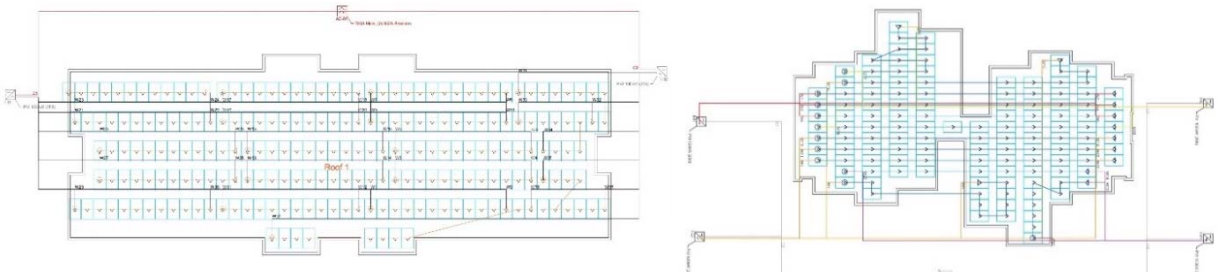

Fig. 7. PV panel modules placed on the roof of the building in Tirana (on the left) and Shkodra (on the right) (source: the authors, extracted from the PVCAD software, 2021)

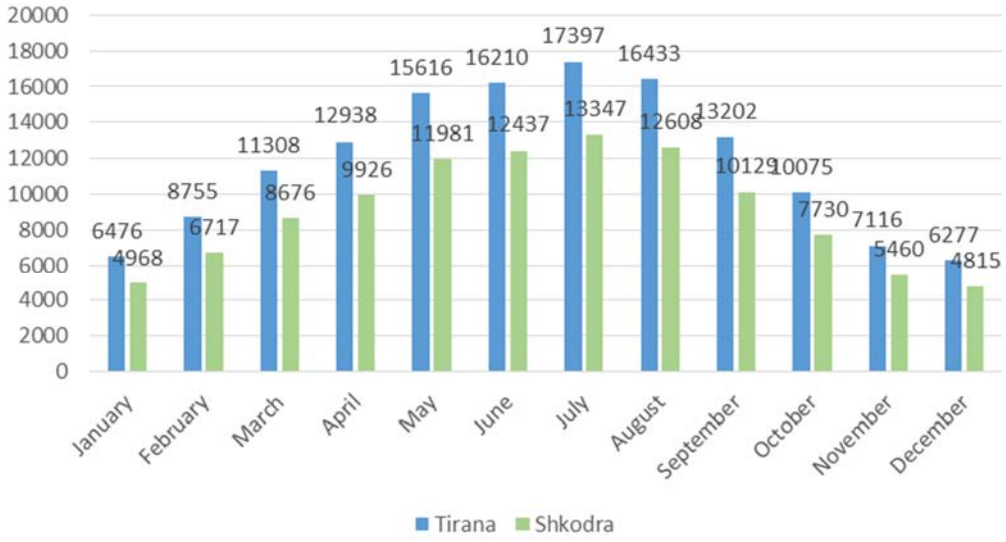

Fig. 8. PV panels' monthly energy performance chart for Tirana and Shkodra cases, kWh

generation of the Tirana building is higher than that of the Shkodra building. However, the climate differences between the two cities are minimal and the average solar radiation received by a square meter of the roof surface is the same for both cases, which is 5.13 kWh/m^2/day. The building located in Tirana can potentially produce in total 141,804 kWh/year, with the highest energy generation in summer months, and the Shkodra building can produce 108,793 kWh/year. Due to the larger total area, the annual production of solar energy per square meter for the Tirana case is 46.34 kWh/year, which is lower than in Shkodra with 50.25 kWh/year per square meter.

– **Annual energy balance**

The energy balance of the two selected buildings of the communist period shows positive results after the renovation with new efficient applications. The two case studies were built using different construction techniques and they are located in places with minor temperature differences. The study proposes two strategies aiming to gain renewable energy by the installation of photovoltaic arrays on the building roof and minimize energy losses through the building envelope and appliances. The contribution of each of the renovation strategies to the annual energy balance of the building can be viewed in Table 7.

The application of the passive strategies for the renovation results in a 56% decrease in energy losses for the Tirana case study and a 57% decrease for the Shkodra building. The annual energy balance is positive for both cases; however, the Tirana case shows higher performance both in terms of energy saving and energy generation. Installation of the photovoltaic panels on the roofs can cover all the heating, cooling, and lighting demands for both cases of renovation being evaluated on

Table 7. **Annual energy balance of the existing and renovated buildings in Shkodra and Tirana**

Building element	Case study 1. Tirana				Case study 2. Shkodra			
	Q existing		Q proposed		Q existing		Q proposed	
	Whole building, kWh	Per m^2, kWh/m^2	Whole building, kWh	Per m^2, kWh/m^2	Whole building, kWh	Per m^2, kWh/m^2	Whole building, kWh	Per m^2, kWh/m^2
Energy losses								
Walls	108,975	35.61	24,716	8.08	134,399	62.08	51,509	23.79
Windows	40,636	13.28	9021	2.95	45,838	14.98	11,292	5.22
Roof	46,958	15.35	43,571	14.24	37,948	12.40	35,210	16.26
Lighting system	19,272	6.30	3854	1.26	19,710	9.10	3942	1.82
Total	185,831	60.73	81,162	26.62	237,895	109.88	101,953	47.09
Energy gains								
PV panels	0	0	141,804	46.34	0	0	108,793	50.25
Total energy balance								
	-185,831	-60.73	60,642	19.82	-237,895	-109.88	6840	3.16

a yearly basis. In the case of Tirana, the generated energy overpasses the needs of the building after the retrofit by 75%, while in the case of Shkodra, the positive difference is only 7%. However, it is necessary to evaluate the performance of the PV system during the coldest month, which is January. Based on the solar panel performance data (NREL, 2021), the daily production of solar energy by the whole building in January is 1.97 kW for the Tirana case and 1.35 kW for the Shkodra case, while the heating loads are 24.94 kW and 27.76 kW, respectively. During the heating period, for both buildings, the contribution of the PV panels into the energy balance is minimal. In the case of Shkodra, the number of photovoltaic panels is minimal, which covers the energy needs, while in the case of Tirana, the number of panels can be reduced since the energy production exceeds the heating, cooling, and lighting demands.

Discussion

The study evaluates the energy performance of the retrofitted mass-housing apartment buildings constructed in all the main cities of Albania. The energy consumption of a typical building can be taken as reference for the evaluation of performance of a similar building (Kmeťkovä and Krajčik, 2015), therefore, the results of the analysis of these two case studies can be applied to all similar buildings constructed during the communist period in the coastal areas and the lowlands of Albania.

Based on the European experience, the reduction of energy losses by 80–90% can be considered as a goal for any retrofit project. In the northern countries, there is a complex approach towards retrofit strategies aiming to decrease energy consumption and demand, control energy use, and generate energy on site. In the southern and Mediterranean countries, modifications of the building envelope as well as solar panels and water heaters are commonly used, while other strategies are not applied. In Albania, the studies are focused mainly on the thermal insulation of walls and windows, which results in a relatively low reduction in energy demands of 47–54%; however, a more complex approach is found in a work by Sherifi (2017). In the present study, the passive retrofit strategies result in a 56–57% reduction in the energy demands, which is slightly higher than the average score for Albania.

The thermal insulation of the exterior walls brings the greatest reduction in the heating and cooling loads. Energy losses through the walls reach 56% in the case of Tirana and 58% in the case of Shkodra. The 5 cm insulation layer is added following the recommendations of Simaku (2017) and Sherifi (2017) for Albania. In the case of Tirana, this resulted in a reduction in energy losses through the walls of up to 30%, which is similar to the average value for Albania of 29.9–32.4% (Simaku, 2017). In the case of Shkodra, the rate dropped to 50%, which is caused by the complex building shape with low compactness. The energy losses through the roof in the Tirana case reach 20%, which is higher than in Shkodra with 16% and higher than the average value for Albania of 7.7–11.2% (Simaku, 2017). The thermal insulation of the roof does not affect significantly the overall performance of the two buildings; however, it should affect positively the thermal comfort in the apartments located at the top floors.

The energy losses through the windows reach 22% and 19% for case study 1 and 2, respectively. According to the literature (Başarır et al., 2012; Djebbar et al., 2018; Höfler et al., 2014), double glazing is the most commonly used retrofit option in the southern countries. Triple glazing and low-e glazing are commonly applied in the northern European countries (Urbikain, 2019), China (Ahn et al., 2015) and South Korea (He et al., 2019). In Albania, double glazing was selected by Sherifi (2017), while Bajraktari et al. (2019) suggest applying triple glazing for retrofit. In the case of Tirana, the application of the triple-glazed windows causes 22% reduction in the energy losses, while in Shkodra it reaches 26%.

The installation of the energy-efficient LED lighting systems brings 80% reduction in the lighting needs, which is higher than the results expected by Gavioli et al. (2015). The difference can be explained by the different location of Albania with the higher amount of natural light and solar radiation. However, Dubois et al. (2015) state that there is a greater potential of energy savings through the application of smart systems and controlled lighting.

The evaluation of the performance of the PV panels goes along with a study of Buchinger et al. (2017), where the authors state that due to the low annual energy demands and large amount of solar radiation, it is possible to reach zero-energy balance through the installation of photovoltaic and solar thermal systems. The application of the PV panels on the entire roof surface results in the high annual energy production, which exceeds the energy demands in the case of Tirana by 75% and in the case of Shkodra by 7%. The results of the study are valid for mid-story buildings having 4–5 floors. In higher buildings, the number of households and interior energy consumption will be higher, while the rooftop photovoltaic panels will produce the comparable amount of energy.

Conclusion

The goal of this study was to estimate the energy performance of the residential buildings of the communist period in Tirana and Shkodra under the existing conditions and apply a number of passive and active retrofit strategies in order to make them more energy-efficient. Particular decisions were made at the level of the building envelope, such as

the installation of triple-glazed windows and 5 cm thermal insulation of the roof and walls, and at the level of appliances, such as the replacement of incandescent light bulbs with LED lamps. Additionally, photovoltaic panels were installed on the roofs, providing an extra source of renewable energy. The evaluation methods included the development of a Revit 3D model for the buildings, application of the PW CAD and PW Watts software in order to calculate the layout and the productivity of the solar panels, use of the LED Bulb Power Consumption Calculator, and calculation of annual energy transfers by the building elements using the DesignBuilder and EnergyPlus software. The comparison of the results shows considerable reduction in the energy losses after the retrofit. Solar panels cannot supply all the heating needs during the cold season but they can provide energy for cooling during summer and cover other household demands during the rest of the year. The study shows that maximum energy losses occur through the building walls, however, other elements of the building envelope and building systems cannot be neglected, since they bring considerable contribution to the annual energy balance.

Despite similar climate conditions and similar building materials, the case study of Tirana has better energy performance in comparison to the case study of Shkodra. This can be explained by some parameters of the building volume, such as the simple shape of the building, rectangular plan, smaller windows, and smaller number of apartments. Due to the complex shape, the energy losses of the Shkodra building through the outer envelope are higher, and the shape of the roof allows solar panels to be installed efficiently, covering all the roof surface. Additionally, the Shkodra building has more floors, which means higher occupancy demands.

The evaluated case studies have the least estimated energy reduction in comparison with the best European practices. Similar retrofit strategies can be used for all brick buildings constructed in Albania during the communist period. The choice of the interventions is explained by the economic conditions of Albania, therefore, low-cost measures, which are easy to implement, were selected. To reach the higher level, additional strategies should be applied, such as adding mechanical ventilation with heat recovery, installing solar water heaters, central water heating systems and hot water distribution, ensuring thermal insulation of the basement, closing open staircases and terraces, providing exterior shading systems as well as lighting management and control.

References

Abazaj, A. (2019). Prefabrication and modular construction dwellings in Albania. *International Journal of Scientific & Engineering Research*, Vol. 10, Issue 8, pp. 811–819.

AboKhalil, A. G. and Ahemd, S. S. (2013). A new approach to improve the energy efficiency of Middle-East buildings. *7th Conference on Future of Renewable and New Energy in the Arab World*, Assiut University, Assiut, Egypt, February 12–14, 2013.

Adly, B. and El-Khouly, T. (2022). Combining retrofitting techniques, renewable energy resources and regulations for residential buildings to achieve energy efficiency in gated communities. *Ain Shams Engineering Journal*, Vol. 13, Issue 6, 101772. DOI: 10.1016/j.asej.2022.101772.

Ahn, B.-L., Kim, J.-H., Jang, C.-Y., Leigh, S.-B., and Jeong, H. (2015). Window retrofit strategy for energy saving in existing residences with different thermal characteristics and window sizes. *Building Services Engineering Research and Technology* , Vol. 37, Issue 1, pp. 18–32. DOI: 10.1177/0143624415595904.

Ahuja, S., Chopson, P., Haymaker, J., and Augenbroe, G. (2015). *Practical energy and cost optimization methods for selecting massing, materials, and technologies.* Chicago: Architectural Research Centers Consortium (ARCC), pp. 280–287.

Aldegheri, F., Baricordi, S., Bernardoni, P., Brocato, M., Calabrese, G., Guidi, V., Mondardini, L., Pozzetti, L., Tonezzer, M., and Vincenzi, D. (2014). Building integrated low concentration solar system for a self-sustainable Mediterranean villa: The Astonyshine house. *Energy and Buildings*, Vol. 77, pp. 355–363. DOI: 10.1016/j.enbuild.2014.03.058.

Aliaj, B. (2003). *Housing Models in Albania between 1945-1999.* Tirana: Co-PLAN Institute for Habitat Development, pp. 1-14.

Baggio, M., Tinterri, C., Dalla Mora, T., Righi, A., Peron, F., and Romagnoni, P. (2017). Sustainability of a historical building renovation design through the application of LEED® rating system. *Energy Procedia*, Vol. 113, pp. 382–389. DOI: 10.1016/j.egypro.2017.04.017.

Bajraktari, E., Nushi, V., and Almeida, M. (2019). Cost efficiency of retrofit measures for typical masonry houses in Kosovo. *International Review of Applied Sciences and Engineering*, Vol. 10, Issue 1, pp. 87–91. DOI: 10.1556/1848.2019.0013.

Başarır, B., Diri, B. S., and Diri, A. C. (2012). Energy efficient retrofit methods at the building envelopes of the school buildings. *Retrofit 2012*, University of Salford, January 24–26, 2012.

Bertoldi, P., Ricci, A., and Almeida, A. (2001). *Energy efficiency in household appliances and lighting.* Berlin, Heidelberg: Springer, 856 p. DOI: 10.1007/978-3-642-56531-1.

Bonakdar, F., Kalagasidis, A. S., and Mahapatra, K. (2017). The implications of climate zones on the cost-optimal level and cost-effectiveness of building envelope energy renovation and space heat demand reduction. *Buildings*, Vol. 7, Issue 2, 39. DOI: 10.3390/buildings7020039.

Botta, M. (2005). *Towards sustainable renovation: three research projects.* PhD Thesis. School of Architecture Royal Institute of Technology.

Brannigan, A. and Booth, C. A. (2013). Building envelop energy efficient retrofitting options for domestic buildings in the UK. *WIT Transactions on Ecology and the Environment*, Vol. 179, pp. 475–486. DOI: 10.2495/SC130401.

Buchinger, J., Karner, A., Kamberi, M., and Profka, D. (2017). *The Country Programme of Albania under the Global Solar Water Heating Market Transformation and Strengthening Initiative.* Tirana: UNDP*, 65 p.*

Carpino, C., Bruno, R., and Arcuri, N. (2017). Statistical analysis of the heating demand in residential buildings located in Mediterranean climate and proposals for refurbishment. *Energy Procedia*, Vol. 133, pp. 16–27. DOI: 10.1016/j.egypro.2017.09.365.

Chen, D. and Chen, H. W. (2013). Using the Köppen classification to quantify climate variation and change: An example for 1901–2010. *Environmental Development*, Vol. 6, pp. 69–79. DOI: 10.1016/j.envdev.2013.03.007.

Chen, J., Peng, Z., and Yang, P. P.-J. (2019). The energy performance evaluation of roof retrofit under uncertainties for the Shanghai's Worker Village. *Energy Procedia*, Vol. 158, pp. 3170–3176. DOI: 10.1016/j.egypro.2019.01.1020.

Ciriminna, R., Albanese, L., Pecoraino, M., Meneguzzo, F., and Pagliaro, M. (2019). Solar energy and new energy technologies for Mediterranean countries. *Global Challenges*, Vol. 3, Issue 10, 1900016. DOI: 10.1002/gch2.201900016.

climate-data.org (2021a). *Shkoder climate (Albania).* [online] Available at: https://en.climate-data.org/europe/albania/shkoder/shkoder-3429/#temperature-graph [Date accessed February 23, 2021].

climate-data.org (2021b). *Tirana climate (Albania).* [online] Available at: https://en.climate-data.org/europe/albania/tirana/tirana-714992/#temperature-graph [Date accessed February 23, 2021].

de Almeida, M., Ferreira, M., Rodrigues, A., and Baptista, N. (2017). *Cost-effective energy and carbon emissions optimization in building renovation.* Braga: University of Minho, 35 p.

Department of Energy (2015). *Quadrennial technology review. An assessment on energy technologies and research opportunities.* Washington: Department of Energy*, 489 p.*

Djebbar, K. E.-B., Salem, S., and Mokhtari, A. (2018). A multi-objective optimization approach of housing in Algeria. A step towards sustainability. *Urbanism. Arhitectură. Construcţii*, Vol. 9, Issue 2, pp. 131–158.

Djebbar, K. E.-B., Salem, S., and Mokhtari, A. (2019). Assessment of energy performance using bottom-up method: Exemplified by multi-storey buildings in Tlemcen (Algeria). *International Journal of Building Pathology and Adaptation*, Vol. 38, No. 1, pp. 192–216. DOI: 10.1108/IJBPA-11-2017-0056.

Dobjani, E. (2020). Requalification of residential space in Tirana - methodologies and intervention strategies. *European Journal of Formal Sciences and Engineering*, Vol. 3, No. 1, pp. 84–101. DOI: 10.26417/ejef.v4i1.p79-92.

Dubois, M.-C., Bisegna, F., Gentile, N., Knoop, M., Matusiak, B., Osterhaus, W., and Tetri, E. (2015). Retrofitting the electric lighting and daylighting systems to reduce energy use in buildings: a literature review. *Energy Research Journal*, Vol. 6, No. 1, pp. 25–41. DOI: 10.3844/erjsp.2015.25.41.

EEA (2016). *More from less — material resource efficiency in Europe. 2015 overview of policies, instruments and targets in 32 countries.* Copenhagen: European Environment Agency*, 151 p.*

Electrical4u (2021). *LED Light Power Consumption Calculation & LED Energy Bill Calculator.* [online] Available at: https://www.electrical4u.net/electrical-basic/led-bulb-power-consumption-calculation-led-energy-bill-calculator/ [Date accessed February 17, 2021].

EUROSTAT (2020). *Enlargement countries - energy statistics.* [online] Available at: https://ec.europa.eu/eurostat/statistics-explained/index.php/Enlargement_countries_-_energy_statistics [Date accessed October 7 2020].

Felius, L. C., Dessen, F. and Hrynyszyn, B. D. (2020). Retrofitting towards energy-efficient homes in European cold climates: a review. *Energy Efficiency*, Vol. 13, Issue 1, pp. 101–125. DOI: 10.1007/s12053-019-09834-7.

Figueiredo, A., Rebelo, F., Castanho, R. A., Oliveira, R., Lousada, S., Vicente, R., and Ferreira, V. M. (2020). Implementation and challenges of the passive house concept in Portugal: lessons learnt from successful experience. *Sustainability*, Vol. 12, Issue 21, 8761. DOI: 10.3390/su12218761.

Fina, B., Auer, H., and Friedl, W. (2019). Profitability of active retrofitting of multi-apartment buildings: Building-attached/integrated photovoltaics with special consideration of different heating systems. *Energy and Buildings*, Vol. 190, pp. 86–102. DOI: 10.1016/j.enbuild.2019.02.034.

Ganguly, A., Chowdhury, D., and Neogi, S. (2016). Performance of building roofs on energy efficiency – a review. *Energy Procedia*, Vol. 90, pp. 200–208. DOI: 10.1016/j.egypro.2016.11.186.

Gavioli, M., Tetri, E., Baniya, R. R., and Halonen, L. (2015). Lighting retrofitting: improving energy efficiency and lighting quality. *Proceedings of 28th CIE session*, Manchester, UK, June 28 – July 4, 2015.

Glushkov, S., Kachalov, N., Senkiv, E., and Glushkova, V. (2016). Estimation of energy efficiency of residential buildings. *MATEC Web of Conferences*, Vol. 92, 01072. DOI: 10.1051/matecconf/20179201072.

Habibi, S., Obonyo, E. A., and Memari, A. M. (2020). Design and development of energy efficient re-roofing solutions. *Renewable Energy*, Vol. 151, pp. 1209–1219. DOI: 10.1016/j.renene.2019.11.128.

Harmathy, N., Urbancl, D., Goričanec, D., and Magyar, Z. (2019). Energy efficiency and economic analysis of retrofit measures for single-family residential buildings. *Thermal Science*, Vol. 23, Issue 3, pp. 2071–2084. DOI: 10.2298/TSCI170518298H.

He, Q., Ng, T., Hossain, U., and Skitmore, M. (2019). Energy-efficient window retrofit for high-rise residential buildings in different climatic zones of China. *Sustainability*, Vol. 11, Issue 22, 6473. DOI: 10.3390/su11226473.

Hoxha, O., Nepravishta, F., and Tola (Panariti), A. (2018). Exploration of housing evolution in Tirana during the years 1929-1943. *International Journal of Business and Technology*, Vol. 6, Issue 3, 12. DOI: 10.33107/ijbte.2018.6.3.12.

Höfler, K., Maydl, J., Venus, D., Mørck, O. C., Østergaard, I., Thomsen, K. E., Rose, J., Jensen, S. Ø., Kaan, H., Almeida, M., Ferreira, M., Brito, N., Baptista, N., Fragoso, R., Blomsterberg, Å., Citherlet, S., and Périsset, B. (2014). *Shining examples of cost-effective energy and carbon emissions optimization in building renovation.* Braga: University of Minho*, 109 p.*

Huovila, P., Ala-Juusela, M., Melchert, L., and Pouffary, S. (2007). *Buildings and climate change: status, challenges and opportunities.* Paris: United Nations Environment Programme, 78 p.

Jaber, S. and Hawa, A. A. (2016). Optimal design of PV system in passive residential building in Mediterranean climate. *Jordan Journal of Mechanical and Industrial Engineering*, Vol. 10, No. 1, pp. 39–49.

Kass, K., Blumberga, A., and Zogla, G. (2015). Energy performance of historical brick buildings in Northern climate zone. *Energy Procedia*, Vol. 72, pp. 238–244. DOI: 10.1016/j.egypro.2015.06.034.

Këshilli i Ministrave (2015). *Ligji nr. 124/2015 "Për Efiçencën e Energjisë".* Tirana: Fletore Zyrtare, 15 p.

Këshilli i Ministrave (2016). *Ligji nr. 116/2016 "Për performancën e energjisë së ndërtesave".* Tirana: Fletore Zyrtare*, 12 p.*

Kmet'kovä, J. and Krajčik, M. (2015). Energy efficient retrofit and life cycle assessment of an apartment building. *Energy Procedia*, Vol. 78, pp. 3186–3191. DOI: 10.1016/j.egypro.2015.11.778.

Konstantinou, T. and Knaack, U. (2011). Refurbishment of residential buildings: a design approach to energy-efficiency upgrades. *Procedia Engineering*, Vol. 21, pp. 666–675. DOI: 10.1016/j.proeng.2011.11.2063.

Laustsen, J. (2008). *Energy efficiency requirements in building codes,energy efficiency policies for new buildings.* Paris: International Energy Agency*, 85 p.*

Ma, Z., Cooper, P., Daly, D., and Ledo, L. (2012). Existing building retrofits: Methodology and state-of-the-art. *Energy and Buildings*, Vol. 55, pp. 889–902. DOI: 10.1016/j.enbuild.2012.08.018.

Ndreçka, O. and Nepravishta, F. (2014). The impact of socialist realism ideology in the Albanian architecture in 1945-1990. *Architecture and Urban Planning*, Vol. 9, pp. 27–32. DOI: 10.7250/aup.2014.004.

Novikova, A., Szalay, Z., Horváth, M., Becker, J., Simaku, G., and Csoknyai, T. (2020). Assessment of energy-saving potential, associated costs and co-benefits of public buildings in Albania. *Energy Efficiency*, Vol. 13, pp. 1387–1407. DOI: 10.1007/s12053-020-09883-3.

NREL (2021). *NREL's PVWatts® Calculator.* [online] Available at: https://pvwatts.nrel.gov/index.php [Date accessed February 23, 2021].

Pitts, A. (2017). Passive house and low energy buildings: barriers and opportunities for future development within UK practice. *Sustainability*, Vol. 9, Issue 2, 272. DOI: 10.3390/su9020272.

Ray, K. L. (2010). *Photovoltaic cell efficiency at elevated temperatures.* BSc Thesis in Mechanical Engineering. Massachusetts Institute of Technology.

Romeo, C. and Zinzi, M. (2013). Impact of a cool roof application on the energy and comfort performance in an existing non-residential building. A Sicilian case study. *Energy and Buildings*, Vol. 67, pp. 647–657. DOI: 10.1016/j.enbuild.2011.07.023.

Sherifi, M. (2017). *Development of a sustainability framework for greening the construction sector in Albania.* MSc Thesis. Harvard University.

Simaku, G. (2017). Albanian building stock typology and energy building code in progress towards national calculation methodology of performance on heating and cooling. *European Journal of Multidisciplinary Studies*, Vol. 2, Issue 5, pp. 8–30. DOI: 10.26417/ejms.v5i1.p13-35.

Struga, M. and Marko, O. (2019). *Financing energy efficiency retrofits in the built environment in Albania: barriers and opportunities.* Tirana: Friedrich-Ebert Stifftung*, 23 p.*

Synnefa, A., Vasilakopoulou, K., De Masi, R. F., Kyriakodis, G.-E., Londorfos, V., Mastrapostoli, E., Karlessi, T., and Santamouris, M. (2017). Transformation through renovation: an energy efficient retrofit of an apartment building in Athens. *Procedia Engineering*, Vol. 180, pp. 1003–1014. DOI: 10.1016/j.proeng.2017.04.260.

Urbikain, M. K. (2019). Energy efficient solutions for retrofitting a residential multi-storey building with vacuum insulation panels and low-E windows in two European climates. *Journal of Cleaner Production*, Vol. 269, 121459. DOI: 10.1016/j.jclepro.2020.121459.

Usta, P. and Zengin, B. (2021). The energy impact of building materials in residential buildings in Turkey. *Materials*, Vol. 14, Issue 11, 2793. DOI: 10.3390/ma14112793.

Villegas, R. R. (2017). *A methodology to assess impacts of energy efficient renovation – a Swedish case study.* Gävle: Gävle University Press*, 22 p.*

Weather Spark (2021a). *Climate and average weather year round in Shkodër.* [online] Available at: https://weatherspark.com/y/84405/Average-Weather-in-Shkod%C3%ABr-Albania-Year-Round [Date accessed February 23, 2021].

Weather Spark (2021b). *Climate and average weather year round in Tirana.* [online] Available at: https://weatherspark.com/y/84331/Average-Weather-in-Tirana-Albania-Year-Round [Date accessed February 23, 2021].

Weather Spark (2022). *Compare the climate and weather in Shkodër and Tirana.* [online] Available at: https://weatherspark.com/compare/y/84405~84331/Comparison-of-the-Average-Weather-in-Shkod%C3%ABr-and-Tirana [Date accessed September 11, 2022].

Yüksek, I. and Karadayi, T. T. (2017). Energy-efficient building design in the context of building life cycle. In: Yap, E.-H. (ed.). *Energy Efficient Buildings.* London: InTech, pp. 93–123. DOI: 10.5772/66670.

МОДЕРНИЗАЦИЯ МНОГОКВАРТИРНЫХ ДОМОВ В АЛБАНИИ С УЧЕТОМ ЭНЕРГЕТИЧЕСКИХ ХАРАКТЕРИСТИК НА ПРИМЕРЕ ТИПОЛОГИЙ МАССОВОГО ЖИЛИЩНОГО СТРОИТЕЛЬСТВА

Анна Юницына*, Ильда Садрия

Университет Эпока, Тирана, Албания

*E-mail: ayunitsyna@epoka.edu.al

Аннотация
Введение: Исследование посвящено анализу энергоэффективности жилых домов массовой застройки в Албании и дальнейшей оценке возможностей энергетической модернизации данных зданий. На данный момент в Албании оценка энергоэффективности обязательна для новых зданий, однако в отношении существующего фонда зданий не разработано ни одного соответствующего подхода. **Методы:** Цель данной работы — выполнить оценку многоквартирных зданий коммунистического периода в Тиране и Шкодере и применить ряд стратегий пассивной и активной модернизации, подходящих для условий средиземноморского климата. **Результаты и обсуждение:** Улучшение теплопроводности и энергетического баланса может быть достигнуто за счет дополнительного утепления стен и крыш зданий и замены окон, установки фотоэлектрических панелей и устройства освещения с низким энергопотреблением. Применение пассивных стратегий приводит к снижению потерь энергии на 56% в Тиране и на 57% в Шкодере. **Заключение:** Установка фотоэлектрических панелей позволяет покрыть потребности в охлаждении и освещении в теплый период, однако в зимнее время их работа не может обеспечить удовлетворение потребностей в отоплении.

Ключевые слова: модернизация многоквартирных зданий, энергоэффективность здания, энергоэффективность, фотоэлектрические системы, энергетический баланс.

Urban Planning and Development

DOI: 10.23968/2500-0055-2023-8-3-77-91

ANALYSIS OF URBAN TRANSFORMATIONS AND THEIR IMPACT ON THE COLONIAL URBAN FABRIC IN DJELFA (ALGERIA) USING SPACE SYNTAX TECHNIQUE

Brahim Ahmed[1]*, Khalfallah Boudjemaa[2]

[1] Ziane Achour University, Djelfa, Algeria

[2] Mohamed Boudiaf University, Msila, Algeria

*Corresponding author: a.brahim@univ-djelfa.dz

Abstract

Introduction: The paper examines the urban transformations that Djelfa underwent over time, from its colonial inception to the present day, characterized by rapid demographic and urban growth as well as excessive consumption of urban space. **Purpose of the study:** We aimed to study the urban transformations of the city of Djelfa over time, provide a quantitative description of the urban and social characteristics that shape the built environment, and identify the city's most integrated (easily accessible) and secluded areas. **Methods:** We utilized the spatial syntax technique to analyze the stages of city development, which is based on modeling city maps into axial maps and quantitatively measuring various factors such as connectivity and integration (Rn). **Results:** We obtained significant results notably that the historical city center still maintains its importance in terms of easy access, interconnected axes, and chess layout that facilitated its expansion. Additionally, residential neighborhoods, isolated from the rest of the city, emerged at certain periods. Restructuring operations, such as the opening of Mohamed Boudiaf Square in the city center, contributed to increasing connectivity with its neighboring axes.

Keywords: Urban transformation, colonial city, spatial syntax, Djelfa, connectivity, integration.

Introduction

The city is the most complex urban pattern created by human thought, with distinct characteristics and features that define its historical identity as well as its social and cultural heritage. According to Kevin Lynch, The city may be looked on as a story, a pattern of relations between human groups, a production and distribution space, a field of physical force, a set of linked decisions, or an arena of conflict. Values are embedded in these metaphors: historic continuity, stable equilibrium, productive efficiency, capable decision and management, maximum interaction, or the progress of political struggle. Certain actors become the decisive elements of transformation in each view: political leaders, families and ethnic groups, major investors, the technicians of transport, the decision elite, the revolutionary classes (Lynch, 2008).

Intellectuals and historians have long considered the city to be an important field of scientific research for its social, economic, cultural, and political functions.

In this study, we will attempt to analyze the city of Djelfa at different time points, relying on Djelfa's population and housing statistics. In order to align the available demographic data with the urban transformations in Djelfa, we can rely on decennial census conducted to systematically acquire, record, and calculate population information. The United Nations (UN) defines the essential features of population and housing censuses as "individual enumeration, universality within a defined territory, simultaneity and defined periodicity", and recommends that population censuses be taken at least every ten years (UN Department of Economic and Social Affairs Statistics Division, 2008). We relied on these statistics as reference points in time to study the transformations that the city of Djelfa underwent. The delay in the last census was due to political reasons experienced by Algeria. However, we collected population and geographical data for the last period through our own sources (study offices). We utilized the Space Syntax technique to analyze the influence of the spatial structure on human behavior and economic movement within the system. Our goal was to answer the following question: What is the effect of these urban transformations on the urban fabric of Djelfa, with its colonial core?

To answer the question, we relied on two assumptions: that urbanization has affected the spatial structure of the city of Djelfa in terms of morphology and functionality, and that the spatial structure of the old urban fabric (colonial) has contributed to the city's modern morphological formation.

Materials and methods

Space Syntax

Space Syntax is a novel computational language proposed to describe the spatial patterns of contemporary cities. Syntax is a linguistic concept that refers to the relationships between different elements or the interactions between space and society. Urban planners can gain a better understanding of urban development and gather more ideas to help design new urban schemes by conducting structural analyses of the urban environment.

The patterns of human movement in the city can be analyzed using Space Syntax principles, primarily by considering the degree of integration and interconnectedness of urban spaces (El-Agouri, 2004). Bill Hillier and other researchers at the Bartlett Faculty of the Built Environment at University College London developed space syntax in the late 1970s and early 1980s as a morphological approach to the urban and social development of major British cities of the time. It then rapidly evolved during the 1980s and 1990s (Hillier, 1996) developing into a method to analyze the spatial formations of architectural objects and urban areas through the interpretation of social behavior, using various theories and techniques that resulted in several interpretative models of numerous social and spatial phenomena. Examples include social segregation, crime, business location, activities, and urban mobility (Hillier, 2005). In his paper, Hillier (1999) emphasizes this point and contends that if the spatial complexity variable cannot be controlled, its effects and consequences cannot be measured. In fact, urban research using the Space Syntax approach aims to bridge this gap by first addressing the problem of description, namely, how to accurately and consistently describe the physical complexity of the city in order to use it as a variable.

Space Syntax studies the composition of road networks and spaces across cities, analyzing the resulting attraction or separation characteristics that significantly impact the distribution of activities as well as users' behavior and, more specifically, mobility. Using modeling tools developed by the Space Syntax Laboratory (SSL), this composition can be compared to various statistical variables. It enables the assessment of the strength of its association with different factors, such as pedestrian and vehicle flows, property value, distribution of activities, and even crime (Perrin, 2001a). Space syntax theory offers useful tools to understand the logic of configurations through its engagement with social structure (Rahmane and Abbaoui, 2021).

They are used in land use planning, city planning, and transportation. Its scope has expanded in recent years to include archaeology, urban and human geography, as well as anthropology and the environment (Perrin, 2001b). Typical applications of space syntax include pedestrian modeling, urban crime mapping, road-finding processes in complex built environments, and analysis of other hidden spatial and social dimensions in the built environment. All these investigations tend to be based on the assumption that spatial patterns or structures have a significant impact on human activities and behavior in urban environments. Several empirical studies demonstrated the importance of spatial syntax for modeling and understanding urban patterns and structures (El-Agouri, 2004).

The space syntax technology has been used in numerous research projects. Hanson described the social and cultural implications of various plans to rebuild London (Hanson, 1989). In 1989, Miller used spatial syntax as a tool in the urban renewal process in Swedish cities (Miller, 1989). In the same year, Hillier and others attempted to predict spatial patterns of crime in urban areas. In 1984, Hillier and Hanson published a book entitled "The Social Logic of Space", which addressed the impact of spatial formation on social life and vice versa. The theory demonstrated how the arrangement of spaces influences users' behavior, thus determining the efficiency and suitability of the design for the activity (Elporolosy and Elfalafly, 2020). Peponis and colleagues investigated the functional role of building morphological structure (Peponis, 1993). In 1989, Mills demonstrated how the spatial structure of towns functions as a controlling mechanism for apartheid ideology (Mills, 1989). Besides, the relationship between urban morphology and movement patterns (primarily related to pedestrians) was extensively studied (Teklenburg et al., 1993).

Study area

The mandate of Djelfa, resulting from the 1974 administrative division, is located in the central part of northern Algeria, south of Algiers, between latitudes 33° 35' and 36° 12' north and longitudes 2° and 5° east. It is located in the center of the steppe highlands and covers a vast area of 32,362 km2, which is equivalent to 1.36% of Algeria's total area.

The Djelfa province occupies land stretching from north to south for more than 300 km, while its maximum width from east to west is only 150 km. This vast area borders nine other provinces: Medea and Tissemsilt in the north; M'sila and Biskra in the east; Ouargla and El Oued in the southeast; Laghouat and Ghardaia in the southwest; and Tiaret in the west.

Djelfa city's urban development

Colonialism is regarded as a mainly regional phenomenon because colonized societies needed space, raw materials, labor force, manufacturers, and consumers. Consequently, colonial cities were established in specific locations, such as transit areas or strategic zones. The primary objective of these cities was to oversee and control the respective

territories. During the first years of the colonization of Algeria, the colonizers established a network of cities in specific regions. The French policy aimed to secure the regions, attract European settlers, and establish the center of power. The colonial cities in Algeria were designed to recreate what existed in Europe at the beginning of the 19th century: a chess layout and the image of a Roman city (Amokrane, 2016). All of the old centers are characterized by a high density of buildings lined up along the streets and around the squares and monuments, and the lands are frequently of a special legal nature. However, the focus is on the square, which typically includes three elements commonly seen in French villages: the school, the town hall, and the monument. In this regard, Malverti stated that the colonial city centers are military cities, whose mission is to house the military forces, after which the urban neighborhood is planned (Malverti & Picard, 1988). Vacher (1997) defines the colonial city as a chessboard of straight streets, which delineate a group of land plots, often square in shape, in the city center, some of which are removed to make way for the most significant structures: the church, the town hall, the homes of merchants, and the wealthiest settlers (Vacher, 1997).

Djelfa's urban development has gone through several stages over time to give us the city we see today (Fig. 1). The city of Djelfa has a colonial origin (1852–1962), and its ancient nucleus serves as the center from which various expansions were launched. This occurred particularly after the demolition of the perimeter protective fence in 1960. As a result, the city expanded along the axis of National Road 1, which has remained one of the city's important spatial axes. This urban development has followed the same pattern as the ancient perpendicular nucleus, despite the emergence of other structured axes in subsequent periods of time, such as the National Road 46 axis east of the Mellah valley and the Ben M'hidi axis in the west. Algeria was subjected to French colonization from July 5, 1830, to July 5, 1962.

Digital modeling of Djelfa City

After finishing the urban schemes for each period with XDF extension, we converted these schemes into axial maps, which are defined as the minimum set of axial lines passing through each convex area (Turner et al., 2005). Depth is the measure of the shortest path from a specific root line to all other lines in the system (Turner, 2004). Let us perform an axial analysis with DepthmapX of the latest version 0.8.0, examining the most important metrics in this type of analysis (global and local measures) to accurately identify the transformations that have affected the spatial structure and their effects.

Depth Map is a multi-platform software developed to perform multiple spatial network analyses in order to explore the complexity of social behavior in a given built environment (Fareh and Alkama, 2022). After modeling and conducting complex calculations, the DepthmapX program utilizes the color spectrum of the spatial system axes to measure the strength or weakness of the factor. The colors used for this purpose are red, orange, yellow, green, light blue, and dark blue, representing varying levels of strength or weakness. The colors symbolize very strong, relatively strong, above average, medium, weak, and very weak relationships, respectively.

Due to the length of these studies and the time required to work on them, the visual and convex analysis of the Djelfa city will be the subject of future research.

Results and discussions

Connectivity

The value of connectivity is measured by the number of axes that are directly connected to each individual axis in the urban system, and an increase in the number of axes that are directly connected to each other indicates the high mobility provided by the space. Sukor and Fisal (2020) stated that connectivity is an important attribute to ensure high-quality public transit.

Djelfa before 1962

The city of Djelfa had 86 axes in its spatial structure. The axes that showed high connectivity, indicated in red on the axial map of the Djelfa city using the connectivity index before 1962 as shown in Fig. 2, were a single axial line intersected by 16 axes. This particular axis is represented by National Road 1, which marked the starting point of the colonial nucleus. Its significance lies in being the only existing landmark and serving as the only axis facilitating continuous movement from north to south. The orange axis to the east is parallel to this axis, but it is shorter and has a connectivity value of 14. As we move further away from the main axis, the connectivity values gradually decrease.

Djelfa in the period between 1962 and 1977

The number of axes in Djelfa increased to 574 (more than 6.5 times), as indicated by the development of several neighborhoods stretching from the northwest to the southwest and northeast of the Mellah valley.

The results of calculating the connectivity values at the city level, as shown in Fig. 2, revealed that Khemisti Street (the borders of the old nucleus) in the south had the highest connectivity value at the city level, with a value of 24. This value increased from 11 before 1962. Additionally, the connectivity of the axis of National Road 1 was 19, also showing an increase from 16 before 1962.

The reason for this difference in growth is the city's expansion to the east and west rather than to the north and south. Khemisti Street benefited from this expansion because it runs east-west, resulting

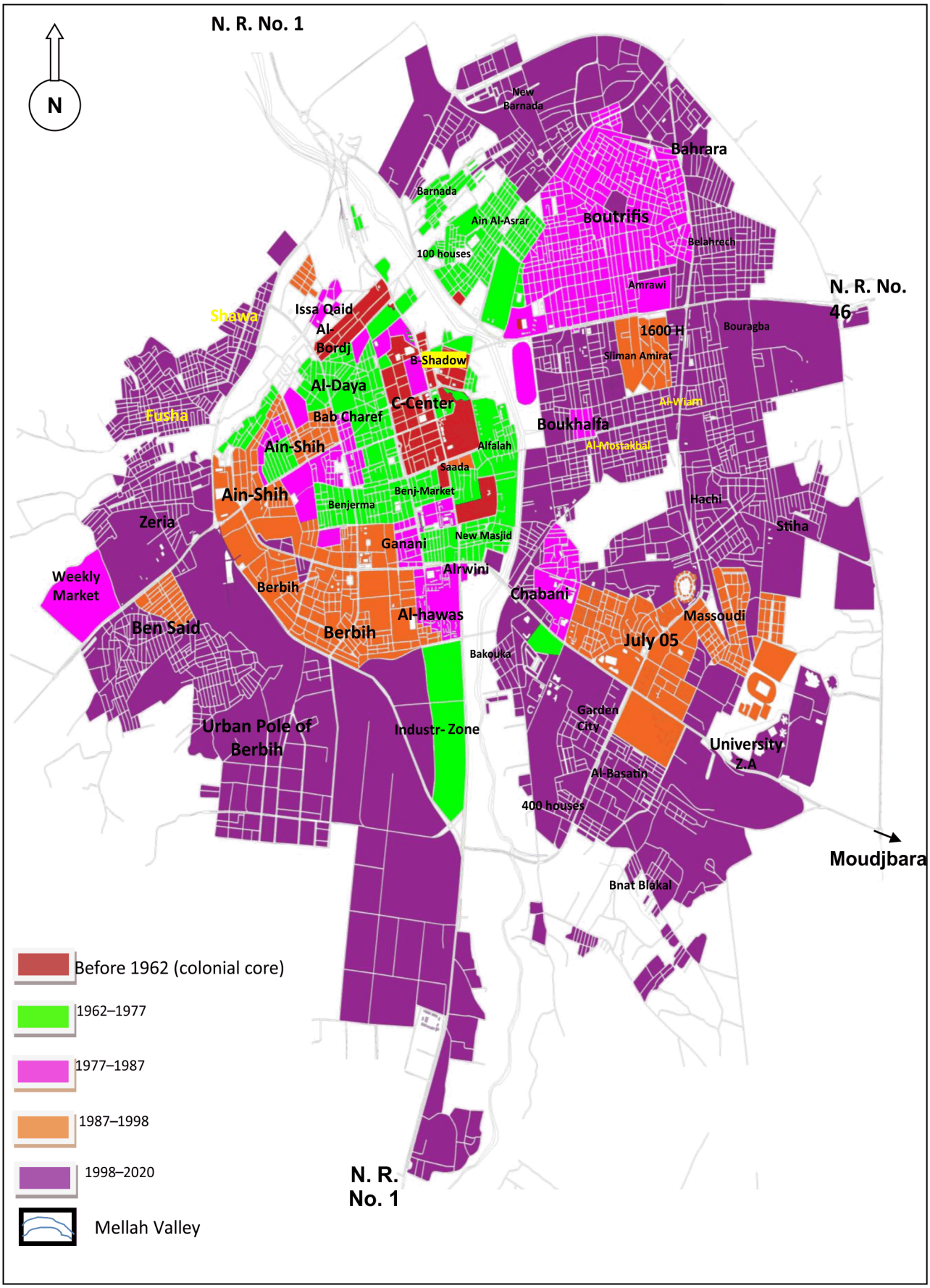

Fig. 1. Urban development of the city of Djelfa. Source: authors

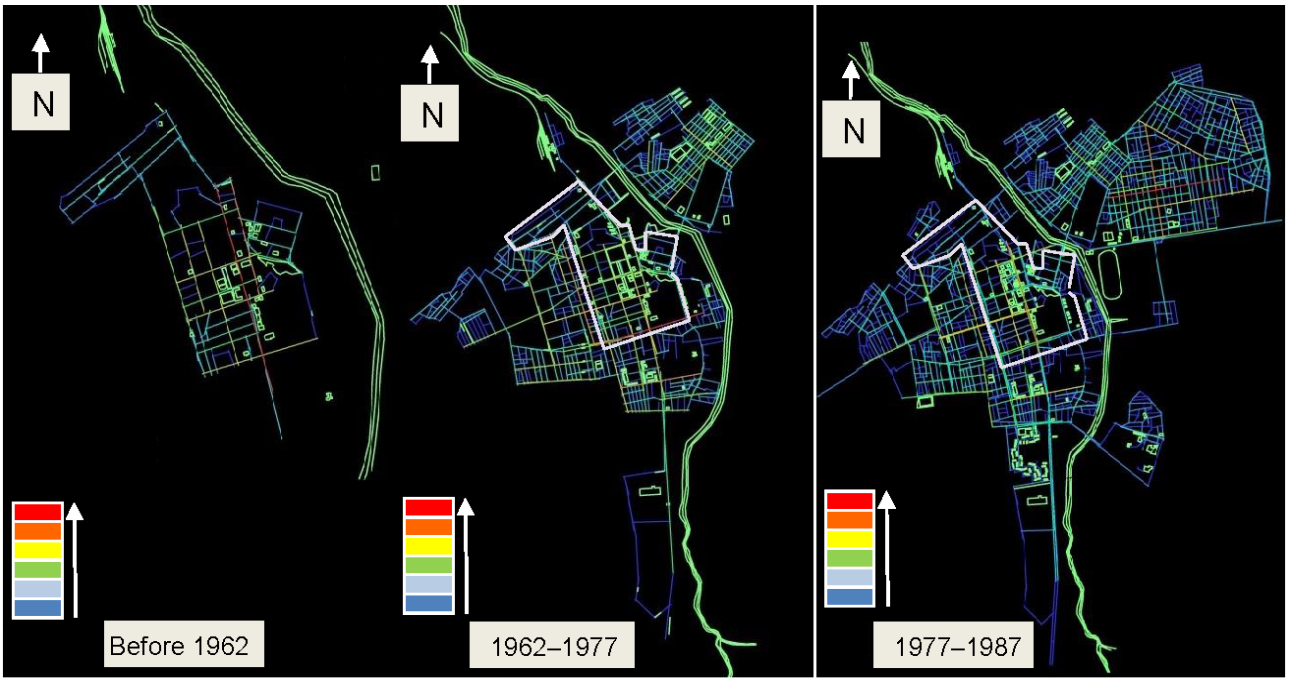

Fig. 2. Axial map of Djelfa before 1962, in 1962–1977, and in 1977–1987 (connectivity). Source: authors

in a higher number of intersecting axes and making it easily accessible from 24 streets that directly intersect it. The axial map, analyzed using the connectivity indicator, reveals that the old city center has most of the axes with high connectivity.

The new neighborhoods developed to the east of the Mellah valley demonstrate two perpendicular axes with the highest connectivity value. The intersection of these axes will later give rise to a significant commercial center in the area, known as the Al-Rahma Market.

Djelfa in the period between 1977 and 1987

The digital modeling of the Djelfa city for 1987 reveals some interesting findings. For the first time, the axis with the highest connectivity value shifted to the eastern side of the Mellah valley, specifically within the axes of the new expansions of the Boutrifis neighborhood. This axis has a connectivity value of 32, indicating its significant role in enhancing kinetic flexibility at this level. The axis that ranks second in terms of connectivity, with a value of 28, is perpendicular to it, and the axis that ranks third, with a value of 24, runs parallel to it at the system-wide level. These three axes with the highest connectivity index values, along with other axes with lower values, will help create the first nucleus of a secondary center for commercial activities in this neighborhood in the future.

The restructuring of the city center, along with the opening of Mohamed Boudiaf Square, considered the focal point of the vibrant city center, helped increase the values of the connectivity index of the adjacent axes, especially the northern axis (the AL-Ma'rad axis), which ends at the Sidi Nael axis. Its connectivity index increased from 14 to 20, making it one of the most important axes for movement and trade, connecting the city center with the previously somewhat isolated northern area.

The retreat of the Khemisti axis towards the south was a significant setback for the overall spatial system. This axis had a connection value of 24 in 1977, making it crucial in connecting different areas. However, it later became a less important axis with a connectivity value of 17. The reason behind this decline was the oversight in considering its continuity during the planning of new neighborhoods to the west. The end of the axis was blocked, which hindered its function of connecting sub-axes. This lack of connectivity weakened its fluidity and movement. That was a result of poor and random planning, with a lack of foresight.

Djelfa in the period between 1987 and 1998

This stage was distinguished by accelerated construction and the implementation of major housing programs, including:

- The establishment of a new urban residential area in the eastern part, represented by the July 05 district.
- The establishment of a new urban residential area in the western part, represented by the newly developed Ain Al-Shih neighborhood.
- Restructuring of Larbi Ben M'hidi Street by expanding it through the middle of the Ben Jerma neighborhood (demolition of about 200 m on both sides of the street) and extending it to the south to meet the Western bypass road (Algiers–Laghouat). Along with demolishing the western part of the Al-Bordj neighborhood to make way for Larbi Ben M'hidi

Street, the bypass road (Algiers–Laghouat) will be connected in its northern part.

The city of Djelfa experienced a significant expansion over a ten-year period, with the number of system axes increasing to 1801, which is about a third more than its original size. The axial map of the city, when analyzed using the connectivity indicator (Fig. 3), provides valuable insights into the changes in the city center, outskirts, and new neighborhoods, as well as the impact of urban interventions on the main axes.

The connectivity value of National Road 1 remains at 28, which is the highest in the city center and on the western side as a whole.

The axes of the old city center remained unchanged in their high or medium values from the previous period. As a result, both the center and the surrounding area were fully developed without any urban interventions that could disrupt the interconnectedness of the axes. It should be noted that the axis of the AL-Dhil AL-Jamil neighborhood in the city center did not witness any intervention made to enhance its connectivity and therefore keep up with the other axes in the city center.

The digital modeling of the Larbi Ben M'hidi axis revealed that it consists of a series of straight axes connected to form a circular line. The longest straight axis is 818.6 m long and has a correlation value of 21 (orange). It ranks second in terms of importance for the spatial network of the city. This area is where commercial activities are concentrated, providing kinetic fluidity and intersecting with the largest number of sub-axes. This relieves the pressure on the city center and facilitates travel from the center to the north and south of the city. The expansion in the south transformed the Ganani–Ben Jerma axis, which intersects it, into one of the most important axes with a value of 24. Despite having one blind end, this axis saw the flourishing of commercial activities and services. It includes a school for blind children, a municipal playground, and a court headquarters. It also intersects an important axis with a connectivity value 23, of which is the axis of the Ben Jerma market. This market is the heart of the western-south region, attracting movement and providing easy access from the side streets, thus reducing pressure on the old city center. The new urban residential area in the eastern part, represented by the July 05 district, seems to be an isolated block within the city. Most of the axes in this area have low connectivity (dark blue and light blue), making it difficult to move around. As a result, this area experienced significant isolation and became a predominantly residential area. The lack of axes with high connectivity and the collective housing character contribute to this isolation. However, there is a bridge across the Mellah valley that connects this area to the rest of the city.

The Boutrifis neighborhood continues to have the axis with the highest connectivity value (32), along with the previously mentioned axes. However, it is worth noting that the crossroads axis (horse racing area) is starting to emerge towards Bou Saada with a connectivity index value of 15. This is due to the construction activities in the area south of it, including the establishment of a neighborhood with 1600 housing units and the development of the first nucleus of the Boukhalfa neighborhood. Additionally, sub-axes are being opened that lead to this axis. In the future, this axis will undergo a transformation and will become the most important axis in connecting the Boutrifis neighborhood with the future neighborhoods due to its length, straightness, and central location among these neighborhoods.

Djelfa in the period between 1998 and 2020

The number of axes in this period increased to 4036, which is more than double the previous amount. The maximum value of the connectivity index at the system level is 32, and the minimum is 1, which is consistent with the values from the previous period. In addition, the average connectivity in the city's spatial system is 5.1, which is considered high given the size of the city. That is, on average, each axis in the spatial system is intersected by five other axes, indicating good kinetic fluidity in the city and providing the user with an average of five choices in their movements within the city.

When examining the axial map and the connectivity index values of the city of Djelfa during this period (Fig. 3), several noteworthy observations come to light. Firstly, the axes of the city center maintained their significance and even increased their values due to their connection with important axes in the new expansions. This facilitated easy access to the city center from different directions and enabled comfortable outward expansion towards the borders of the Mellah valley to the east and the Larbi Ben M'hidi axis to the west. Moreover, within this space, the facades of the sub-streets underwent transformations, giving rise to diverse commercial and service fronts. However, it is important to note that certain neighborhoods lack the presence of interconnected axes, resulting in a higher degree of privacy. One such example is the old tower neighborhood located north of the old city center. Built by local residents during the colonial period, it possesses a distinct character that prevented its streets from turning into bustling commercial areas, despite its proximity to the city center. Additionally, this neighborhood did not benefit from restructuring programs aimed at integrating it into the city center's activities.

The new neighborhoods that emerged on the far-western side of the city resemble a cord extending from the northwest to the southwest, following the path of the Western bypass road (Algiers–Laghouat). These neighborhoods include Hay Al-Sha'wa, Al-Fusha, Al-Zariah, Ben Said, and the Urban Pole of

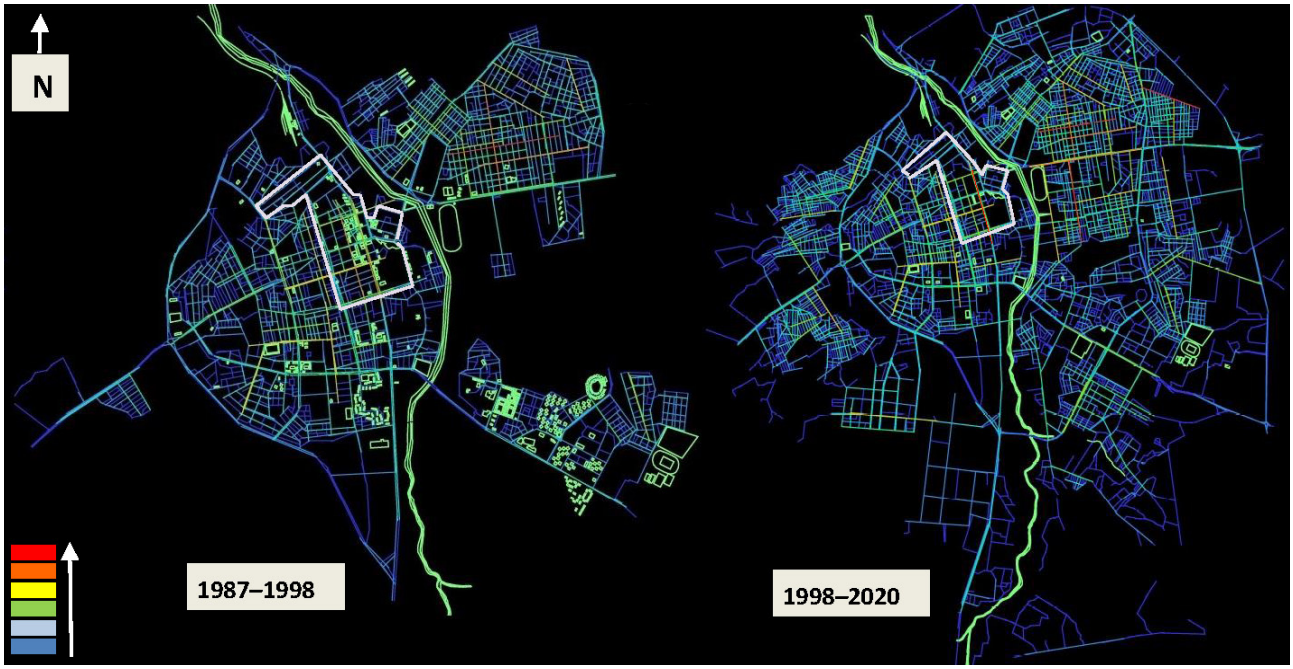

Fig. 3. Axial map of Djelfa in 1987–1998 and in 1998–2020 (connectivity). Source: authors

Berbih. These neighborhoods have a gradient in color and therefore differ in connectivity values. The axes with the highest connectivity values represent important axes within the neighborhood, where many streets converge. These axes provide kinetic fluidity as they represent public spaces within these neighborhoods. Next, there are less interconnected axes, which represent semi-public spaces. Finally, there are those axes that represent semi-private and private spaces within these neighborhoods. Since these areas are primarily residential, the number of axes with high connectivity values within one neighborhood is limited. Regarding the planned territorial divisions that were established in the mid-1990s, the main axis is located in the middle of the neighborhood. Numerous sub-axes branch out from it, creating a sense of balance within the neighborhood. This is in contrast to the illegal neighborhoods of Al-Fusha, Al-Zariah, and Ben Said, which grew and developed unnoticed by the authorities. Their status was later settled under the law of 08/15. These neighborhoods were planned spontaneously, with privacy in mind, leaving the important hubs on their borders impermeable to their fabric. Then the new pole emerged in Berbih, which was a planned residential neighborhood. It should be noted that the most significant axis situated in this neighborhood has a connectivity value of 21. This important axis is located in the middle of the neighborhood and extends from east to west. A large part of collective housing adjacent to it does not face it, and there are no ground-floor shops that benefit from the significance of this axis. The exception being a few shops located in its far west. This important axis, which provides good mobility, has not been utilized up to now and will not be utilized in the future due to the type of housing adjacent to it (collective housing). It is impossible to open shops at its level. This axis, which would have represented a commercial pole, attracts various commercial and service activities and saves the residents the trouble of traveling long distances. This reduces the need for mechanical transportation, which in turn minimizes energy waste and decreases air pollution.

The emergence of significant shifts in the spatial structure of the eastern side, particularly in the new neighborhoods, can be observed. The spatial axes of these neighborhoods follow the same planning and direction as the axes of the Boutrifis neighborhood. These neighborhoods were planned as public plots designated for individual private housing. This planning facilitated the formation of several important axes within the heart of these neighborhoods. They are characterized by high connectivity, and the biggest beneficiary of these planned expansions is the axis of National Road 46. Its connectivity value increased from 15 in the period of 1987–1998 to 27 in this period because it benefited from 12 new axes that intersect it. As a result, it became an important link between the city center and such neighborhoods as Boutrifis, Boukhalfa, Al-Mostakbal, Suleiman Omairat, Al-Wiam, Hashi, and Bahrara. This is due to the significant kinetic fluidity that it provides.

Global Integration Index (Rn)

Djelfa before 1962

The axial map that represents the global integration index for the city of Djelfa before independence (Fig. 4) shows that most of the axes

of the colonial core, which represent the streets where the colonists lived, are axes with high integration values. Where the axis colors range from red to orange to yellow to green, these are the streets that represent the axes that can be reached with the fewest number of steps. It is clear that the areas with low integration, which can only be reached with the greatest number of steps, appear isolated from the rest of the urban fabric. The axes that appear on the map in dark blue are axes located in the Al-Bordj neighborhood, which is inhabited by locals. A distinction between the residents of these neighborhoods is observed. The average global integration of the spatial structure of the urban fabric is 1.35, indicating a high level of integration. The National Road 1 axis has the highest integration value of 2.38, while the Al-Bordj district's sub-axis has the lowest value of 0.67.

Djelfa in the period between 1962 and 1977

The average global integration is 1.14, indicating a high level of integration within the spatial system as a whole. However, this value slightly decreased compared to the period before independence (1.35). This decline resulted from the city's expansion beyond the boundaries of the initial colonial core and the development of eastern and western neighborhoods in the Mellah Valley. The axial map displaying the global integration index (Rn) for the city of Djelfa (Fig. 5) shows that the areas exhibiting high integration, represented by red, orange, and yellow colors, are primarily located in the city center. This leads to the conclusion that the historical city center remained unaffected by the expansions, maintaining its prominence. Notably, axes such as the Emir Abdelkader axis, the AL-Ma'rad axis, the Sidi Nael axis, the city center–Bab Al-Charef axis, and the old post office–Ben Jerma axis, all appear in red. These axes denote the commercial and kinetic significance of the city center in relation to the outskirts. In contrast, the new neighborhoods on the outskirts of the city are depicted in blue due to their lack of global integration. This indicates their great depth, which makes it difficult to access them from other areas, particularly the Zahaf neighborhood, 100 houses, and the northern part of the old Ain Al-Shih neighborhood.

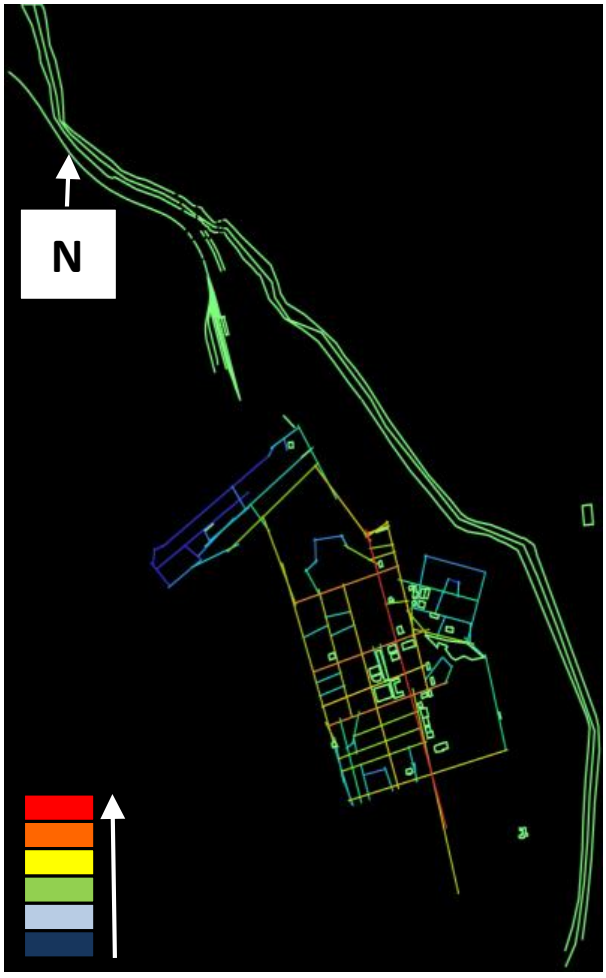

Fig. 4. Axial map of Djelfa before 1962 (global integration (Rn)). Source: authors

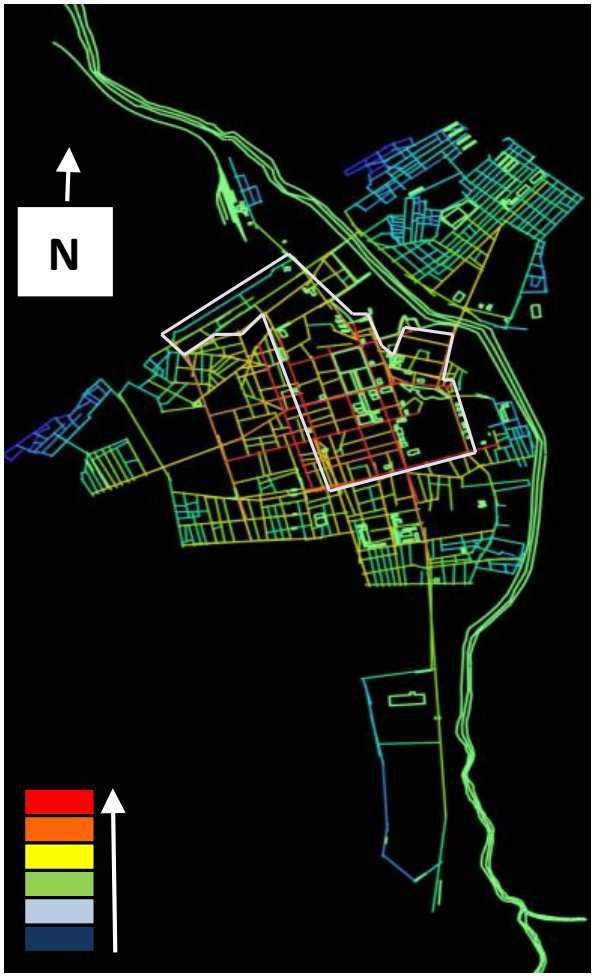

Fig. 5. Axial map of Djelfa in 1962–1977 (global integration (Rn)). Source: authors

Djelfa in the period between 1977 and 1987

The average global integration for the entire spatial network of the system is 1.02. This value suggests that integration is at its lowest level. However, when we examine the axial map representing global integration (Rn) for the city of Djelfa from 1977 to 1987 (Fig. 6), we can see that there is a concentration of important axes with high integration depicted in red. These axes are primarily located in the colonial center of the city and were expanded through the restructuring process of the city center, which involved the opening of Mohamed Boudiaf Square on the site of old dwellings. This contributed to raising the global integration of the AL-Ma'rad axis to its highest value within the entire spatial system, up to 1.61. It is worth noting that this was accomplished while the city's size nearly doubled compared to the previous period.

Global integration, even if it had lesser value, extended to most parts of the city, particularly the newer ones like the Boutrifis neighborhood on the eastern side of the Mellah valley. Its connection with the Ain Al-Asrar neighborhood contributed to raising the integration of the latter, which had previously experienced low global integration. This connection increased the number of axes that can be accessed from any other axis with the fewest number of steps and thus reduced its isolation. The Al-Bordj neighborhood endured isolation and lack of connectivity within the previous period. However, the emergence of the Issa Al-Qaed neighborhood to the north, and the expansion of the Al-Daya neighborhood to the southwest, along with their connection to Al-Bordj through various spatial axes, contributed to its transformation. It went from being an isolated neighborhood lacking movement to becoming a neighborhood that shows remarkable recovery, acting as a link connecting the Al-Daya and Ain Al-Shih neighborhoods in the west, the Ain Al-Asrar and Boutrifis neighborhoods in the east, and the Issa Al-Qaed neighborhood in the north with the city center in the south. This is evident in the colors of the structured axes (yellow and green).

Djelfa in the period between 1987 and 1998

We note that the average global integration (Rn) decreased to 0.82 after being 1.02 in the period of 1977–1987. This value indicates that the spatial system as a whole is not integrated and is characterized by depth. It means that moving from one axis to another requires many detours, thereby increasing the difficulty of movement. By analyzing the axial map displaying the global integration index (Rn) (Fig. 7), we can identify the reason for this decline. We can see that the city expanded during this period, with its size increasing by approximately one-third. The growth includes the development

Fig. 6. Axial map of Djelfa in 1977–1987 (global integration (Rn)). Source: authors

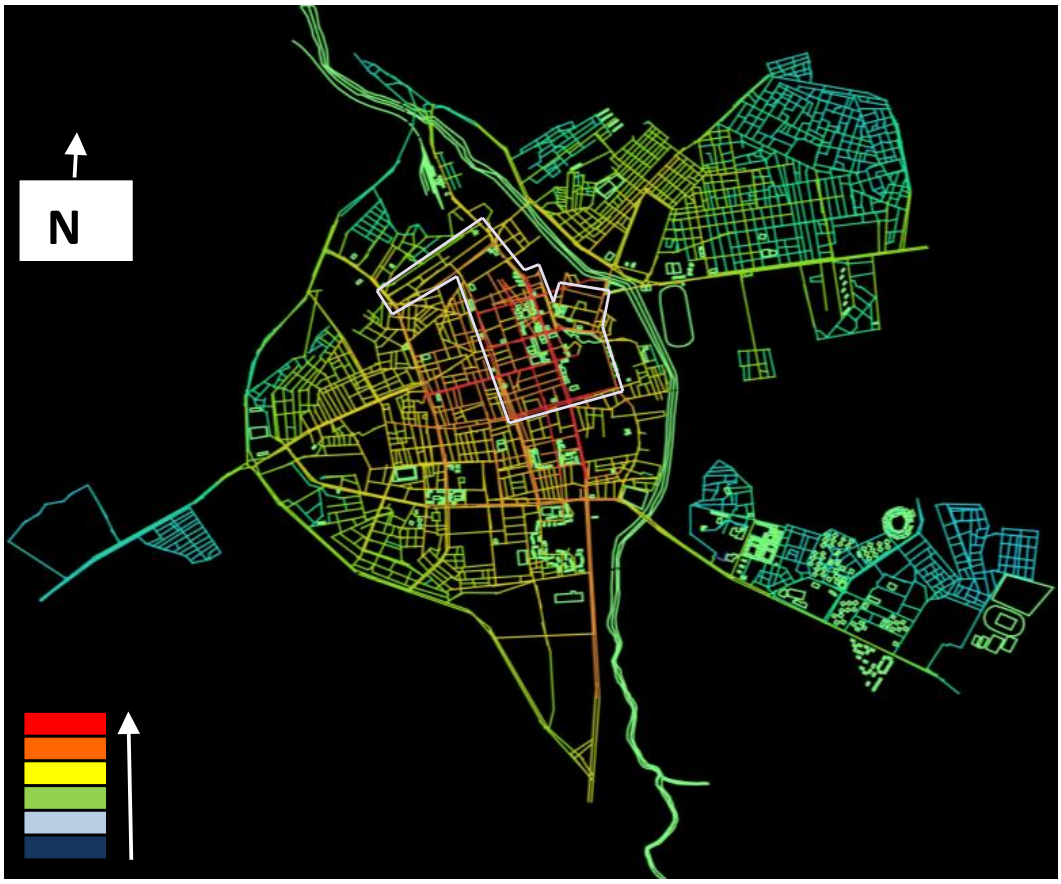

Fig. 7. Axial map of Djelfa in 1987–1998 (global integration (Rn)). Source: authors

of a new urban residential area in the eastern part represented by the July 05 neighborhood. Despite its large size, this neighborhood is isolated and connected to the rest of the city only through one axis, which is the July 05–Al-Ruwaini axis.

Most of the affected neighborhoods are displayed on the axial map showing the global integration index (Rn) in yellow. This indicates their highly acceptable integration, as they transformed from semi-private areas to semi-public areas. These neighborhoods can now be accessed from every axis in the city's spatial system, with an average number of steps. With adequate pedestrian and vehicle traffic, these neighborhoods can potentially evolve into an extension of the city center and serve as an outlet when it becomes saturated in the future.

Regarding the city center, it witnessed significant transformations. Its most important spatial axes are marked in red, and they are the most well-integrated axes within the overall spatial system. These axes are the least deep, which makes them the easiest to access with the fewest number of steps. These axes witness intense movement, whether by pedestrians or vehicles, because they represent areas that provide high liquidity. On the other hand, we have observed the expansion of the historical city center beyond its original borders in the west, reaching the Larbi Ben M'hidi axis. The restructuring and extension to the north and south, highlighted in red, facilitated the movement of both pedestrians and vehicles, particularly after its connection to several important axes originating from the city center in the west and leading towards it. Furthermore, the global integration index (Rn) of most of the sub-streets that flow into it increased, attracting more commercial and service activities. Consequently, these streets transformed from semi-public spaces to bustling public streets, further enhancing the city center's appeal. The old one serves as an outlet to the west, as well as a means of relieving pressure from pedestrians and vehicles. No urban intervention was made on the eastern side of the old city center to repair the damage caused by blocking the ends of the beautiful AL-Dhil AL-Jamil axis. As a result, the latter neither contributed to the flow of pedestrians and vehicles nor attracted substantial activities in line with the city center's level. Consequently, it became a mere back street for parking vehicles.

Djelfa in the period between 1998 and 2020

The average global integration index (Rn) for the city of Djelfa in the period of 1998–2020 was low, decreasing from 0.82 in the period of 1987–1998 to 0.74. This suggests that the city lacks integration and is dominated by depth. A user had to take many detours to reach other axes in the city, but when looking at the axial map displaying the

global integration index (Rn) (Fig. 8), we find some interesting observations:

The global integration index (Rn) accurately shows us the most integrated areas within the space system, which can be accessed with the least number of steps. These areas are the historical (colonial) city center, with its highly integrated axes (in red) and the adjacent neighborhoods.

The variation in colors, evident in the axial map of the global integration index, provides us with an accurate understanding of the kind of space and its position in relation to the city's overall spatial system. The color gradient is as follows: red and orange represent public spaces; yellow and green represent semi-public spaces; light blue represents semi-private spaces, and dark blue represents private spaces. The red and orange axes, representing the most integrated spaces in the spatial system that can be reached with the fewest number of steps, are located in the historical city center and the adjacent axes. The city center expanded southward with the National Road 1 axis to the northern border of the industrial zone. To alleviate pressure on this axis, a west-east axis parallel to the Al-Ruwaini–Shabani axis was opened, with a bridge over the Mellah valley connecting the southwest and southeast of the city. This intervention greatly increased the integration of this axis. Furthermore, a bridge connecting this axis with the crossroads of July 05, Shabani, and Al-Ruwaini had a significant impact on its integration, transforming it from weak to strong (red color). This axis attracted intense movement, which will likely affect the future land occupation and the diversity of activities on this axis.

The Larbi Ben M'hidi axis remains on the western side as a dividing line between the expanding city center and the semi-private and private areas. In other words, at this stage, the city center did not extend beyond the north-south axis of Larbi Ben M'hidi, particularly on its northern side, unlike its southern side, which saw a slight expansion along the Al-Hawas–Ain Al-Shih axis.

The neighborhood of July 05 is still considered isolated in relation to the spatial system of the city in this modern period. Unlike the Shabani neighborhood, which benefited from its association with the Ben Tiba neighborhood and transformed most of its main axes into public and semi-public areas, access to it requires the fewest number of steps within the entire spatial system. However, the July 05 neighborhood is isolated and failed to benefit from the expansion of the Ben Tiba and Al-Mostakbal neighborhoods to the north. This is due to a natural obstacle, namely a forest located to the north, which prevents the neighborhood from connecting with the new neighborhoods with good global integration.

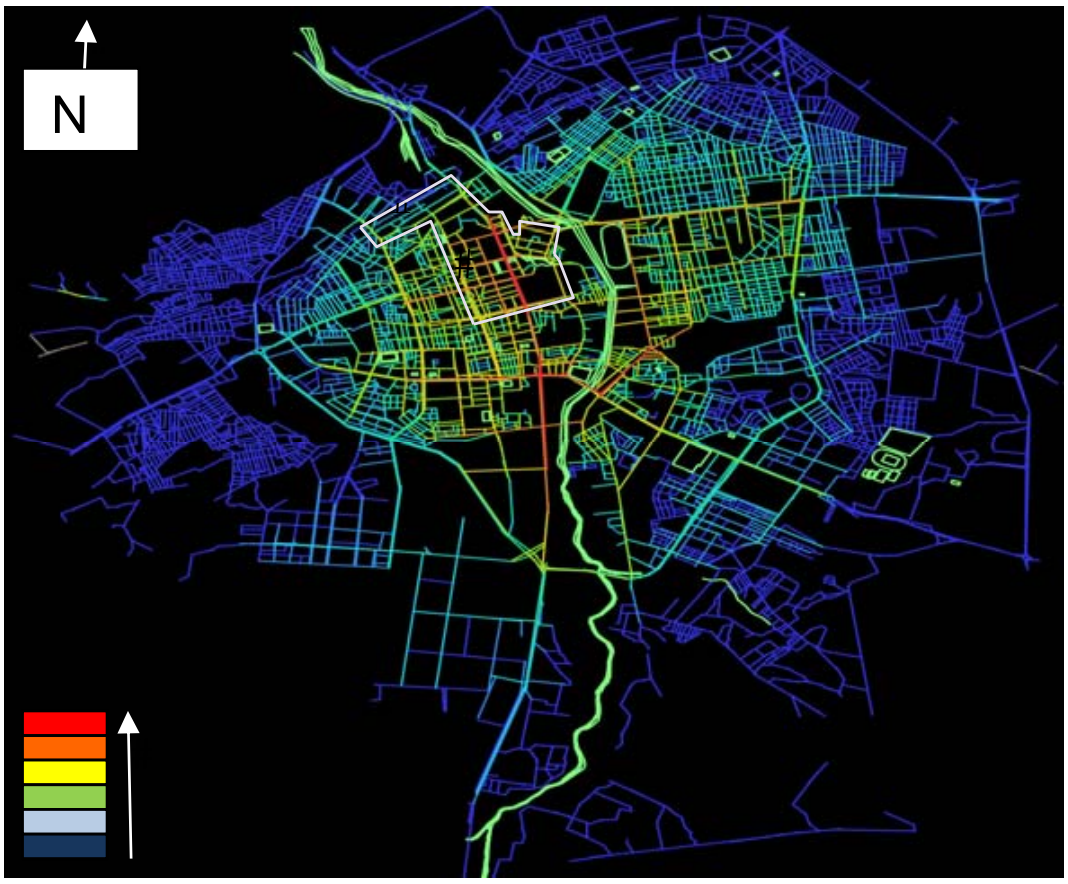

Fig. 8. Axial map of Djelfa in 1998–2020 (global integration (Rn)). Source: authors

Conclusions

Djelfa before 1962 (before independence)

The number of axes in its urban fabric was 86, with an average connectivity of 4.13. This means that each axis intersects with four other axes. The highest value was estimated at approximately 16, which was carried by National Road 1 (Algiers–Laghouat or Emir Abdelkader later). This road is considered the first point of reference on which the initial nucleus of the city was established. With an average global integration (Rn) of 1.35, the ancient Al-Bordj neighborhood, inhabited by local residents, is the least integrated in the entire urban fabric and therefore isolated from the spatial structure as a whole.

Djelfa in the period between 1962 and 1977

During this period, the number of its axes increased to 574, with an average connectivity of 5.1. The Khemisti axis became (within the limits of the colonial nucleus) the highest in terms of connectivity, reaching 24, as the city expanded on the western side. This expansion benefited this axis. During this period, the historical city center maintained its status and remained unaffected by the new expansions. This is confirmed by the average global integration (Rn), which had a value of 1.14. The axial map indicated that areas with high global integration were concentrated in the city center.

Djelfa in the period between 1977 and 1987

During this period, the number of axes in the urban fabric of the city of Djelfa increased to 1127, which is approximately twice as many as in the previous period. This indicates that the city doubled in size. Additionally, the average connectivity index of the city increased to 5.5, which is the highest among all the periods studied. The higher connectivity axis further shifted towards the eastern side. This period witnessed the emergence of new axes with high connectivity, particularly in the Boutrifis neighborhood. However, other axes experienced a decline in connectivity due to their inability to keep up with the city's expansion, poor planning, discontinuity as the Khemisti axis in the city center, and the restructuring of the city center. The opening of Mohamed Boudiaf Square also played a role in increasing the connectivity index of the nearby axes, particularly the AL-Dhil AL-Jamil axis. The average global integration (Rn) during this period was the lowest at 1.02. (An Rn value below 1 indicates that the city is not integrated, meaning it has a significant level of isolation.) Even in this period, the most easily accessible (with the fewest number of steps) and integrated axes can be found in the colonial city center.

Djelfa in the period between 1987 and 1998

During this period, the number of axes in the urban fabric of the city of Djelfa increased to 1801, which accounts for about a third of the city's size in the previous period. The average connectivity index is 5.3, meaning that each axis in the spatial system intersects with approximately five other axes. This value is considered good, as it indicates that the spatial system of the city remains coherent despite its expansion and growth. By examining the axial map of Djelfa displaying the connectivity index, we can make important and accurate observations regarding the city center, the outskirts, and the new neighborhoods. However, the average global integration index (Rn) decreased to 0.82, indicating that the overall spatial system of the city is not well-integrated. This means that reaching desired destinations within the city requires traversing numerous streets. The reason for this decline is due to the emergence of a new urban residential area in the eastern part, represented by the July 05 neighborhood. Despite its large size, it is isolated and not well connected to the city, except through a single axis (July 05–Alrwini axis).

Djelfa in the period between 1998 and 2020

During this period, the number of axes in the spatial system of the city of Djelfa increased to 4036, which is more than twice. This period was characterized by significant demographic growth and rapid reconstruction. The city also witnessed significant transformations, with an average connectivity index of 5.1, which is considered high. Given the size of the city, this indicates good fluidity and suggests that users have an average of five transportation options available to them. The analysis of the connectivity index has revealed some important observations. Firstly, the axes of the city center have maintained their values and have become even stronger due to their connection to important axes in the new expansions. This connectivity allows for easy access to the city center from various directions, and enables the expansion of the city towards the Mellah valley in the east and the Larbi Ben M'hidi axis in the west. However, it is worth mentioning that the average global integration index (Rn) decreased to 0.74, indicating that the city as a whole lacks depth and integration. This means that users often have to navigate through multiple depths to reach different axes within the city. Nonetheless, when we examine the axial map displaying the global integration index (Rn), we can clearly observe a gradation of spaces. The most integrated spaces are public areas, followed by semi-public areas with moderate integration. In contrast, semi-private areas have lower integration, while private areas are isolated and situated deeper within the spatial system.

From all of the above, it becomes clear to us that analyzing the city using the spatial syntax methodology has helped us reveal the important transformations that the city witnessed from its colonial inception to the latest stage. The morphological composition of the first colonial nucleus with its chess layout center and the continued expansion of the city greatly

contributed to the distinction of the city center as a commercial center. This expansion also allowed the city to grow beyond its original borders. The high connectivity and integration indices further indicate the ease of movement and accessibility from different parts of the city. The results also showed that the restructuring and construction of Mohamed Boudiaf Square greatly affected the adjacent axes and led to an increase in traffic and commercial activities, especially along the AL-Dhil AL-Jamil axis. However, they also revealed that the illegal and unplanned neighborhoods, such as Al-Fusha and Ben Said, faced significant isolation due to their limited connectivity and integration with the rest of the city. Commercial activities are driven by the most interdependent axes and integrated areas, which highlights the influence of the spatial structure on human behavior.

References

AMOKRANE, R. (2016). *Mutations urbaines et architecturales du centre ville (noyau colonial) d'Ain Beida Etat des lieux et perspectives futures* (Doctoral dissertation, Université Mohamed Khider-Biskra).

El-Agouri, F. A. (2004). *Privacy and segregation as a basis for analyzing and modelling the urbain space composition of the Libyan traditional city. Case study: the city of Ghadames*. PhD Thesis in City and Regional Planning. Middle East Technical University.

Elporolosy, L. A. and Elfalafly, M. H. S. M. (2020). Mosques functional efficiency. A comparative study using space syntax theory. *International Research Journal of Engineering and Technology (IRJET)*, Vol. 07, Issue 12, pp. 1552–1569.

Fareh, F. and Alkama, D. (2022). The effect of spatial configuration on the movement distribution behavior: the case study of Constantine Old Town (Algeria). *Engineering, Technology & Applied Science Research*, Vol. 12, No. 5, pp. 9136–9141. DOI: 10.48084/etasr.5169.

Hanson, J. (1989). Order and structure in urban design: The plans for the rebuilding of London after the Great Fire of 1666. *Space Syntax: Social implications of urban layouts*, Vol. 56, No. 334/335, pp. 22-42.

Hillier, B. (1996). *Space is the machine: a configurational theory of architecture*. Cambridge: Cambridge University Press, 368 p.

Hillier, B. (1999). The common language of space : a way of looking at the social, economic and environmental functioning of cities on a common basis. *Journal of Environmental Sciences*, Vol. 11, pp. 344–349.

Hillier, B. (2005). Between social physics and phenomenology: explorations towards an urban synthesis? In: van Nes, A. (ed.). *Space Syntax 5th International Symposium*, Vol. 2, pp. 3–23.

Lynch, K. A. (2008). What Is the Form of a City, and How Is It Made?. *Urban ecology: an international perspective on the interaction between humans and nature*, 677-690.

Malverti, X. and Picard, A. (1989). *Les villes coloniales fondées entre 1830 et 1870 en Algérie (II). Les tracés de ville et le savoir des ingénieurs du génie*. [Rapport de recherche] 576/89, Ministère de l'équipement et du logement / Bureau de la recherche architecturale (BRA); Ministère de la recherche; Ecole nationale supérieure d'architecture de Grenoble. 1989. hal-01905850

Miller, J. (1989). Growth and renewal: The Swedish model. *Space Syntax: Social implications of urban layouts*, Vol. 56, No. 334/335, pp. 56-64.

Mills, G. (1989). Space and power in South Africa: The township as a mechanism of control. *Space Syntax: Social implications of urban layouts*, Vol. 56, No. 334/335, pp. 65–74.

Peponis, J. (1993). Evaluation and formulation in design - the implications of morphological theories of function. *Nordic Journal of Architectural Research*, Vol. 2, pp. 53–62.

Perrin, L. (2001a). La syntaxe spatiale entre dans le vocabulaire des urbanistes. *Diagonal*, No. 152, pp. 23–24.

Perrin, L. (2001b). La syntaxe spatiale : configuration de l'espace urbain et pratiques sociales. *Etudes foncières*, No. 93, pp. 32–34.

Rahmane, A. and Abbaoui, M. (2021). The architectural genotype approach in contemporary housing (1995 to 2010): the case study of Setif, Algeria. *Engineering, Technology & Applied Science Research*, Vol. 11, No. 1, pp. 6810–6818. DOI: 10.48084/etasr.4006.

Sukor, N. S. A. and Fisal, S. F. M. (2020). Safety, connectivity, and comfortability as improvement indicators of walkability to the bus stops in Penang Island. *Engineering, Technology & Applied Science Research*, Vol. 10, No. 6, pp. 6450–6455. DOI: 10.48084/etasr.3849.

Turner, A. (2004). *DepthMap4: a researcher's handbook.* London: UCL, 52 p.

Turner, A., Penn, A., and Hillier, B. (2005). An algorithmic definition of the axial map. *Environment and Planning B: Planning and Design*, Vol. 32, Issue 3, pp. 425–444. DOI: 10.1068/b31097.

Teklenburg, J. A. F., Timmermans, H. J. P., and van Wagenberg, A. F. (1993). Space syntax: standardized integration measures and some simulations. *Environment and Planning B: Planning and Design*, Vol. 20, Issue 3, pp. 347–357. DOI: 10.1068/b200347.

UN Department of Economic and Social Affairs Statistics Division (2008). *Principles and recommendations for population and housing censuses. Revision 2*. New York: UN, 420 p.

Vacher, H. (1997). *Projection coloniale et ville rationalisée: Le rôle de l'espace colonial dans la constitution de l'urbanisme en France*. Ph.D. Thesis. Copenhagen: Aalborg University.

ИССЛЕДОВАНИЕ ГОРОДСКИХ ПРЕОБРАЗОВАНИЙ И ИХ ВЛИЯНИЯ НА КОЛОНИАЛЬНУЮ ГОРОДСКУЮ ЗАСТРОЙКУ В ДЖЕЛЬФЕ (АЛЖИР) С ПОМОЩЬЮ ПРОСТРАНСТВЕННОГО СИНТАКСИСА

Брахим Ахмед[1], Хальфалла Буджемаа[2]

[1] Университет Зиан Ачур, Джельфа, Алжир

[2] Университет Мохамеда Будиафа, Мсила, Алжир

E-mail: a.brahim@univ-djelfa.dz

Аннотация
Введение: В данной статье рассматриваются городские преобразования Джельфы, которым подвергался город с момента его формирования в качестве колонии до настоящего времени, характеризующиеся стремительным демографическим ростом и урбанизацией, а также обширным использованием городского пространства. **Цель работы:** Исследование городских преобразований Джельфы в динамике и количественное описание городских и социальных характеристик, формирующих застройку; определение наиболее интегрированных (легкодоступных) и уединенных районов города. **Методы:** Для анализа этапов развития города мы использовали методику пространственного синтаксиса, которая основана на моделировании карт городов в виде схем осей и количественном измерении ряда показателей, таких как связанность и интегрированность (Rn). **Результаты:** Были получены значимые результаты, в том числе следующие: исторический центр города по-прежнему сохраняет свое значение с точки зрения доступности, увязанных осей и шахматной планировки, которые способствовали его расширению. Кроме того, в определенные периоды появились жилые кварталы, изолированные от остальной части города. Деятельность по перестройке, в частности, открытие площади Мохамеда Будиафа в центре города, внесла вклад в увеличение связанности соседних осей.

Ключевые слова: городские преобразования, колониальный город, пространственный синтаксис, Джельфа, связанность, интегрированность.

Guide for Authors
for submitting a manuscript for publication in the «Architecture and Engineering»

The journal is an electronic media and accepts the manuscripts via the online submission. Please register on the website of the journal http://aej.spbgasu.ru/, log in and press “Submit article” button or send it via email aejeditorialoffice@gmail.com.

Please ensure that the submitted work has neither been previously published nor has been currently submitted for publication in another journal.

Main topics of the journal:

1. Architecture
2. Civil Engineering
3. Geotechnical Engineering and Engineering Geology
4. Urban Planning
5. Technique and Technology of Land Transport in Construction

Title page

The title page should include:

The title of the article in bold (max. 90 characters with spaces, only conventional abbreviations should be used); The name(s) of the author(s); Author’s(s’) affiliation(s); The name of the corresponding author.

Abstract and keywords

Please provide an abstract of 100 to 250 words. The abstract should not contain any undefined abbreviations or unspecified references. Use the IMRAD structure in the abstract (introduction, methods, results, discussion).

Please provide 4 to 6 keywords which can be used for indexing purposes. The keywords should be mentioned in order of relevance.

Main text

It should have the following structure:
1) Introduction,
2) Scope, Objectives and Methodology (with subparagraphs),
3) Results and Discussion (may also include subparagraphs, but should not repeat the previous section or numerical data already presented),
4) Conclusions,
5) Acknowledgements (the section is not obligatory, but should be included in case of participation of people, grants, funds, etc. in preparation of the article. The names of funding organizations should be written in full).

General comments on formatting:

- Subtitles should be printed in Bold,
- Use MathType for equations,
- Tables should be inserted in separate paragraphs. The consecutive number and title of the table should be placed before it in separate paragraphs. The references to the tables should be placed in parentheses (Table 1),
- Use “Top and Bottom” wrapping for figures. Figure captions should be placed in the main text after the image. Figures should be referred to as (Fig. 1) in the text.

References

The journal uses Harvard (author, date) style for references:
- The recent research (Kent and Park, 1990)...
- V. Zhukov (1999) stated that…

Reference list

The list of references should only include works that are cited in the text and that have been published or accepted for publication. Personal communications and unpublished works should only be mentioned in the text. Do not use footnotes or endnotes as a substitute for a proper reference list. All references must be listed in full at the end of the paper in alphabetical order, irrespective of where they are cited in the text. Reference made to sources published in languages other than English or Russian should contain English translation of the original title together with a note of the used language.

Peer Review Process

Articles submitted to the journal undergo a double blind peer-review procedure, which means that the reviewer is not informed about the identity of the author of the article, and the author is not given information about the reviewer.
On average, the review process takes from one to five months.